OCTOBER 2021 | VOLUME 3 | No. 1

JOURNAL OF MATHEMATICAL SCIENCES & COMPUTATIONAL MATHEMATICS

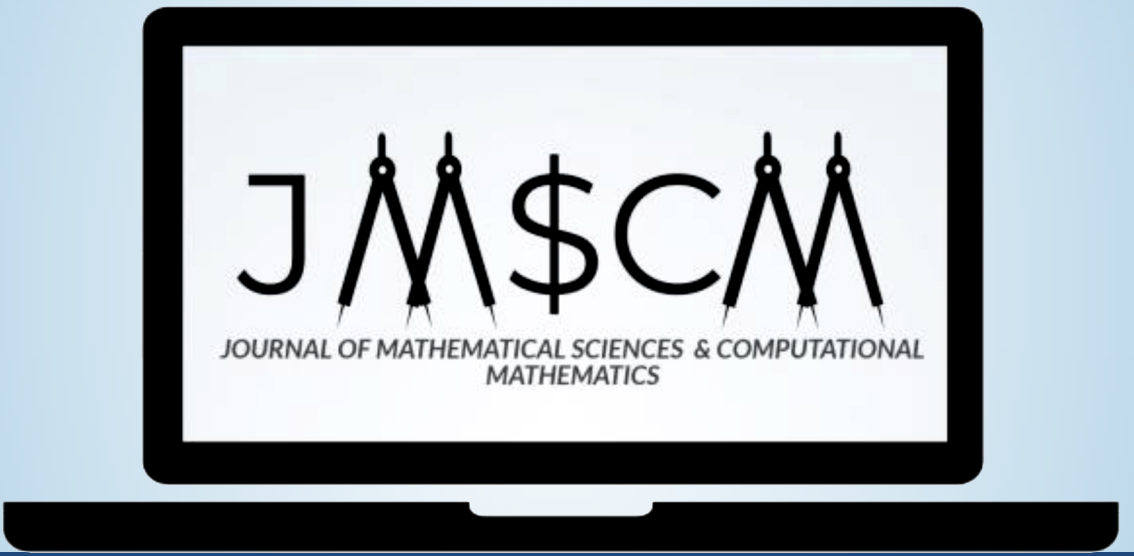

US ISSN Center at the Library of Congress

ISSN 2688-8300 (Print)

ISSN 2644-3368 (Online)

in association with

University of Engineering & Management

Institute of Engineering & Management

A Publication of SMART.

Society for Makers, Artists, Researchers and Technologists
6408 Elizabeth Avenue SE, Auburn, Washington 98092, USA

https://jmscm.smartsociety.org

JOURNAL OF MATHEMATICAL SCIENCES & COMPUTATIONAL MATHEMATICS

VOLUME 3, NO.1

(OCTOBER, 2021)

SOCIETY FOR MAKERS, ARTISTS, RESEARCHERS AND TECHNOLOGISTS

6408 ELIZABETH AVENUE SE, AUBURN, WA 98092, USA

SMART

SOCIETY FOR MAKERS, ARTISTS, RESEARCHERS AND TECHNOLOGISTS

SMART is a publishing organization which seeks to bring to light new and innovative research ventures and publish original works of study. All publications by SMART is undertaken with due authorization of the related author(s).

Journal of Mathematical Sciences & Computational Mathematics is a publication by SMART.

Published in October, 2021

Auburn, USA

ISSN 2688-8300(Print)

ISSN 2644-3368(Online)

SMART

SOCIETY FOR MAKERS, ARTISTS, RESEARCHERS AND TECHNOLOGISTS

6408 ELIZABETH AVENUE SE, AUBURN, WA 98092, USA

Price :USD 200

Editorial and Administrative Information

From Managing Editor's Desk

"Mathematics is a more powerful instrument of knowledge than any other that has been bequeathed to us by human agency" - 'Descartes'

The Journal of Mathematical Sciences & Computational Mathematics (JMSCM) is a peer reviewed, international journal which promptly publishes original research papers, reviews and technical notes in the field of Pure and Applied Mathematics and Computing. It focuses on theories and applications on mathematical and computational methods with their developments and applications in Engineering, Technology, Finance, Fluid and Solid Mechanics, Life Sciences and Statistics.

The spectrum of the Journal is wide and available to exchange and enrich the learning experience among different strata from all corners of the society. The contributions will demonstrate interaction between various disciplines such as mathematical sciences, engineering sciences, numerical and computational sciences, physical and life sciences, management sciences and technological innovations. The Journal aims to become a recognized forum attracting motivated researchers from both the academic and industrial communities. It is devoted towards advancement of knowledge and innovative ideas in the present world.

It is the first issue of third volume and we expect to bring it to the zenith through the cooperation of my friends and colleagues.

We sincerely believe that the quarterly issues of the Journal will receive patronage from our esteemed readers and contributors throughout the globe.

Valuable suggestions from any corner for further improvement of the Journal are most welcome and highly appreciated.

Our thanks are due to the SMART SOCIETY, USA in bringing out the Journal in an orderly manner.

Saktipada Nanda

Biswadip Basu Mallik

Managing Editors

Editorial Board and Editorial Advisory Board members:

Editor in Chief:

Dr. Pooja Bansal
Assistant Professor,
Department of Mathematics,Ram Lal Anand,
College, University of Delhi, New Delhi - 110021,
Email:poojabansal811@gmail.com

Dr. Mohit Kumar Assistant
Professor, Department of
Mathematics,
School of Applied and Life Sciences,
Uttaranchal University, Dehradun, Uttarakhand-248007, India,
Contact No: +91-9627340771
Email: mkdgkv@gmail.com

Dr. Md Tabrez Nafis
Assistant Professor,
Department of Computer Science & Engineering,
School of Engineering Sciences & Technology,
JAMIA HAMDARD (DEEMED UNIVERSITY),
New Delhi - 110062, INDIA
Email: tabrez.nafis@jamiahamdard.ac.in

Dr. Sanket Tikare
Assistant Professor of Mathematics,
Ramniranjan Jhunjhunwala College, Mumbai, India.
Email: sankettikare@rjcollege.edu.in

Dr. Kirti Verma
Associate Professor in Mathematics,
Lakshmi Narain College of Technology, Bhopal, India,
Email: kirtivrm3@gmail.com

Dr. Qazi Aftab Kabir
Assistant Professor in Mathematics,
Govt. Gandhi memorial science college, Jammu, India.
Email: qaziaftabkabir@gmail.com

Prof. Dr. Ihtiram Raza Khan
Professor,
Computer science Department,
JAMIA HAMDARD (DEEMED UNIVERSITY),
New Delhi - 110062, INDIA,
Email: erkhan2007@gmail.com

Joydeep Dey
Head & State Aided College Teacher,
Department Of Computer Science, M.U.C. Women's College,
Burdwan, West Bengal, India.
Email: joydeepmcabu@gmail.com

Dr. Sk Samim Ferdows
Department of Mathematics,
M.U.C. Women's College (Under Burdwan University),
Burdwan, West Bengal, India.
Email: samimstat@gmail.com

Anirban Bhowmik
State Aided College Teacher,
Department of Computer Science,
M.U.C. Women's College, Burdwan,
India
E-mail: animca2008@gmail.com

Dr. George Albert Toma
Lecturer,
Department of Mathematics,
Faculty of Sciences,
Aleppo University, Aleppo,
Syria
Email: george.toma.1987@gmail.com,
Official email: george.toma.1987@alepuniv.edu.sy

Dr. Shaza Alturky
Lecturer.
Department of Mathematics,
Faculty of Sciences,
Aleppo University, Aleppo, Syria.
Email: shazaalturkey@gmail.com

Prasenjit Bhadra
Founder & CEO,
Ranial Systems
Address: Forest Hills Tower, 118-35 Queens Blvd, Suite # 400
Forest Hills, NY 11375
USA.
Telephone: +1(917) 435 – 0700
Email: prasenjit@ranial.com

Contact us :

- **Society for Makers, Artist, Researchers and Technologists**
  6408 Elizabeth Avenue SE, Auburn,
  WA 98092, USA.
  Email: **editor.jmscm@gmail.com**
  Phone: 1-425-605-0775

CONTENTS	Page No.

SOLUTION OF AN INTEGRO-DIFFERENTIAL EQUATION WITH DIRICHLET CONDITIONS USING TECHNIQUES OF THE INVERSE MOMENTS PROBLEM

[1,2]María B. Pintarelli

[1]*Departamento de Matematica de la Facultad de Ciencias Exactas*
Universidad Nacional de La Plata, LaPlata -1900. Argentina

[2]*Departmento de Ciencias Basicas de la Facultad de Ingenieria*
Universidad Nacional de La Plata -1900. Argentina
Email: mariabpintarelli@gmail.com

Abstract

It will be shown that finding solutions from some integro-differential equation under Dirichlet conditions is equivalent to solving an integral equation, which can be treated as a generalized two-dimensional moment problem over a domain $E = \{(x,t),\ 0 < x < L;\ t > 0\}$. We will see that an approximate solution of the equation integro-differential can be found using the techniques of generalized inverse moments problem and bounds for the error of the estimated solution. First the problem is reduced to solving a hyperbolic or parabolic partial derivative equation considering the unknown source. The method consists of two steps. In each one an integral equation is solved numerically using the two-dimensional inverse moment problem techniques.
We illustrate the different cases with examples.

Keywords*: integro-differential equation, integral equations, generalized moment problem.*

INTRODUCTION

Integral and integro-differential equations are found in numerous applications in different fields of science and engineering. For instance, in the mathematical modelling of spatio temporal developments, epidemic modelling and various biological and physical problems. Analytical solutions of integral and integro-differential equations, however, either do not exist or it is often hard to find. It is precisely due to this fact that several numerical methods have been developed for finding approximate solutions of integral and integro-differential equations.

The issue of solving different types of integro-differential equations has been widely discussed in the literature and a great variety of methods have been proposed for its numerical resolution.

Biorthogonal spline wavelet method is proposed for the numerical solution of Linear and nonlinear integral and integro-differential equations in [1]. In [2] it is proposed a new hybrid method to find

analytical approximate or exact solutions for various many linear and nonlinear integro – differential equations. In [3] the paper presents an iterative technique based on homotopy analysis method for solving system of Volterra integro-differential equations. The technique provides us series solutions to the problems which are combined with the diagonal Padé approximants and Laplace transform to obtain closed-form solutions. In [4] the paper is concerned with modification of the Adomian Decomposition Method for solving linear and non-linear Volterra and Volterra-Fredholm Integro-Differential equations. In [5] this paper, we introduced the modified differential transform which is a modified version of a two-dimensional differential transform method. In [6] different classes of integral and integro-differential equations are solved using a modified differential transform method. This proposed technique is based on differential transform method (DTM), Laplace transform (LT) procedure and Padé approximants (PA). In [7] a new modification of homotopy perturbation method was proposed to find analytical solution of high-order integro-differential equations. The Modification process yields the Taylor series of the exact solution. Canonical polynomials are used as basis function equations. The Modification process yields the Taylor series of the exact solution. Canonical polynomials are used as basis function. [8] presents an effective hybrid semi-analytical method for dealing with the integro-differential equations. This new technique is based on the combining of the Kharrat-Toma integral transform with the homotopy perturbation method to find the exact or approximate solutions of both linear and nonlinear models. In [9] a combination between a Sumudu transform (ST) and the homotopy perturbation method (HPM) is presented. Other recent works are [10, 11], to name a few.

Some study inverse boundary problems for one dimensional linear integro-differential equation of the Gurtin – Pipkin type with the Dirichlet to Neumann map as the inverse data [12].

Other jobs study the stability of solutions for a heat equation with memory [13].

In [14] study decay properties in energy norm for solutions of a class of partial differential equations with memory are studied by means of frequency domain methods.

In [15] it is tested that the one-dimensional heat equation with memory cannot be controlled to rest for large classes of memory kernels and controls. The approach is based on the application of the theory of interpolation in Paley–Wiener spaces.

In this work we want to find $w(x,t)$ such that

$$w_t(x,t) = \int_0^t k(t-s)\, w_{xx}(x,s)ds + f(x,t)\,.$$

about a domain $E = \{(x,t),\ 0 < x < L;\ t > 0\}$
with conditions

$$w(x,0) = h_1(x); \qquad w(0,t) = k_1(t); \quad ; \qquad w(L,t) = k_2(t).$$

where $k(t)$ has continuous derivate on $x = 0$, the value of $k(0)$ is known, $f(x,t)$ known and derivative with respect to *t* continuous, using the problem generalized moments techniques.

The objective of this work is to show that we can solve the problem using the techniques of inverse moments problem. We focus the study on the numerical approximation. It is not the objetive to compare with other methods.

The generalized moments problem [16, 17, 18], is to find a function $f(x)$ about a domain $\Omega \subset R^d$ that satisfies the sequence of equations

$$\mu_i = \int_\Omega g_i(x) f(x) dx \quad i \epsilon N ---------- \quad (1)$$

Where N is the set of the natural numbers, $(g_i(x))$ is a given sequence of functions in $L^2(\Omega)$ linearly independent known and the succession of real numbers $\{\mu_i\}_{i\epsilon N}$ are known data. The problem of Hausdorff moments [17,18] , is to find a function $f(x)$ in (a,b) such that

$$\mu_i = \int_a^b x^i f(x) dx \quad i \epsilon N .$$

In this case $g_i(x) = x^i$ with *i* belonging to set *N*.

If the integration interval is $(0,\infty)$ we have the problem of Stieltjes moments; if the integration interval is $(-\infty,\infty)$ we have the problem of Hamburger moments [16,17].

The moments problem is an ill-conditioned problem in the sense that there may be no solution and if there is no continuous dependence on the given data [16,17,18]. There are several methods to build regularized solutions. One of them is the truncated expansion method [17].

This method is to approximate (1) with the finite moments problem

$$\mu_i = \int_\Omega g_i(x) f(x) dx \quad i = 1,2,\dots,n. ------- \quad (2)$$

where it is considered as approximate solution of $f(x)$ to $p_n(x) = \sum_{i=0}^{n} \lambda_i \phi_i(x)$, and the functions $\{\phi_i(x)\}_{i=1,..,n}$ result of orthonormalize $\langle g_1, g_2, \dots, g_n \rangle$ being λ_i the coefficients based on the data μ_i. In the subspace generated by $\langle g_1, g_2, \dots, g_n \rangle$ the solution is stable. If $n \epsilon N$ is chosen in an appropriate way then the solution of (2) it approaches the solution of the problem (1).

In the case where the data μ_i are inaccurate the convergence theorems should be applied and error estimates for the regularized solution (pages 19 - 30 of [17]).

ARTICLE ORGANIZATION

To find $w(x,t)$ such that

$$w_t(x,t) = \int_0^t k(t-s)\, w_{xx}(x,s)ds + f(x,t)\,.$$

about a domain $E = \{(x,t),\ 0 < x < L;\ t > 0\}$
with conditions

$$w(x,0) = h_1(x); \qquad w(0,t) = k_1(t); \quad ; \qquad w(L,t) = k_2(t).$$

we will do it in two steps.
The next section describes the first step.
Then it is explained how the generalized moment problem is solved with the truncated expansion method.
The section that follows explains the second step.
Finally the numerical example and the conclusions.

RESOLUTION OF THE INTEGRO-DIFFERENTIAL EQUATION – FIRST STEP

We want to find $w(x,t)$ such that

$$w_t(x,t) = \int_0^t k(t-s)\, w_{xx}(x,s)ds + f(x,t). - - - - - - - (3)$$

about a domain $E = \{(x,t),\ 0 < x < L;\ t > 0\}$.

We derive with respect to *t*:

$$w_{tt}(x,t) = \int_0^t k_t(t-s)\, w_{xx}(x,s)ds + k(t-t)w_{xx}(x,t) + f_t(x,t).$$

Then

$$w_{tt}(x,t) - k(0)w_{xx}(x,t) = \int_0^t k_t(t-s)\, w_{xx}(x,s)ds + f_t(x,t).$$

We considerer

$$w_{tt}(x,t) - k(0)w_{xx}(x,t) = G(x,t). - - - - - - (4)$$

We can solve (4) as a Klein-Gordon equation with Dirichlet conditions where $G(x,t)$ is unknown.

We consider as auxiliary function

$$u(m,r,x,t) = e^{-m(x+1)}e^{-r(t+1)}\,.$$

We write $k = k(0)$

and

$$w(x,0) = h_1(x); \qquad w(0,t) = k_1(t); \quad ; \qquad w(L,t) = k_2(t)\ .$$

We define the vector field

$$F^* = (F_1(w), F_2(w)) = (-kw_x, w).$$

As $u\ div(F^*) = u\ G(x,t)$ we have to:

$$\iint_E u\ div(F^*)dA = \iint_E u\ G(x,t)dA.$$

Moreover, as $u\ div(F^*) = div(u\ F^*) - F^*.\nabla\ u$, then

$$\iint_E u\ div(F^*)dA = \iint_E div(u\ F^*)dA - \iint_E F^*.\nabla u\ dA. - - - - - - - 5$$

where $\nabla u = (u_x, u_t)$.

Besides that

$$\iint_E div(u\ F^*)dA = \iint_E (-k\ u\ w_x)_x + (u\ w_t)_t dA = \_\_\_\_\_6$$

$$\iint_E u\ div(F^*)dA + \iint_E (-k\ u_x w_x + u_t w_t)dA.$$

Then from (5) and (6):

$$\iint_E (-\ k\ u_x w_x + u_t w_t)dA = \iint_E F^*.\nabla u\ dA\ . - - - - - - - - - 7$$

On the other hand, it can be proven, after several calculations that, integrating by parts:

$$\iint_E F^*.\nabla u\ dA = A(m,r) + B(m,r) - \iint_E u\ w\ (-k\ m^2 + r^2)dA = \varphi(m,r) - - - - 8$$

with

$$A(m,r) = \int_0^\infty (-m)(-k)u(m,r,L,t)w(L,t) - (-m)(-k)u(m,r,0,t)w(0,t)dt$$

$$B(m,r) = \int_0^L -(-r)u(m,r,x,0)w(x,0)dx\ .$$

If $\sqrt{k}\ m = r$, instead of (7) and (8)

$$\iint_E (-k)(-m)u\,w_x - \sqrt{k}\,m\,w_t u dA = \varphi\left(m, \sqrt{k}\,m\right).$$

$$\therefore \quad \iint_E u\left(kw_x - \sqrt{k}\ w_t\right)dA = \frac{\varphi\left(m, \sqrt{k}\,m\right)}{m}.$$

with

$$\frac{\varphi\left(m, \sqrt{k}\,m\right)}{m} = \int_0^\infty k\,u\left(m, \sqrt{k}\,m, L, t\right)w(L,t) - k\,u\left(m, , \sqrt{k}\,m, 0, t\right)w(0,t)dt +$$

$$+ \int_0^L u\left(m, \sqrt{k}\,m, x, 0\right)\sqrt{k}\ w(x,0)dx\ .$$

We note $\varphi_1(m) = \frac{\varphi(m,\sqrt{k}\,m)}{m}$, then

$$\iint_E u\left(kw_x - \sqrt{k}\ w_t\right)dA = \varphi_1(m)\,. - - - - - - - - - - 9$$

To solve this integral equation we take a base $\psi_i(m) = m^i e^{-m} \quad i = 0,1,2,\ldots,n$ Then we multiply both members of (9) by $\psi_i(m) = m^i e^{-m}$ and we integrate with respect to *m*, we obtain

$$\iint_E H_i(x,t)\left(kw_x - \sqrt{k}\,w_t\right)dA = \int_0^\infty \varphi_1(m)\psi_i(m)dm = \mu_i \quad i = 0,1,2,\ldots,n\,. - - - - - 10$$

where $H_i(x,t) = \int_0^\infty u(m, \sqrt{k}\,m, x, t)\psi_i(m)dm.$

We can interpret (10) as a generalized two-dimensional moment problem. We solve it numerically with the truncated expansion method and we found an approximation $p_n\,(x,t)$ for $kw_x - \sqrt{k}\ w_t$.

SOLUTION OF THE GENERALIZED MOMENTS PROBLEM

We can apply the detailed truncated expansion method in [18] and generalized in [15] and [19] to find an approximation $p_n\,(x,t)$ of $kw_x - \sqrt{k}\ w_t$ for the corresponding finite problem with $i = 0,1,2,\ldots,n$ where *n* is the number of moments μ_i. We consider the basis $\phi_i(x,t)\ i = 0,1,2,\ldots,n$ obtained by applying the Gram-Schmidt orthonormalization process on $H_i(x,t)\ \ i = 0,1,2,\ldots,n.$

We approximate the solution $kw_x - \sqrt{k}\ w_t$ with [18] and generalized in [19] and [20]:

$$p_n(x,t) = \sum_{i=0}^n \lambda_i\phi_i(x,t) \quad \text{where} \quad \lambda_i = \sum_{j=0}^i C_{ij}\ \mu_j \quad \text{i} = 0,1,2,\ldots,n\,.$$

And the coefficients C_{ij} verify

$$C_{ij} = \left(\sum_{k=j}^{i-1} (-1) \frac{\langle H_i(x,t) | \phi_k(x,t) \rangle}{\|\phi_k(x,t)\|^2} C_{kj} \right) . \|\phi_i(x,t)\|^{-1} \quad 1 < i \leq n \, ; 1 \leq j < i \, .$$

The terms of the diagonal are $\|\phi_i(x,t)\|^{-1} \;\; i = 0,1, \dots, n$.

The proof of the following theorem is in [20,21]. In [21] the demonstration is made for b_2 finite. If $b_2 = \infty$ instead of taking the Legendre polynomials we take the Laguerre polynomials. En [22] the demonstration is made for the one-dimensional case.

This Theorem gives a measure about the accuracy of the approximation.

Theorem

Sea $\{\mu_i\}_{i=0}^n$ be a set of real numbers and suppose that $f(x,t) \, \epsilon \, L^2((a_1,b_1) \times (a_2,b_2))$ for two positive numbers ε and M verify:

$$\sum_{i=0}^{n} \left| \iint_E H_i(x,t) f(x,t) dt dx - \mu_i \right|^2 \leq \varepsilon^2 \quad .$$

$$\iint_E (x \, f_x^{\,2} + t \, f_t^{\,2}) \, Exp[x+t] dt dx \leq M^2 \;\; .$$

then

$$\int_{a_1}^{b_1} \int_{a_2}^{\infty} |f(x,t)|^2 \, dt dx \leq min_i \left\{ \|C^T C\| \varepsilon^2 + \frac{1}{8(n+1)^2} M^2 ; i = 0,1, \dots, n \right\}$$

and

$$\int_{a_1}^{b_1} \int_{a_2}^{\infty} |f(x,t) - p_n(x,t)|^2 \, dt dx \leq \|C^T C\| \varepsilon^2 + \frac{1}{8(n+1)^2} M^2 .$$

And it must be fulfilled that

$$t^i f(x,t) \to 0 \quad \text{si} \quad t \to \infty \quad \text{para todo} \quad i \in N \; . \blacksquare$$

RESOLUTION OF THE INTEGRO-DIFFERENTIAL EQUATION – SECOND STEP

So we have an equation in first order partial derivatives of the form

$$k w_x(x,t) - \sqrt{k} w_t(x,t) = p_n(x,t)$$

that is, it can be written as

$$A_1(x,t) w_x(x,t) + A_2(x,t) w_t(x,t) = p_n(x,t) \, .$$

where $A_1(x,t) = k$ and $A_2(x,t) = -\sqrt{k}$

It is resolved as in [21], that is, we can prove that solving this equation is equivalent to solving the integral equation

$$\int_0^L \int_0^\infty K(m,r,x,t)w(x,t)dtdx = \varphi_2(m,r). - - - - - - - - - 11$$

with $K(m,r,x,t) = u(m,r,x,t)\left(-m_1k(m+1) + m_2\sqrt{k}(r+1)\right)$

where now it is taken as an auxiliary function

$$u(m,r,x,t) = e^{-m_1(m+1)(x+1)}e^{-m_2(r+1)(t+1)}\,.$$

The values of m_1 and m_2 are chosen in a convenient way to avoid discontinuities, and

$$\varphi_2(m,r) = \int_0^L u(m,r,x,0)\sqrt{k}\,w(x,0)dx +$$
$$+\int_0^\infty u(m,r,L,t)k\,w(L,t) - u(m,r,0,t)k\,w(0,t)dt - \int_0^\infty \int_0^L p_n(x,t)udxdt\,.$$

Again we take a base:

$$\psi_{ij}(m,r) = m^i r^j e^{-(m+r)} \qquad i = 0,1,2,\ldots,n_1 \qquad j = 0,1,2,..,n_2\,.$$

And we multiply both members of (11) by $\psi_{ij}(m,r)$ and we integrate with respect to *m* and *r*.

We have then the generalized moments problem

$$\int_0^L \int_0^\infty w(x,t)H_i(x,t)\ dtdx = \mu_{ij}$$

where

$$\mu_{\{ij\}} = \int_{\{0\}}^{\{L\}} \int_0^\infty \varphi_2(m,r)\psi_{ij}\,(m,r)dmdr\,.$$

$$H_{ij}(x,t) = \int_0^L \int_0^\infty K(m,r,x,t)\psi_{ij}(m,r)dmdr\,.$$

We apply the truncated expansion method and find a numerical approximation for $w(x,t)$.

We can solve in an analogous way the equations

$$w_{tt} = aw_{xx} + \int_0^t k(t-s)w_{xx}(x,s)ds + f(x,t) - - - - - - - - 12$$

and

$$w_t = w_{xx} + \int_0^t k(t-s)w_{xx}(x,s)ds + f(x,t) - - - - - - - - 13$$

In both cases the domain is $E = \{(x,t),\ 0 < x < L;\ t > 0\}$ with Dirichlet conditions.

If (12) the equation would be solved

$$w_{tt} - aw_{xx} = G(x,t),$$

if (13) the equation would be solved

$$w_{tt} - w_{xx} = G(x,t)\ .$$

with $G(x,t) = \int_0^t k(t-s)w_{xx}(x,s)ds + f(x,t)$ where $G(x,t)$ unknown.

This last case was resolved in [23].

NUMERICAL EXAMPLE:

We consider the equation

$$w_t = \int_0^t cos(t-s)w_{xx}(x,s)ds - \frac{1}{5}\, e^{-1-x-2t}(8 + 2e^{2t}\cos(t) + e^{2t}\sin(t))$$

in $(0,3) \times (0,\infty)$.

Conditions:

$$w(0,t) = e^{-2t-1} \qquad w(3,t) = e^{-4-2t} \qquad w(x,0) = e^{-x-1}\ .$$

The solution is: $w(x,t) = e^{-2t-1-x}$

For the first step we take $n = 5$ moments and we approximate $w_x(x,t) - w_t(x,t) = G1(x,t)$.

with accuracy $\int_0^3 \int_0^\infty (p_{15}(x,t) - G1(x,t))^2 = 0.0324621.$

In the Fig. 1 we show $p_{15}(x,t)$ and $G1(x,t)$overlapping.

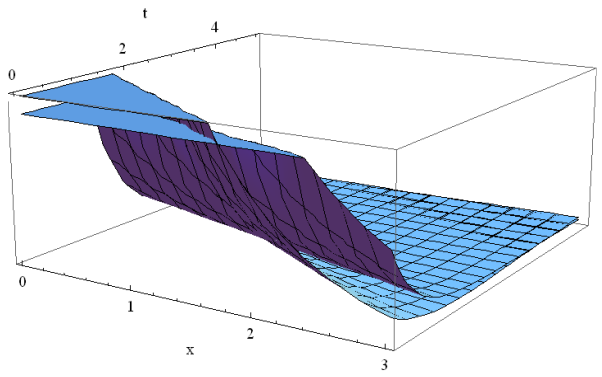

Fig. 1 $p_{15}(x,t)$ and $G1(x,t)$

For the second step we take $m_1 = m_2$=1. We also consider $n_1 = 3$ and $n_2 = 2$, that is 6 moments.

We approximate $w(x,t)$ with accuracy $\int_0^3 \int_0^\infty (p_{26}(x,t) - w(x,t))^2 = 0.0135942.$

In the Fig. 2 we show $p_{26}(x,t)$ and $w(x,t)$ overlapping.

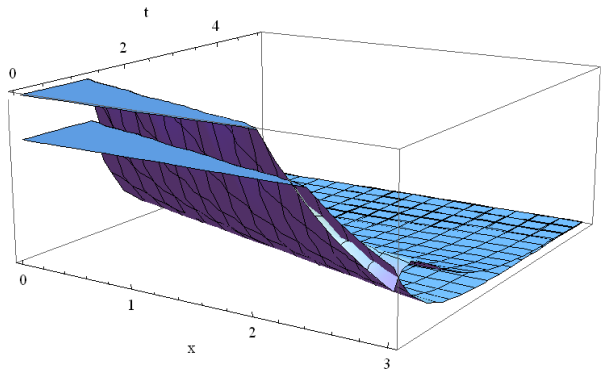

Fig. 2 $p_{26}(x,t)$ and $w(x,t)$

CONCLUSION

An equation integro-differential of the form $w_t(x,t) = \int_0^t k(t-s)\, w_{xx}(x,s)ds + f(x,t)$ where the unknown function $w(x,t)$ is defined in $(0,L) \times (0,\infty)$ under the Dirichlet conditions can be solved numerically by applying inverse problem techniques of moments in two steps considering the equation in partial derivatives $w_{tt}(x,t) - k(0)w_{xx}(x,t) = G(x,t)$ where $k(0)$ is known and $G(x,t)$ unknown.

1. First we consider the integral equation

$$\iint_E u\left(kw_x - \sqrt{k}\ w_t\right)dA = \varphi_1(m)\,.$$

we can solve it numerically as a inverse moments problem, and we get an approximate solution for $kw_x(x,t) - \sqrt{k}\ w_t(x,t)$.

2. as a second step we consider the integral equation

$$\int_0^L \int_0^\infty K(m,r,x,t)w(x,t)dtdx = \varphi_2(m,r)\,.$$

and again it can be solved numerically by applying inverse moments problem techniques, and we get an approximate solution for $w(x,t)$.

We can solve in an analogous way the equations $w_{tt} = aw_{xx} + \int_0^t k(t-s)w_{xx}(x,s)ds + f(x,t)$ and $w_t = w_{xx} + \int_0^t k(t-s)w_{xx}(x,s)ds + f(x,t)$.

In both cases the domain is $(0,L)\times(0,\infty)$ under the Dirichlet conditions.

REFERENCES:

1. R. A. Mundewadi, and B. A. Mundewadi: "Numerical Solution of Linear and Nonlinear Integral and Integro-Differential Equations using Biorthogonal Spline Wavelet Transform Method": Int. J. Math. And Appl., **8(1)**, 7–31 (2020)
2. George. A. Toma:" A Hybrid Semi-Analytical Method with Natural Transform for Solving Integro-Differential Equations": International Journal of Scientific Research in Mathematical and Statistical Sciences: **7(3**), 01-07 (2020)
3. A. O. Adewumi, R. A. Adetona, and B.S. Ogundare: "On Closed-Form Solutions to Integro-Differential Equations": Journal of Numerical Mathematics and Stochastics, **12 (1)**, 28-44 (2021)
4. R. O. Ijaiya , O. A. Taiwo1 and K. A. Bello: "Modified Adomian Decomposition Method for the Solution of Integro-Differential Equations": Asian Research Journal of Mathematics **17(2)**, 111-124 (2021)
5. Yuvraj G. Pardeshi , Vineeta Basotia and Ashwini P. Kulakarni: "Solving Partial Integro Differential Equations using Modified Differential Transform Method": Asian Journal of Applied Science and Technology **4(3),**109-118 (2020)
6. S. Al-Ahmad, Ibrahim Mohammed Sulaiman , and M. Mamat: "An efficient modification of differential transform method for solving integral and integro-differential equations": Aust. J. Math. Anal. Appl. **17 (2),** 5-15 (2020)
7. Micheal .O. Omotosho and Taiwo. O. Adebayo: "Modified Homotopy Perturbation Method For Solving High Order Integro-Differential Equation": Mathematical Theory and Modeling: **10(1),** 15-29 (2020)
8. George Albert Toma, Shaza Alturky: "A Hybrid Kharrat-Toma Transform with Homotopy Perturbation Method for Solving Integro-Differential Equations": Journal of Mathematical Analysis and Modeling: **2(2),** 50-62 (2021)
9. Bachir Nour Kharrat and George Toma: "A New Hybrid Sumudu Transform With Homotopy Perturbation Method For Solving Boundary Value Problems": Middle-East Journal of Scientific Research: **28 (2),** 142-149 (2020)
10. Boukary Béyi, Joseph Bonazebi-Yindoula, Longin Some and Gabriel Bissanga: "Application of the Laplace-Adomian method and the SBA method to solving the partial differential and integrodifferential equations": Journal of Mathematical Sciences: Advances and Applications: (61), 17-35 (2020)

11. Samaneh Soradi-Zeid and Mehdi Mesrizadeh: "The method of lines for parabolic integro-differential equations": Journal of Mathematical Modeling 8(3), 291–308 (2020)
12. Sergei A. Avdonin,Sergei A. Ivanov and Jun-Min Wang: "Inverse problems for the heat equation with memory": Inverse Problems and Imaging: **13(1)**, 31–38 (2019)
13. Nasser-Eddine Tatar, SebtiI Kerbal and Asma Al-Ghassani: "Stability of solutions for a heat equation with Memory": Electronic Journal of Differential Equations: **2017(303)**, 1–16 (2017)
14. Jan Pruss: "Decay properties for the solutions of a partial differential equation with memory": Archiv der Mathematik: **92**, 158–173 (2009)
15. S. Ivanov and L. Pandolfi: "Heat equation with memory: Lack of controllability to rest: "Journal of Mathematical Analysis and Applications: **355**, 1–11 (2009)
16. J.A. Shohat and J.D. Tamarkin: "The problem of Moments": Mathematic Surveys, Am. Math. Soc., Providence, RI (1943)
17. D.D. Ang, R. Gorenflo, V.K. Le and D.D. Trong: "Moment theory and some inverse problems in potential theory and heat conduction": Lectures Notes in Mathematics, Springer-Verlag,Berlin (2002)
18. G. Talenti: "Recovering a function from a finite number of moments": Inverse Problems: **3**, 501- 517, (1987)
19. M. B. Pintarelli and F. Vericat: "Stability theorem and inversion algorithm for a generalize moment problem": Far East Journal of Mathematical Sciences: **30**, 253-274 (2008)
20. M.B. Pintarelli and F. Vericat: "Bi-dimensional inverse moment problems": Far East Journal of Mathematical Sciences: **54** , 1-23, (2011)
21. M.B.Pintarelli: " Linear partial differential equations of first order as bi-dimensional inverse moment problem": Applied Mathematics: **6(6),** 979-989 (2015)
22. M.B.Pintarelli: " Parabolic partial differential equations as inverse moments problem": Applied Mathematics: **7 (1**), 77-99 , (2016)
23. M.B.Pintarelli: "Parabolic Partial Differential Equations with Border Conditions of Dirichlet as Inverse Moments Problem": Applied Mathematics: **8 (1**), 15-25, (2017)

APPLICATION OF BOX-JENKINS MODELS TO THE TOURIST INFLOW IN BHUTAN

Dorji Om, ChompunoochThamanukornsri, kado and MontipTiensuwan

Department of Mathematics, Faculty of Science, Mahidol University, Bangkok, 10400, Thailand

Gongzim Ugyen Dorji Central school, Haa , Bhutan

Email: om_dorji@yahoo.com; Chompunooch.tha@student.mahidol.ac.th; kadoscs@education.gov.bt; montip.tie@mahidol.ac.th

Abstract

Bhutan has now increasingly become a popular destination for many international tourists. Tourism in Bhutan is considered as one of the largest foreign earning industries. The number of tourist inflow in the country is increasing year by year. Forecasting is very necessary for administration and tourist agent for creating awareness and planning for the future development. It can also predict the future trends as accurately as possible and helps in staying one step ahead of the competition. This study aims to apply mathematical model for forecasting monthly tourist inflow from Malaysia, Singapore, China, USA, England, France, Germany, Thailand, Australia and Japan to Bhutan. The Box-Jenkins model is used to identify the parameters of Autoregressive integrated moving average (ARIMA) model of monthly tourist visited data of above mentioned countries in the period 2011-2015 obtained from Tourism Council of Bhutan. An Akaike's Information Criterion, Schwartz's Bayesian Criterion and estimate variance of white noise are used throughout to test for the identification of best fit model. Further, the periodogram analysis was used to confirm the seasonal period of the model. The results showed ARIMA model for Thai, Chinese, Malaysian and Japanese, while seasonal ARIMA for American, Australian, British, French, Singaporean and German. Further, seasonal ARIMA model was obtained as the best fit model for the overall data. These models are illustrated and could possibly forecast the monthly tourist inflow of one year ahead with acceptable accuracy.

Keywords: *Akaike's information criterion, Box-Jenkins model, Schwartz's Bayesian criterion, variance of white noise*

1. Introduction

Bhutan's tourism industry began in 1974. It was introduced with the primary objective of generating revenue, especially foreign exchange; publicizing the country's unique culture and traditions to the outside world, and to contribute to the country's socio-economic development. Bhutan has now increasingly become a popular destination for many international tourists (Dorji, 2014). The number of tourist inflow in the country is increasing year by year. So forecasting is

very necessary for administration and tourist agent for creating awareness and planning for the future development (Honey & Gilpin, 2009). It can also predict the future trends as accurately as possible and helps in staying one step ahead of the competition (Singha, 2012).

In spite of the great importance of tourism in Bhutan's economy, there is an incomprehensible lack of systematic and up to date quantitative research oriented on analyzing the core determinant and patterns of the visitors from different countries in Bhutan. Therefore it is very important to analyze the determinant and the core pattern tourist inflow in Bhutan. Such a study can be used in formulation of future macroeconomic development strategies, pricing strategies and tourism routing strategies in Bhutan as a one of the most popular destination in the world (Mahmood & Ali, 2016).

Given the importance of the tourism industry to Bhutan it is essential to generate the accurate forecast of the future trends of tourist flows from the major origin countries. This research paper aimed is one-period-ahead forecasts of international tourism demand for Bhutan, and to seek provide the best model for forecasting international tourist arrivals to Bhutan for these periods using Box Jenkins Methods with non-seasonal and seasonal modification.The advantages ofBox Jenkins Methodology involve selecting a great quantum of information from the analyzed empirical time series, using a small number of parameters (Nanthakumar & Ibrahim, 2010).

2. Data and methodology

2.1 Data

For the study, we used the monthly tourist inflow series includes data from top ten market sources that is Malaysia, Singapore, China, America, Australia, USA, France, Thailand, Germany and Japan during 2011-2015 obtained from Tourism Council of Bhutan. (Tourism Council of Bhutan, n.d) The series consist of 60 observations where first 54 sample observations are analyzed by using the Box-Jenkins method and the rest 6 observations out of sample are used to compare the forecast in all the nationalities.

2.2 Methodology

In this study, the Box-Jenkins model is used to analyze tourist inflow series which include data from top ten market sources that is Malaysia, Singapore, China, America, Australia, USA, France, Thailand, Germany, Japan and total tourist visitedduring 2011 – 2015.The Box-Jenkins method consists of following steps. (Singh, 2013).

The first step is to identify the all tentative model. Identification consists of specifying appropriate AR, MA or ARMA and order of the model. The identification is done by looking at the ACF and PACF of the interested stationary series.

The second step is to estimate the parameters of the model. Parameters of models can be estimated by least-square method. The estimation of parameter usually requires more complicated iteration procedure but the computer programming automatically generate it.

The third step is to check the model. This step is also called diagnostic checking or verification. Two important elements in checking are to ensure that the residuals of the model are random and white noise i.e. uncorrelated and constant variance $\hat{\sigma}_a^{\,2}$, and also to make sure that the estimated parameters are strictly significant (Newbold, 2013).

The fourth step is to elect the best model from the various ARIMA models which might be suitable for the series. Thus we use Akaike's Information Criteria (AIC) and Schwarz's Bayesian Criterion (SBC) for model selection to find the best model of the monthly tourist inflow in Bhutan.

2.2.1 ARIMA model

If the process is not stationary, we have to take differencing term $(1-B)^d$ in the process. When model ARMA (*p, q)* model on a time series which has been differenced *d* times we call this an ARIMA (*p, d, q*) model [4].Thus the general ARIMA (*p, d, q*) written using backshift operator as:

$$f_p(B)(1-B)^d X_t = q_0 + q_q(B)a_t$$

where $\phi_p(B) = 1-\phi_1 B-\phi_2 B^2 -\cdots-\phi_p B^p$ is the stationary AR operator,

$\theta_q(B) = 1-\theta_1 B-\theta_2 B^2 -\cdots-\theta_q B^q$ is the invertible MA operator

and $\theta_0 = \mu(1-\phi_1-\phi_2-\cdots-\phi_p)$ which is known as deterministic trend term.(Ekpenyong, 2016)

2.2.2 Seasonal ARIMA

The Seasonal ARIMA model includes both seasonal and non-seasonal factors in multiplicative model called ARIMA $(p,d,q)\times(P,Q,D)_s$ where *p* is non-seasonal AR order, d is non-seasonal differencing,*q* is non-seasonal MA order,*P* is seasonal AR order,*D* is seasonal differencing,*Q* is seasonal MA orderand*S* is seasonal periodwhere the general equation of the model is

$$\Phi_P(B^s)\phi_p(B)(1-B)^d(1-B^s)^D X_t = \theta_q(B)\Theta_Q(B)^s a_t$$

(Baldigara & Mumula, 2015) where $\phi_p(B)$ is the non-seasonal autoregression component of order *p*, $\Phi_p(B^s)$ is the seasonal autoregression of order *s*, X_t is the current value of the time series examined, *B* is the backward shift operator $X_t(B^i) = X_{t-i}$, $(1-B)^d$ is non-seasonal difference term, $(1-B^s)^D$ is the seasonal difference term, $\theta_q(B)$ is the non-seasonal moving average of order *q* and $\Theta_Q(B)^s$ is the seasonal moving average of order *Q* (1990, p. 106)

.

2.2.3 Periodogram analysis

To confirm the seasonality, we perform periodogram analysis. Periodogram help us to find the hidden periodicities. If model contains a single periodic component at frequency ω, the periodogram $I(\omega_k)$ at Fourier frequency ω_k closest to ω will be maximum. Thus the maximum periodogram ordinate will be

$$I^{(1)}(\omega_{(1)}) = \max\left\{I(\omega_k)\right\}$$

where $\omega_{(1)}$ is to indicate the maximum periodogram ordinate of the Fourier frequency.

Under the nul1 hypothesis H_0, including a period in a time series, an exact test statistic of $I^{(1)}(\omega_{(1)})$ is known as Fisher's test which is based on the equation below

$$T = \frac{I^{(1)}(\omega_{(1)})}{\sum_{k=1}^{[n\ 2]} I(\omega_k)}.$$

3. Results

The monthly tourist visited from top ten market source during 2011 – 2015 is analyzed by using Box – Jenkins's model. Out of which we will present only one nationality with all the process and rest will be presented with best fit models. The Box-Jenkins model consist of following steps: model identification, parameter estimation, diagnostic checking and model forecasting.

3.1.1 Model identification.

1. To use Box - Jenkins methodology, the series should be stationary. In this study, the graphical methods have been used to check the stationary of the series. In graphical method, graph and correlogram have been used. Figure 1 shows the graph of monthly American tourist visited

during 2011 – 2015. The data set suggests that the series is not stationary in variance. To stabilize the variance, we used Box-Cox transformation (Buthmann, n.d.). The preliminary residual mean square errors are calculated using the power transformation by SAS system software version 9.1 and we need logarithm transformation. Figure 2 shows the graph of monthly logarithm transformed American tourist visited which is stationary in the mean and variance. (Sample ACF and Properties of AR(1) Model. n.d.).

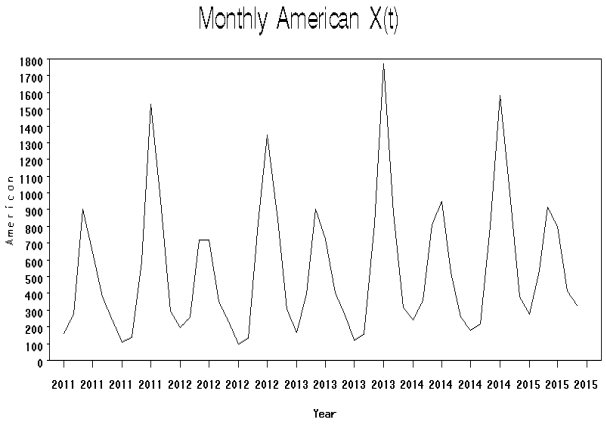

Fig. 1 The monthly American tourist visited during 2011 -2015

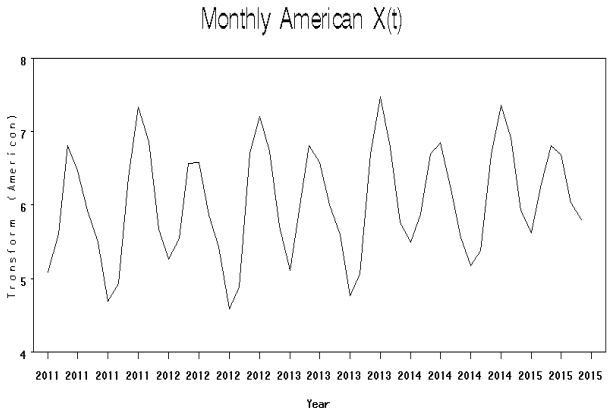

Fig. 2 The monthly logarithm transformed American tourist visited during 2011 -2015

Autocorrelations

Lag	Covariance	Correlation	-1 9 8 7 6 5 4 3 2 1 0 1 2 3 4 5 6 7 8 9 1	Std Error
0	0.561199	1.00000	|********************|	0
1	0.275484	0.49088	|**********. |	0.136083
2	-0.211709	-.37724	| ********. |	0.166660
3	-0.403305	-.71865	|**************. |	0.180870
4	-0.201307	-.35871	| .*******. |	0.227689
5	0.182113	0.32451	| .******. |	0.237924
6	0.369330	0.65811	| .************. |	0.245984
7	0.166376	0.29647	| .******. |	0.276675
8	-0.205447	-.36608	| .********. |	0.282496
9	-0.370559	-.66030	|**************. |	0.291149
10	-0.163669	-.29164	| .******. |	0.317672
11	0.232442	0.41419	| .********. |	0.322593
12	0.422760	0.75332	| .**************. |	0.332295
13	0.196771	0.35063	| .*******. |	0.362543
14	-0.181317	-.32309	| .*******. |	0.368769
15	-0.315143	-.56155	| .**********. |	0.373975
16	-0.144071	-.25672	| .******. |	0.389277
17	0.141215	0.25163	| .*****. |	0.392399
18	0.270134	0.48135	| .**********. |	0.395376
19	0.104389	0.18601	| .*****. |	0.406084
20	-0.169342	-.30175	| .*******. |	0.407658
21	-0.271148	-.48316	| .**********. |	0.411774
22	-0.117488	-.20935	| .*****. |	0.422142
23	0.158044	0.28162	| .******. |	0.424060
24	0.281238	0.50114	| .**********. |	0.427509
25	0.115719	0.20620	| .*****. |	0.438253
26	-0.134712	-.24004	| .******. |	0.440046
27	-0.216128	-.38512	| .********. |	0.442464
28	-0.098576	-.17565	| .*****. |	0.448629
29	0.087099	0.15520	| .***. |	0.449901
30	0.166823	0.29726	| .******. |	0.450891
31	0.055755	0.09936	| .**. |	0.454506
32	-0.119651	-.21321	| .*****. |	0.454908
33	-0.170948	-.30461	| .******. |	0.456754
34	-0.062858	-.11201	| .**. |	0.460501
35	0.083772	0.14927	| .***. |	0.461005
36	0.136559	0.24333	| .*****. |	0.461900
37	0.050700	0.09034	| .**. |	0.464267
38	-0.078288	-.13950	| .***. |	0.464593
39	-0.109674	-.19543	| .*****. |	0.465368
40	-0.038594	-.06877	| .*. |	0.466885
41	0.044261	0.07887	| .**. |	0.467073
42	0.066537	0.11856	| .**. |	0.467319
43	0.014848	0.02646	| .*. |	0.467876
44	-0.050552	-.09008	| .**. |	0.467904
45	-0.060831	-.10839	| .**. |	0.468225

Partial Autocorrelations

Lag	Correlation	-1 9 8 7 6 5 4 3 2 1 0 1 2 3 4 5 6 7 8 9 1
1	0.49088	| . |********** |
2	-0.81447	|**********. | . |
3	0.06720	| . |*. |
4	-0.16551	| . ***. | . |
5	0.40795	| . |******** |
6	-0.11096	| . **. | . |
7	-0.04343	| . *. | . |
8	-0.21393	| .****. | . |
9	-0.08071	| . **. | . |
10	0.11430	| . |**. |
11	0.29950	| . |****** |
12	0.15104	| . |***. |
13	-0.03529	| . *. | . |
14	0.26627	| . |***** |
15	0.11914	| . |**. |
16	-0.16907	| . ***. | . |
17	0.00811	| . | . |
18	-0.17551	| .****. | . |
19	0.04048	| . |*. |
20	-0.00685	| . | . |
21	-0.05333	| . *. | . |
22	-0.09942	| . **. | . |
23	0.04321	| . |*. |
24	-0.10964	| . **. | . |
25	-0.05546	| . *. | . |
26	0.04109	| . |*. |
27	-0.11091	| . **. | . |
28	0.00272	| . | . |
29	-0.05802	| . *. | . |
30	-0.04405	| . *. | . |
31	-0.02622	| . *. | . |
32	0.00633	| . | . |
33	0.03281	| . |*. |
34	0.00397	| . | . |
35	-0.20075	| .****. | . |
36	0.03751	| . |*. |
37	-0.03745	| . *. | . |
38	-0.05589	| . *. | . |
39	0.04150	| . |*. |
40	0.01359	| . | . |
41	-0.04034	| . *. | . |
42	0.02825	| . |*. |
43	0.08096	| . |**. |
44	-0.02458	| . | . |
45	0.03890	| . |*. |

Figure 3 Sample ACF and PACF of monthly logarithm transformation of American tourist visited (Nau, n.d.).

Figure 3 shows sample ACF and PACF with 95% confidence limits. (Adhikari & Agrawal, 2013, pp. 1–3) The ACF shows damp sine cosine wave and slow decaying of the spikes indicates cyclic or seasonal movement of the correlation (Keshvani, 2013). Therefore to confirm the seasonality, we perform periodogram analysis. The periodogram analysis of the logarithm of monthly American tourist visited is clearly dominated by a very large peak at frequency, 1.04720. This frequency corresponds to a period of Pequals 6. It indicates that the data exhibit an approximate of 6 months cycle. So we need first seasonal differencing of period 6 months. Figure 4 shows sample ACF and PACF of monthly logarithm transformation of American tourist visited for first seasonal differencing at period 6 months. The sample ACF shows spike at lag 1, 6 and 12 and PACF cuts off after lag 6. Therefore, the tentative models are ARIMA (1, 0, 0) × (0, 1, 1)6, ARIMA (1, 0, 0) × (0, 1, 2)6, ARIMA (4, 0, 0) × (0, 1, 2)6, ARIMA (5, 0, 0) × (0, 1, 1)6 ,ARIMA (5, 0, 0) × (0, 1, 2)6 ARIMA (0, 0, 1) × (1, 1, 1)6, ARIMA (0, 0, 1) × (1, 1, 0)6 , ARIMA (0, 0, 0) × (1, 1, 0)6 and ARIMA (0, 0, 0) × (0, 1, 1)6..

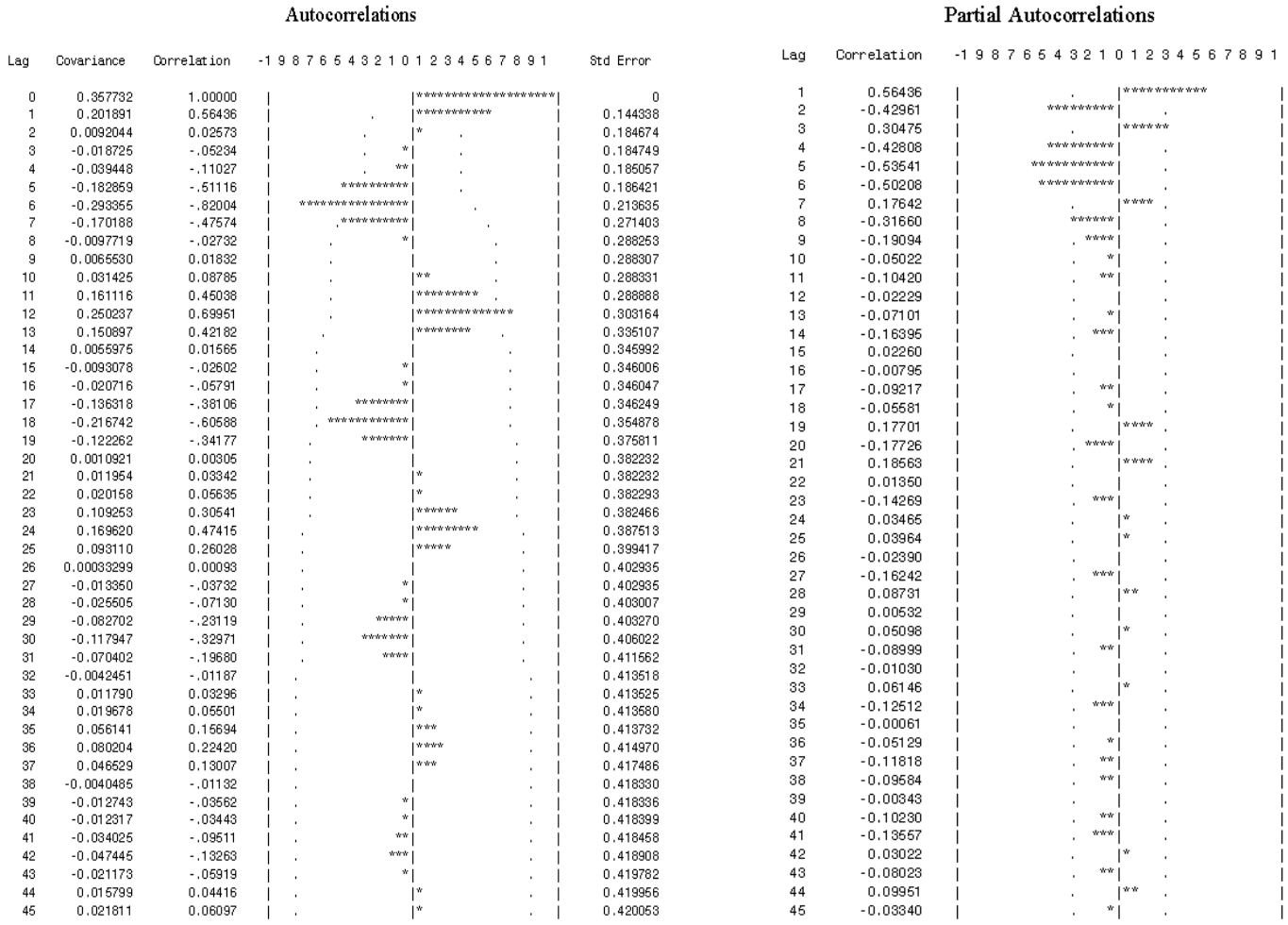

Figure 4 Sample ACF and PACF of monthly logarithm transformation of American tourist visited for first seasonal differencing at period 6 months.

3.1.2 Model estimation and Evaluation

To check model adequacy, we consider whether the residuals of the model are white noise by using a Q statistic test with k = 12. The values of the Q statistic and p-values are given in Table 1. Procedure of choosing the models depends on the value of AIC and SBC (EKPENYONG, 2016). The model with the minimum values is considered as the best model for the data set (Scott, 2019). The models are presented in Table 2. From Table 2 the least AIC and SBC is ARIMA (0, 0, 1) × (1, 1, 0)6 that indicates the ARIMA (0, 0, 1) × (1, 1, 0)6 is the best model for forecasting the monthly American tourist visited during 2011 – 2015. (Yong & Brook, 2014).

Table 1 The Q statistic test for k=12 of the tentative models for monthly American tourist visited.

Model	Q statistic	p-value
1. ARIMA (1, 0, 0) × $(0, 1, 1)_6$	40.23	<.0001
2. ARIMA (1, 0, 0) × $(0, 1, 2)_6$	31.25	0.0005
3. ARIMA (4, 0, 0) × $(0, 1, 2)_6$	25.47	0.0006
4. ARIMA (5, 0, 0) × $(0, 1, 1)_6$	47.51	<.0001
5. ARIMA (5, 0, 0) × $(0, 1, 2)_6$	31.26	0.0005
6. ARIMA (0, 0, 1) × $(1, 1, 1)_6$	**12.51**	**0.1862**
7. ARIMA (0, 0, 1) × $(1, 1, 0)_6$	**9.7**	**0.4676**
8. ARIMA (0, 0, 0) × $(1, 1, 0)_6$	**14.77**	**0.1934**
9. ARIMA (0, 0, 0) × $(0, 1, 1)_6$	50.71	<.0001

Table 2 The summary of AIC and SBC for American visited.

Model	AIC	SBC
6. ARIMA (0, 0, 1) × $(1, 1, 1)_6$	7.997593	13.6112
7. ARIMA (0, 0, 1) × $(1, 1, 0)_6$	**7.056717**	**10.79912**
8. ARIMA (0, 0, 0) × $(1, 1, 0)_6$	20.17794	22.04914

3.1.3 Diagnostic checking

In time series modeling the selection of best fit model is directly related to how well the residual analysis is performed. One of the assumptions of ARIMA model is that for a good model the residual should be white noise (Pelgrin, 2011).

Form the Figure 5 the sample ACF and PACF of the model shows that the autocorrelation of the residual are all close to zero which mean they are uncorrelated, hence the residual assume mean of zero and constant variance. Finally the p-value (0.4676) for the Ljung-Box statistic clearly exceeds 5% for all lag orders. Thus the selected model ARIMA (0, 0, 1) × $(1, 1, 0)_6$ satisfies all the model assumptions.

Table 3 Parameter estimation of appropriate ARIMA (0, 0, 1) × $(1, 1, 0)_6$

Model	MA1	SAR1
Parameter	0.87445	0.7458
SE	0.09300	0.10328

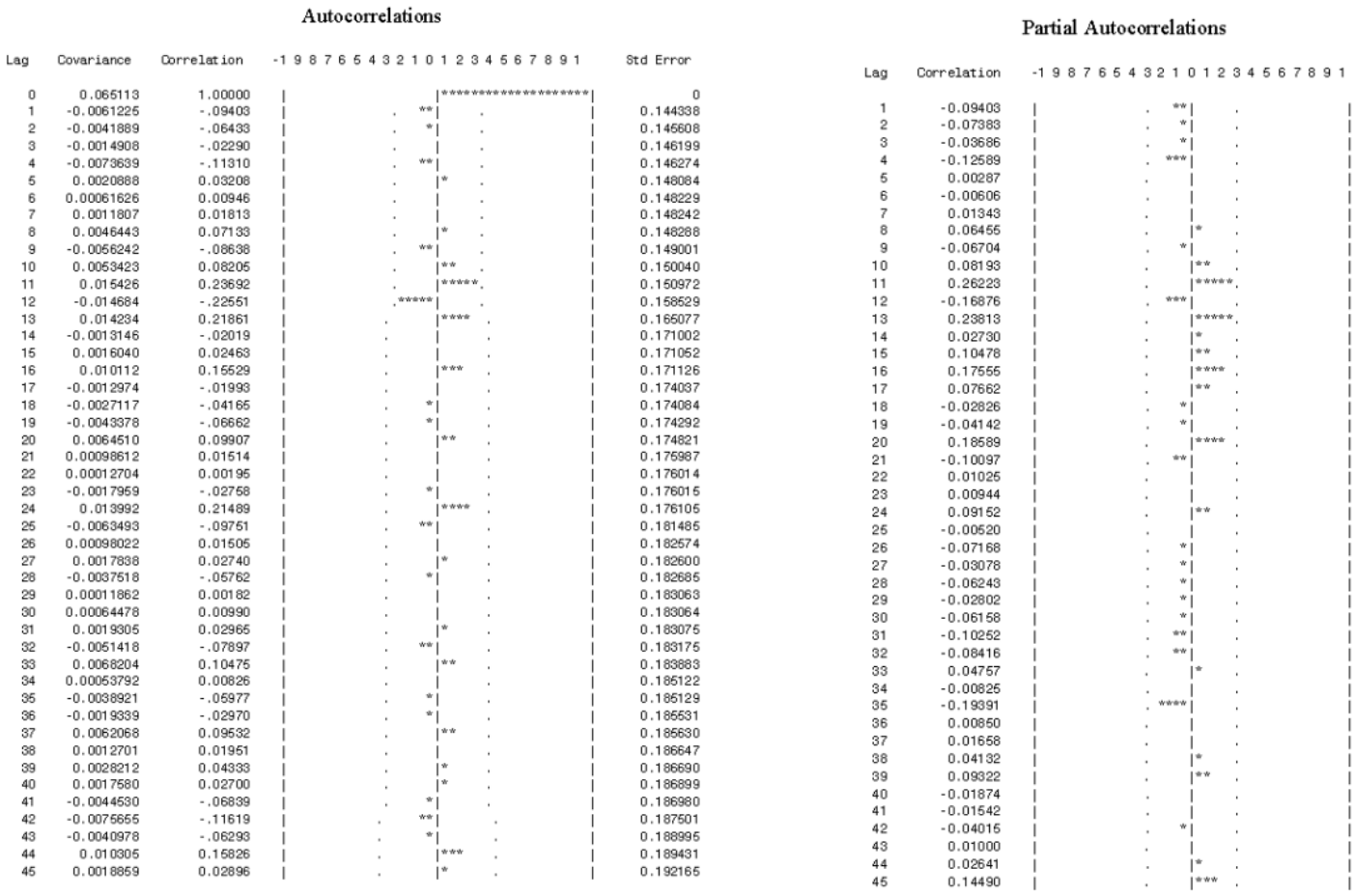

Autocorrelations

Lag	Covariance	Correlation	Std Error
0	0.065113	1.00000	0
1	-0.0061225	-.09403	0.144338
2	-0.0041889	-.06433	0.145608
3	-0.0014908	-.02290	0.146199
4	-0.0073639	-.11310	0.146274
5	0.0020888	0.03208	0.148084
6	0.00061626	0.00946	0.148229
7	0.0011807	0.01813	0.148242
8	0.0046443	0.07133	0.148288
9	-0.0056242	-.08638	0.149001
10	0.0053423	0.08205	0.150040
11	0.015426	0.23692	0.150972
12	-0.014684	-.22551	0.158529
13	0.014234	0.21861	0.165077
14	-0.0013146	-.02019	0.171002
15	0.0016040	0.02463	0.171052
16	0.010112	0.15529	0.171126
17	-0.0012974	-.01993	0.174037
18	-0.0027117	-.04165	0.174084
19	-0.0043378	-.06662	0.174292
20	0.0064510	0.09907	0.174821
21	0.00098612	0.01514	0.175987
22	0.00012704	0.00195	0.176014
23	-0.0017959	-.02758	0.176015
24	0.013992	0.21489	0.176105
25	-0.0063493	-.09751	0.181485
26	0.00098022	0.01505	0.182574
27	0.0017838	0.02740	0.182600
28	-0.0037518	-.05762	0.182685
29	0.00011862	0.00182	0.183063
30	0.00064478	0.00990	0.183064
31	0.0019305	0.02965	0.183075
32	-0.0051418	-.07897	0.183175
33	0.0068204	0.10475	0.183883
34	0.00053792	0.00826	0.185122
35	-0.0038921	-.05977	0.185129
36	-0.0019339	-.02970	0.185531
37	0.0062068	0.09532	0.185630
38	0.0012701	0.01951	0.186647
39	0.0028212	0.04333	0.186690
40	0.0017580	0.02700	0.186899
41	-0.0044530	-.06839	0.186980
42	-0.0075655	-.11619	0.187501
43	-0.0040978	-.06293	0.188995
44	0.010305	0.15826	0.189431
45	0.0018859	0.02896	0.192165

Partial Autocorrelations

Lag	Correlation
1	-0.09403
2	-0.07383
3	-0.03686
4	-0.12589
5	0.00287
6	-0.00606
7	0.01343
8	0.06455
9	-0.06704
10	0.08193
11	0.26223
12	-0.16876
13	0.23813
14	0.02730
15	0.10478
16	0.17555
17	0.07662
18	-0.02826
19	-0.04142
20	0.18589
21	-0.10097
22	0.01025
23	0.00944
24	0.09152
25	-0.00520
26	-0.07168
27	-0.03078
28	-0.06243
29	-0.02802
30	-0.06158
31	-0.10252
32	-0.08416
33	0.04757
34	-0.00825
35	-0.19391
36	0.00850
37	0.01658
38	0.04132
39	0.09322
40	-0.01874
41	-0.01542
42	-0.04015
43	0.01000
44	0.02641
45	0.14490

Figure 5 Sample ACF and PACF of the residual of ARIMA $(0, 0, 1) \times (1, 1, 0)_6$

3.1.4 Forecasting

The forecast values with 95 percent forecast limit of the ARIMA $(0, 0, 1) \times (1, 1, 0)_6$of model for monthly American tourist are shown in Table 4 with standard error, lower and upper limit (Ekpenyong, 2016).

Table 4 Forecasted value for 6 months American tourist visited for 2015

Date	Tourist visited	Forecasted value	95% confidence limit		Error
			Lower	Upper	
Jul-15	131	244.6	148.4	403.4	-113.6
Aug-15	198	242.0	129.8	451.4	-44
Sep-15	681	813.3	436.1	1386.2	-132.3
Oct-15	1514	1449.4	777.1	2702.9	65.6
Nov-15	1020	897.3	481.2	1673.4	122.7
De-15	323	371.6	199.3	693.0	-48.6

3.2 The best fitted model for each nationality

By considering all the steps in Box-Jenkins methodology the best fit model with t-ratio and variance of white noise forall the nationalities are shown in Table 5.

Table 5 The best fitted model for each nationality

Nationality/model	Parameters estimated $\hat{\sigma}_a^2$
1. American ARIMA (0, 0, 1) × $(1, 1, 0)_6$	$(1+0.87445B^6)\ln X_t = (1+0.74358B)a_t$ 0.065113 (0.09300) (0.10328)
2. British ARIMA (0, 0, 1) × $(1, 1, 2)_6$	$(1+0.99004B^6)\sqrt{X_t} = (1+0.39654B)(1-0.43849B^6)a_t$ 7.374285 (0.07764) (0.12700) (0.14988)
3. Australian ARIMA (0, 0, 0) × $(1, 1, 0)_6$	$(1+0.83277B^6)\ln X_t = a_t$ 0.120644 (0.10493)
4. Singaporean ARIMA (1, 1, 0) × $(1, 1, 0)_6$	$(1+0.54467B)(1+0.31214B^6)\sqrt{X_t} = a_t$ 6.467712 (0.11637) (0.12178)
5. French ARIMA (0, 0, 0) × $(1, 1, 0)_6$	$(1+0.94419B^6)\sqrt{X_t} = a_t$ 6.232704 (0.07173)
6. German ARIMA (0, 0, 0) × $(1, 1, 0)_6$	$(1+0.95822B^6)\sqrt{X_t} = a_t$ 19.81132 (0.09604)
7. Chinese ARIMA (4, 1, 0) × (0, 0, 0)	$(1+0.50235B+0.29826B^2+0.81347B^3+0.65127B^4)X_t = a_t$ 24169.85 (0.12606) (0.11889) (0.11812) (0.15240)
8. Thai ARIMA (1, 1, 1) × (0, 0, 0)	$(1+B)\sqrt{X_t} = (1+0.83645B)a_t$ 0.692335 (0.03225) (0.11171)
9. Malaysian ARIMA (5, 1, 1) × (0, 0, 0)	9.524783 $(1+0.23876B+0.80638B^2+0.70042B^3+0.57061B^4+0.43780B^5)\sqrt{X_t} = (1+0.77508B)a_t$ (0.17488) (0.22156) (0.23070) (0.21658) (0.14701)(0.17466)
10. Japanese ARIMA (3, 1, 1) × (0, 0, 0)	$(1+0.38389B^3)X_t = (1-0.52109B)a_t$ 31153.39 (0.13307) (0.11981)
Total ARIMA (0, 0,1) × $(1, 1, 0)_6$	$(1+0.79357B^6)\sqrt{X_t} = 2.24357-(1+0.47057B)a_t$ 68.71606 (0.13374) (0.97511) (0.14447)

4. Conclusion

In this study, a univariate time series models are selected by using the data of the past monthly tourist visited from top ten market sources during 2011 – 2015 obtained from Tourism Council of Bhutan. We applied Box-Jenkins model for forecasting the monthly tourist inflow in Bhutan. The graph, correlogram and periodogram of data show that some of nationalities data sets have seasonality at the period 6. From Table 5 we see that the best model for each nationality is divided into 2 groups. In the first group the model is ARIMA model which consist of Chinese - ARIMA (4 ,1, 0) × (0, 0, 0), Thai - ARIMA (1, 1, 1) × (0, 0, 0), Malaysian - ARIMA (5, 1, 1) × (0, 0, 0) and Japanese - ARIMA (3, 1, 0) × (0, 0, 0) and in the second group it is seasonal ARIMA model which consist of Australian-ARIMA (0, 0, 0) × (1, 1, 0)6, British - ARIMA (0, 0, 1) × $(1, 1, 2)_6$, American- ARIMA (0, 0, 1) × $(1, 1, 0)_6$, Singaporean - ARIMA (0, 1, 1) × $(1, 1, 0)_6$, French - (0, 0, 0) × $(1, 1, 0)_6$, German - ARIMA (0, 0, 0) × $(1, 1, 0)_6$ and overall data - ARIMA (0, 0, 1) × $(1, 1, 0)_6$.Among the visitors, Chinese, Thai, Malaysian and Japanese doesn't show seasonality. [Otieno, Mung'ta & Orwa, 2014).] The main purpose of visitors from these four countries is to experience culture and tradition, and for spiritual and wellness activities which happen throughout the year so the season doesn't hinders the interest of their visit. But for American, Australian, British, Singaporean, French, and Germany shows seasonality as most of them preferred for adventurous tourism. The spring and autumn weather is basically warm and less rainfallwhich makes it favorable for the visitors those who are interested in (Tourism council of Bhutan, n.d.).

5. Acknowledgements

We would like to thank Thai International Cooperation Agency (TICA) for providing the financial support. We also would like to thank Tourism Council of Bhutan (TCB) for providing us latest available data.

References

1. Adhikari, R., & Agrawal, K. R. (2013). *an introductory study on time series modelling and forecasting* (Dragos magu ed.). LAP lambert Acadamic. https://doi.org/10.13140/2.1.2771.8084

2. Baldigara, T., Mumula, M. (2015). Modelling international tourism demand using seasonal ARIMA models. Tourism and Hospitality management (21), 13 pages. https://papers.ssrn.com/sol3/papers.cfm?abstract_id=2624593

3. Buthmann, A. (n.d.). Making Data Normal Using Box-Cox Power Transformation. http://www.isixsigma.com/tools-templates/normality/making-data-normal-Using-box-cox-power-transformation/

4. Dorji, T.(2014, june,21). 2015 is the visit Bhutan year. The Bhutanese

5. Ekpenyong, B. O. (2016). Arma Type Modeling of Certain Non-stationary Time Series in Calabar. *American Journal of Applied Mathematics and Statistics.* 4(4), 118-125. doi: 10.12691/ajams-4-4-4

6. Honey, M. & Gilpin, R. (2009, October 19). Tourism in the Developing World Promoting Peace and Reducing Poverty. *United states institute of peace*, special report. 1200 17th Street NW Washington, DC

7. Keshvani, A. (2013) USING AIC TO TEST ARIMA MODELS. http://coolstatsblog.com/2013/08/14/using-aic-to-test-arima-models-2/

8. Mahmood, Tahir & Ali, Asad. (2016). Forecasting of Daily Gold Price by Using Box-Jenkins Methodology. International Journal of Asian Social Science. 6. 614-624. 10.18488/journal.1/2016.6.11/1.11.614.624.

9. Nanthakumar, L & Ibrahim, Y. (2010). Forecasting international tourism demand in Malaysia using Box –Jenkins's Sarima application. *University Malaysia Terengganus, Malaysia Terengganus,* 3(2).

10. Nau, R. (n.d.). Identifying the numbers of AR or MA terms in an ARIMA model. Fuqua school of Business. Duke University. https://people.duke.edu/~rnau/411arim3.htm

11. Newbold, P. (2013). The Principles of the Box-Jenkins Approach Author(s): Palgrave Macmillan Journals on behalf of the Operational Research Society. https://doi.org/10.1057/jors.1975.88

12. Otieno, G., Mung'ta, J & Orwa George (2014). Time series modeling of tourist accommodation demand in Kenya. 4(10). Mathematical theory and modeling: Research gate.

13. Pelgrin, F. (2011). Box-Jenkins methodology. University of Lausanne, E´cole des HEC Department of mathematics (IMEA-Nice)

14. Sample ACF and Properties of AR(1) Model. (n.d.).

https://online.stat.psu.edu/stat510/lesson/3

15. Scott, G. (2019, june 27) Box-Jenkins model. Investopedia.

https://www.investopedia.com/terms/b/box-jenkins-

16. Singh, H. E. (2013). Forecasting tourist inflow in Bhutan using seasonal ARIMA model. 2(9).

http://citeseerx.ist.psu.edu/viewdoc/download?doi=10.1.1.680.1663&rep=rep1&type=pdf

17. Singha K. (2012). Nexus between Tourism and environment in Bhutan. ;1(1):1-9

18. Tourism Council of Bhutan. *(1).* Annual reports. *https://www.tourism.gov.bt/resources/annual-reports*

19. W.W.W.S. (1990). Time series analysis. In *Time series analysis* (Addison-Wesley, ed., pp. 106). Addison-Wesley, USA.

20. Yong Z, & Brook R. (2014). Modeling and forecasting International Arrivals from China to Australia.

https://doi.org/10.1007/978-3-642-55122-2_85

INJECTIVE EDGE COLORING OF CUBIC GRAPHS

J. Naveen

Department of Mathematics
Government Arts College, Chidambaram, Tamil Nadu, India.
Email. naveenj.maths@gmail.com

Abstract

Three edges e_1, e_2 and e_3 in a graph G are consecutive if they form a cycle of length 3 or a path in this order. A k-injective edge-coloring of a graph G is an edge-coloring of G, (not necessarily proper), such that if edges e_1, e_2, e_3 are consecutive, then e_1 and e_3 receive distinct colors. The minimum k for which G has a k-injective edge-coloring is called the injective edge-coloring number, denoted by $\chi_i'(G)$. In this paper, injective edge-coloring numbers of H- graph and generalized H-graph are determined.

Keywords: *Edge-coloring; k-injective edge-coloring; injective edge-coloring number; H-graph and generalized H-graph.*

1. Introduction

The terminology and notations we refer to Bondy and Murthy [2]. Let G be a finite, simple, undirected and connected graph. Let $\Delta(G)$ denote the maximum degree of G. A *proper vertex (edge) coloring* is a mapping from the vertex (edge) set to a finite set of colors, such that adjacent vertices (edges) receive distinct colors. A k-injective coloring of a graph G is a mapping $\psi : V(G) \to \{1,2,\dots,k\}$ such that if two vertices have a common neighbor, then they receive distinct colors. The injective chromatic number of G, denoted by $\chi_i(G)$, is the minimum k for which G has a k-injective coloring. The injective coloring of graphs was originated from the Complexity Theory on Random Access Machines, which was proposed by Hahn et al. [9] and applied to the theory of error correcting codes and the designing of computer networks [1]. Similarly, Cardoso et al. [6] introduced the concept of injective edge-coloring, motivated by a Packet Radio Network problem. Three edges e_1, e_2 and e_3 in a graph G are consecutive if they form a cycle of length 3 or a path in this order. A k-injective edge-coloring of a graph G is a mapping $\psi : E(G) \to \{1,2,\dots,k\}$, such that if e_1, e_2, e_3 are consecutive, then $\psi(e_1) \neq \psi(e_3)$. If there is a k-injective edge-coloring of G, then we say that G is k-injective edge-colored. The minimum k for which G has a k-injective edge-coloring is called the injective edge-coloring number of G, denoted by

$\chi_i'(G)$. Cardoso et al. [6] showed that it is NP-complete to decide whether $\chi_i'(G) = k$. They determined the injective edge-coloring numbers for paths, cycles, complete bipartite graphs, and Petersen graph and they also gave bounds on some other classes of graphs.

Proposition 1.1. [6]

Let $P_n(C_n)$ be a path (cycle) of order n, $K_{p,q}$ be a complete bipartite graph, and P be the Petersen graph. Then

1. $\chi_i'(P_n) = 2$, for $n \geq 4$.
2. $\chi_i'(C_n) = \begin{cases} 2 & if\ n \equiv 0\ (mod\ 4) \\ 3 & otherwise \end{cases}$
3. $\chi_i'(K_{p,q}) = \min\{p, q\}$.
4. $\chi_i'(P) = 5$.

A graph G is an ω' edge injective colorable (*perfect EIC*-) graph if $\chi_i'(G) = \omega'(G)$, where $\omega'(G)$ is the number of edges in a maximum clique of G. In [11], Yue et al. constructed some perfect EIC-graphs, and gave a sharp bound of the injective edge-coloring number of a 2-connected graph with some forbidden conditions. Bu and Qi [5] and Ferdjallah [8] studied the injective edge coloring of sparse graphs in terms of the maximum average degree. Kostochka [10] studied the injective edge-coloring in terms of the maximum degree. Recently, in [3,4], Bu et al. presented some results on the injective edge-coloring numbers of planar graphs. In this paper, we will consider the injective edge-coloring of H-graph and generalized H-graphs.

1. Injective edge-coloring of H- graph.

In this section, injective edge-coloring number of H-graph will be discussed.

[7] The H-graph $H(r), r \geq 2$, is the 3-regular graph of order $6r$, with vertex set

$$V(H(r)) = \{u_i, v_i, w_i \,/\, 0 \leq i \leq 2r-1\}$$

and edge set (subscripts are taken modulo $2r$)

$$E\big(H(r)\big) = \{(u_i, u_{i+1}), (w_i, w_{i+1}), (u_i, v_i), (v_i, w_i)/0 \leq i \leq 2r-1\}$$

$$\cup \{(v_{2i}, v_{2i+1})/0 \leq i \leq r-1\}$$

Theorem 1.1. If $r \geq 2$, Then $3 \leq \chi_i^{'}(H(r)) \leq 4$,

Proof.

We consider two cases.

Case 1. If r is even, $r \geq 2$.

We define $\psi : E(H(r)) \rightarrow \{1,2,3\}$ as follows:

$$\psi(u_0u_1) = 1 = \psi(u_0u_{2r-1})$$

$$\text{For } i \in \{1,2,\dots,2r-2\},\ \psi(u_iu_{i+1}) = \begin{cases} 2 & if\ i \equiv 1,2\ mod\ 4 \\ 1 & if\ i \equiv 3,0\ mod\ 4 \end{cases}$$

$$\text{For } i \in \{0,1,2,\dots,r-1\},\ \psi(u_{2i}u_{2i+1}) = 3,$$

$$\text{For } i \in \{0,1,2,\dots,2r-1\}, \psi(u_iv_i) = \begin{cases} 1 & if\ i \equiv 0\ mod\ 4 \\ 3 & if\ i \equiv 1,3\ mod\ 4 \\ 2 & if\ i \equiv 2\ mod\ 4 \end{cases}$$

$$\text{For } i \in \{0,1,2,\dots,2r-1\}, \psi(v_iw_i) = \begin{cases} 2 & if\ i \equiv 0\ mod\ 4 \\ 3 & if\ i \equiv 1,3\ mod\ 4 \\ 1 & if\ i \equiv 2\ mod\ 4 \end{cases}$$

$$\psi(w_0w_1) = 2 = \psi(w_0w_{2r-1}),$$

$$\text{For } i \in \{1,2,\dots,2r-2\},\ \psi(w_iw_{i+1}) = \begin{cases} 1 & if\ i \equiv 1,2\ mod\ 4 \\ 2 & if\ i \equiv 3,0\ mod\ 4 \end{cases}$$

It is easy to check that ψ is injective edge-coloring of $H(r)$. Hence, $\chi_i'(H(r)) = 3$.

Case 2. If r is odd, $r \geq 3$.

We define $\psi : E(H(r)) \rightarrow \{1,2,3,4\}$ as follows:

$$\psi(u_0u_1) = 1 = \psi(u_0u_{2r-1})$$

$$\text{For } i \in \{1,2,\dots,2r-4\},\ \psi(u_iu_{i+1}) = \begin{cases} 2 & if\ i \equiv 1,2\ mod\ 4 \\ 1 & if\ i \equiv 3,0\ mod\ 4 \end{cases}$$

$$\psi(u_iu_{i+1}) = 4,\ if\ i = 2r-3, 2r-2,$$

$$\text{For } i \in \{0,1,2,\dots,r-1\},\ \psi(u_{2i}u_{2i+1}) = 3,$$

For $i \in \{0,1,2,\dots,2r-3\}$, $\psi(u_i v_i) = \begin{cases} 1 & if\ i \equiv 0\ mod\ 4 \\ 3 & if\ i \equiv 1,3\ mod\ 4 \\ 2 & if\ i \equiv 2\ mod\ 4 \end{cases}$

$\psi(u_i v_i) = \begin{cases} 4 & if\ i = 2r-2 \\ 3 & if\ i = 2r-1 \end{cases}$

For $i \in \{0,1,2,\dots,2r-5\}$, $\psi(v_i w_i) = \begin{cases} 2 & if\ i \equiv 0\ mod\ 4 \\ 3 & if\ i \equiv 1,3\ mod\ 4 \\ 1 & if\ i \equiv 2\ mod\ 4 \end{cases}$

$\psi(v_i w_i) = \begin{cases} 4 & if\ i = 2r-4 \\ 3 & if\ i = 2r-3, 2r-1 \\ 1 & if\ i = 2r-2 \end{cases}$

$\psi(w_0 w_1) = 2 = \psi(w_0 w_{2r-1})$

For $i \in \{1,2,\dots,2r-6\}$, $\psi(w_i w_{i+1}) = \begin{cases} 1 & if\ i \equiv 1,2\ mod\ 4 \\ 2 & if\ i \equiv 3,0\ mod\ 4 \end{cases}$

$\psi(w_i w_{i+1}) = \begin{cases} 4 & if\ i = 2r-5, 2r-4 \\ 1 & if\ i = 2r-3, 2r-2 \end{cases}$

It is easy to check that ψ is injective edge-coloring of $H(r)$. Hence, $\chi_i'(H(r)) = 4$.

2. Injective edge coloring of Generalized H-graphs.

In this section, we study the injective edge-coloring number of generalized H-graph.

We now consider a natural extension of H-graphs. For every integer $r \geq 2$, the generalised H-graph $H^l(r)$ with l levels, $l \geq 1$, is the 3-regular graph of order $2r(l+2)$, with vertex set

$$V(H^l(r)) = \{u_j^i / 0 \leq i \leq l+1, 0 \leq j \leq 2r-1\}.$$

And edge set (subscripts are taken modulo 2r)

$$E(H^l(r)) = \{(u_j^0 u_{j+1}^0), (u_j^{l+1} u_{j+1}^{l+1}) / 0 \leq j \leq r-1\} \cup \{u_{2j}^i, u_{2j+1}^i / 1 \leq i \leq l, 0 \leq j \leq r-1\}$$

$$\cup \{u_j^i, u_{j+1}^i / 1 \leq i \leq l, 0 \leq j \leq 2r-1\}$$

Theorem 2.1. If $r \geq 3$ *and* $l \geq 2$, then $3 \leq \chi_i'\left(H^l(r)\right) \leq 4$.

Proof.

We consider six cases and in each case, we first define $\psi : E\left(H^l(r)\right) \to \{1,2,3,4\}$ as follows:

$\psi(u_0^0 u_1^0) = 1,$

For $j \in \{1,2,\dots,2r-5\}$, $\psi\left(u_j^0 u_{j+1}^0\right) = \begin{cases} 2 & if\ j \equiv 1,2\ mod\ 4 \\ 1 & if\ j \equiv 3,0\ mod\ 4 \end{cases}$

$\psi(u_0^0 u_{2r-1}^0) = 1,$

For $i \in \{1,2,\dots,l-1\}$ and $j \in \{0,1,2,\dots,r-3\}$

$If\ i \equiv 1\ mod\ 3,\ \psi\left(u_{2j}^i u_{2j+1}^i\right) = 3,\ for\ j \in \{0,1,2,\dots,r-3\}$

$If\ i \equiv 2\ mod\ 3,\ \psi\left(u_{2j}^i u_{2j+1}^i\right) = \begin{cases} 2 & if\ j \in \{0,2,4,\dots,r-4\} \\ 1 & if\ j \in \{1,3,5,\dots,r-3\} \end{cases}$

$If\ i \equiv 0\ mod\ 3,\ \psi\left(u_{2j}^i u_{2j+1}^i\right) = \begin{cases} 1 & if\ j \in \{0,2,4,\dots,r-4\} \\ 2 & if\ j \in \{1,3,5,\dots,r-3\} \end{cases}$

For $j \in \{0,1,2,\dots,2r-5\}$, $\psi\left(u_j^0 u_j^1\right) = \begin{cases} 1 & if\ j \equiv 0\ mod\ 4 \\ 3 & if\ j \equiv 1,3\ mod\ 4 \\ 2 & if\ j \equiv 2\ mod\ 4 \end{cases}$

For $i \in \{1,2,\dots,l-2\}$ and $j \in \{0,1,2,\dots,2r-5\}$

$If\ i \equiv 1\ mod\ 6,\ \psi\left(u_j^i u_j^{i+1}\right) = \begin{cases} 2 & if\ j \equiv 0\ mod\ 4 \\ 3 & if\ j \equiv 1,3\ mod\ 4 \\ 1 & if\ j \equiv 2\ mod\ 4 \end{cases}$

$If\ i \equiv 2\ mod\ 6,\ \psi\left(u_j^i u_j^{i+1}\right) = \begin{cases} 2 & if\ j \equiv 0,3\ mod\ 4 \\ 1 & if\ j \equiv 1,2\ mod\ 4 \end{cases}$

$If\ i \equiv 3\ mod\ 6,\ \psi\left(u_j^i u_j^{i+1}\right) = \begin{cases} 3 & if\ j \equiv 0,2\ mod\ 4 \\ 1 & if\ j \equiv 1\ mod\ 4 \\ 2 & if\ j \equiv 3\ mod\ 4 \end{cases}$

$If\ i \equiv 4\ mod\ 6,\ \psi\left(u_j^i u_j^{i+1}\right) = \begin{cases} 3 & if\ j \equiv 0,2\ mod\ 4 \\ 2 & if\ j \equiv 1\ mod\ 4 \\ 1 & if\ j \equiv 3\ mod\ 4 \end{cases}$

$If\ i \equiv 5\ mod\ 6,\ \psi\left(u_j^i u_j^{i+1}\right) = \begin{cases} 1 & if\ j \equiv 0,3\ mod\ 4 \\ 2 & if\ j \equiv 1,2\ mod\ 4 \end{cases}$

$$If\ i \equiv 0\ mod\ 6,\ \psi\left(u_j^i u_j^{i+1}\right) = \begin{cases} 1 & if\ \ j \equiv 0\ mod\ 4 \\ 3 & if\ \ j \equiv 1,3\ mod\ 4 \\ 2 & if\ \ j \equiv 2\ mod\ 4 \end{cases}$$

Case 1. $If\ l \equiv 3\ mod\ 6$

$$\psi\left(u_{2j}^l u_{2j+1}^l\right) = 4,\ \ for\ j \in \{0,1,2,\dots,r-3\}$$

$$\psi\left(u_0^{l+1} u_1^{l+1}\right) = 1, \psi\left(u_0^{l+1} u_{2r-1}^{l+1}\right) = 1$$

$For\ j \in \{0,1,2,\dots,2r-5\},$

$$\psi\left(u_j^{l-1} u_j^l\right) = \begin{cases} 2 & if\ \ j \equiv 0\ mod\ 4 \\ 4 & if\ \ j \equiv 1,3\ mod\ 4 \\ 1 & if\ \ j \equiv 2\ mod\ 4 \end{cases}$$

$$\psi\left(u_j^l u_j^{l+1}\right) = \begin{cases} 1 & if\ \ j \equiv 0\ mod\ 4 \\ 4 & if\ \ j \equiv 1,3\ mod\ 4 \\ 2 & if\ \ j \equiv 2\ mod\ 4 \end{cases}$$

$$\psi\left(u_j^{l+1} u_{j+1}^{l+1}\right) = \begin{cases} 2 & if\ \ j \equiv 1,2\ mod\ 4 \\ 1 & if\ \ j \equiv 3,0\ mod\ 4 \end{cases}$$

If r is odd

$$\psi\left(u_j^0 u_{j+1}^0\right) = \begin{cases} 2 & if\ \ j = 2r-5, 2r-4 \\ 4 & if\ \ j = 2r-3, 2r-2 \end{cases}$$

$$\psi\left(u_j^0 u_j^1\right) = \begin{cases} 2 & if\ j = 2r-4 \\ 3 & if\ j = 2r-3, 2r-1 \\ 4 & if\ j = 2r-2 \end{cases}$$

$If\ j \in \{r-2,\ r-1\}$ and $i \in \{1,2,\dots,l-1\}$

$$\psi\left(u_{2j}^i u_{2j+1}^i\right) = \begin{cases} 3 & if\ \ i \equiv 1\ mod\ 3 \\ 1 & if\ \ i \equiv 2\ mod\ 3 \\ 2 & if\ \ i \equiv 0\ mod\ 3 \end{cases}$$

$$\psi\left(u_{2j}^l u_{2j+1}^l\right) = 4, if\ j \in \{r-2,\ r-1\}$$

For $i \in \{1,2,\dots,l-2\}$

$$If\ i \equiv 1\ mod\ 6,\ \psi\left(u_j^i u_j^{i+1}\right) = \begin{cases} 1 & if\ \ j = 2r-4, 2r-2 \\ 3 & if\ \ j = 2r-3, 2r-1 \end{cases}$$

$$If\ i \equiv 2\ mod\ 6,\ \ \psi\left(u_j^i u_j^{i+1}\right) = \begin{cases} 1 & if \quad j = 2r-4, 2r-2 \\ 2 & if \quad j = 2r-3, 2r-1 \end{cases}$$

$$If\ i \equiv 3\ mod\ 6,\ \ \psi\left(u_j^i u_j^{i+1}\right) = \begin{cases} 3 & if \quad j = 2r-4, 2r-2 \\ 2 & if \quad j = 2r-3, 2r-1 \end{cases}$$

$$If\ i \equiv 4\ mod\ 6,\ \ \psi\left(u_j^i u_j^{i+1}\right) = \begin{cases} 3 & if \quad j = 2r-4, 2r-2 \\ 1 & if \quad j = 2r-3, 2r-1 \end{cases}$$

$$If\ i \equiv 5\ mod\ 6,\ \ \psi\left(u_j^i u_j^{i+1}\right) = \begin{cases} 2 & if \quad j = 2r-4, 2r-2 \\ 1 & if \quad j = 2r-3, 2r-1 \end{cases}$$

$$If\ i \equiv 0\ mod\ 6,\ \ \psi\left(u_j^i u_j^{i+1}\right) = \begin{cases} 2 & if \quad j = 2r-4, 2r-2 \\ 3 & if \quad j = 2r-3, 2r-1 \end{cases}$$

$$\psi\left(u_j^{l-1} u_j^l\right) = \begin{cases} 1 & if \quad j = 2r-4, 2r-2 \\ 4 & if \quad j = 2r-3, 2r-1 \end{cases}$$

$$\psi\left(u_j^l u_j^{l+1}\right) = \begin{cases} 2 & if\ j = 2r-4 \\ 4 & if\ j = 2r-3, 2r-1 \\ 3 & if\ j = 2r-2 \end{cases}$$

$$\psi\left(u_j^{l+1} u_{j+1}^{l+1}\right) = \begin{cases} 2 & if \quad j = 2r-5, 2r-4 \\ 3 & if \quad j = 2r-3, 2r-2 \end{cases}$$

It is easy to verify that ψ is injective edge-coloring of $H^l(r)$. Hence $\chi_i'\left(H^l(r)\right) = 4$.

If r is even

$$\psi\left(u_j^0 u_{j+1}^0\right) = \begin{cases} 1 & if \quad j = 2r-5, 2r-4 \\ 2 & if \quad j = 2r-3, 2r-2 \end{cases}$$

$$\psi\left(u_j^0 u_j^1\right) = \begin{cases} 1 & if\ j = 2r-4 \\ 3 & if\ j = 2r-3, 2r-1 \\ 2 & if\ j = 2r-2 \end{cases}$$

For $i \in \{1,2, \dots, l-1\}$

$$If\ j = r-2,\ \psi\left(u_{2j}^i u_{2j+1}^i\right) = \begin{cases} 3 & if\ \ i \equiv 1\ mod\ 3 \\ 2 & if\ \ i \equiv 2\ mod\ 3 \\ 1 & if\ \ i \equiv 0\ mod\ 3 \end{cases}$$

$$If\ j = r-1,\ \psi\left(u_{2j}^i u_{2j+1}^i\right) = \begin{cases} 3 & if\ \ i \equiv 1\ mod\ 3 \\ 1 & if\ \ i \equiv 2\ mod\ 3 \\ 2 & if\ \ i \equiv 0\ mod\ 3 \end{cases}$$

$\psi\left(u_{2j}^{l}u_{2j+1}^{l}\right) = 4, if\ j \in \{r-2,\ r-1\}$

For $i \in \{1,2,\dots,l-2\}$

$$If\ i \equiv 1\ mod\ 6,\ \psi\left(u_j^i u_j^{i+1}\right) = \begin{cases} 2 & if\ \ j = 2r-4 \\ 3 & if\ \ j = 2r-3, 2r-1 \\ 1 & if\ \ j = 2r-2 \end{cases}$$

$$If\ i \equiv 2\ mod\ 6,\ \ \psi\left(u_j^i u_j^{i+1}\right) = \begin{cases} 2 & if\ \ j = 2r-4, 2r-1 \\ 1 & if\ \ j = 2r-3, 2r-2 \end{cases}$$

$$If\ i \equiv 3\ mod\ 6,\ \psi\left(u_j^i u_j^{i+1}\right) = \begin{cases} 3 & if\ \ j = 2r-4, 2r-2 \\ 1 & if\ \ j = 2r-3 \\ 2 & if\ \ j = 2r-1 \end{cases}$$

$$If\ i \equiv 4\ mod\ 6,\ \psi\left(u_j^i u_j^{i+1}\right) = \begin{cases} 3 & if\ \ j = 2r-4, 2r-2 \\ 2 & if\ \ j = 2r-3 \\ 1 & if\ \ j = 2r-1 \end{cases}$$

$$If\ i \equiv 5\ mod\ 6,\ \ \psi\left(u_j^i u_j^{i+1}\right) = \begin{cases} 1 & if\ \ j = 2r-4, 2r-1 \\ 2 & if\ \ j = 2r-3, 2r-2 \end{cases}$$

$$If\ i \equiv 0\ mod\ 6,\ \psi\left(u_j^i u_j^{i+1}\right) = \begin{cases} 1 & if\ \ j = 2r-4 \\ 3 & if\ \ j = 2r-3, 2r-1 \\ 2 & if\ \ j = 2r-2 \end{cases}$$

$$\psi\left(u_j^{l-1}u_j^{l}\right) = \begin{cases} 2 & if\ \ j = 2r-4 \\ 4 & if\ \ j = 2r-3, 2r-1 \\ 1 & if\ \ j = 2r-2 \end{cases}$$

$$\psi\left(u_j^{l}u_j^{l+1}\right) = \begin{cases} 1 & if\ \ j = 2r-4 \\ 4 & if\ \ j = 2r-3, 2r-1 \\ 2 & if\ \ j = 2r-2 \end{cases}$$

$$\psi\left(u_j^{l+1}u_{j+1}^{l+1}\right) = \begin{cases} 1 & if\ \ j = 2r-5, 2r-4 \\ 2 & if\ \ j = 2r-3, 2r-2 \end{cases}$$

It is easy to verify that ψ is injective edge-coloring of $H^l(r)$. Hence, $\chi_i'\left(H^l(r)\right) = 4$.

Case 2. $\boldsymbol{If\ l \equiv 4\ mod\ 6}$

$\psi\left(u_{2j}^{l}u_{2j+1}^{l}\right) = 3,\ \ for\ j \in \{0,1,2,\dots,r-3\}$,

$\psi\left(u_0^{l+1}u_1^{l+1}\right) = 2, \psi\left(u_0^{l+1}u_{2r-1}^{l+1}\right) = 1$,

$For\ j \in \{0,1,2,\dots,2r-5\}$,

$$\psi\left(u_j^{l+1}u_{j+1}^{l+1}\right) = \begin{cases} 2 & if\ \ j \equiv 1,0\ mod\ 4 \\ 1 & if\ \ j \equiv 2,3\ mod\ 4 \end{cases}$$

$$\psi\left(u_j^{l-1}u_j^{l}\right) = \begin{cases} 3 & if\ \ j \equiv 0,2\ mod\ 4 \\ 1 & if\ \ j \equiv 1\ mod\ 4 \\ 2 & if\ \ j \equiv 3\ mod\ 4 \end{cases}$$

$$\psi\left(u_j^{l}u_j^{l+1}\right) = \begin{cases} 3 & if\ \ j \equiv 0,2\ mod\ 4 \\ 2 & if\ \ j \equiv 1\ mod\ 4 \\ 1 & if\ \ j \equiv 3\ mod\ 4 \end{cases}$$

If r is odd

$$\psi\left(u_j^{0}u_{j+1}^{0}\right) = \begin{cases} 2 & if\ \ j = 2r-5, 2r-4 \\ 3 & if\ \ j = 2r-3, 2r-2 \end{cases}$$

$$\psi\left(u_j^{0}u_{j}^{1}\right) = \begin{cases} 2 & if\ j = 2r-4,\ 2r-1 \\ 1 & if\ j = 2r-3 \\ 3 & if\ j = 2r-2 \end{cases}$$

For $i \in \{1,2,\dots,l\}$

$$If\ j = r-2,\ \psi\left(u_{2j}^{i}u_{2j+1}^{i}\right) = \begin{cases} 1 & if\ \ i \equiv 1\ mod\ 3 \\ 3 & if\ \ i \equiv 2\ mod\ 3 \\ 2 & if\ \ i \equiv 0\ mod\ 3 \end{cases}$$

$$If\ j = r-1,\ \psi\left(u_{2j}^{i}u_{2j+1}^{i}\right) = \begin{cases} 2 & if\ \ i \equiv 1\ mod\ 3 \\ 1 & if\ \ i \equiv 2\ mod\ 3 \\ 3 & if\ \ i \equiv 0\ mod\ 3 \end{cases}$$

For $i \in \{1,2,\dots,l\}$

$$If\ i \equiv 1\ mod\ 6,\ \psi\left(u_j^{i}u_j^{i+1}\right) = \begin{cases} 3 & if\ \ j = 2r-4 \\ 1 & if\ \ j = 2r-3, 2r-2 \\ 2 & if\ \ j = 2r-1 \end{cases}$$

$$If\ i \equiv 2\ mod\ 6,\ \psi\left(u_j^{i}u_j^{i+1}\right) = \begin{cases} 3 & if\ j = 2r-4,\ 2r-1 \\ 2 & if\ j = 2r-3 \\ 1 & if\ j = 2r-2 \end{cases}$$

$$If\ i \equiv 3\ mod\ 6,\ \psi\left(u_j^{i}u_j^{i+1}\right) = \begin{cases} 1 & if\ \ j = 2r-4 \\ 2 & if\ \ j = 2r-3, 2r-2 \\ 3 & if\ \ j = 2r-1 \end{cases}$$

$$If\ i \equiv 4\ mod\ 6,\ \psi\left(u_j^i u_j^{i+1}\right) = \begin{cases} 1 & if\ j = 2r-4,\ 2r-1 \\ 3 & if\ j = 2r-3 \\ 2 & if\ j = 2r-2 \end{cases}$$

$$If\ i \equiv 5\ mod\ 6,\ \psi\left(u_j^i u_j^{i+1}\right) = \begin{cases} 2 & if\ j = 2r-4 \\ 3 & if\ j = 2r-3, 2r-2 \\ 1 & if\ j = 2r-1 \end{cases}$$

$$If\ i \equiv 0\ mod\ 6,\ \psi\left(u_j^i u_j^{i+1}\right) = \begin{cases} 2 & if\ j = 2r-4,\ 2r-1 \\ 1 & if\ j = 2r-3 \\ 3 & if\ j = 2r-2 \end{cases}$$

$$\psi\left(u_j^{l+1} u_{j+1}^{l+1}\right) = \begin{cases} 3 & if\ j = 2r-4, 2r-3 \\ 1 & if\ j = 2r-2 \end{cases}$$

It is easy to verify that ψ is injective edge-coloring of $H^l(r)$. Hence $\chi_i'\left(H^l(r)\right) = 3$.

If r is even

$$\psi\left(u_j^0 u_{j+1}^0\right) = \begin{cases} 1 & if\ \ j = 2r-4, 2r-3 \\ 2 & if\ \ j = 2r-2 \end{cases}$$

$$\psi\left(u_j^0 u_j^1\right) = \begin{cases} 1 & if\ j = 2r-4 \\ 3 & if\ j = 2r-3, 2r-1 \\ 2 & if\ j = 2r-2 \end{cases}$$

For $i \in \{1,2, \dots, l\}$

$$If\ j = r-2,\ \psi\left(u_{2j}^i u_{2j+1}^i\right) = \begin{cases} 3 & if\ \ i \equiv 1\ mod\ 3 \\ 2 & if\ \ i \equiv 2\ mod\ 3 \\ 1 & if\ \ i \equiv 0\ mod\ 3 \end{cases}$$

$$If\ j = r-1,\ \psi\left(u_{2j}^i u_{2j+1}^i\right) = \begin{cases} 3 & if\ \ i \equiv 1\ mod\ 3 \\ 1 & if\ \ i \equiv 2\ mod\ 3 \\ 2 & if\ \ i \equiv 0\ mod\ 3 \end{cases}$$

$$If\ i \equiv 1\ mod\ 6,\ \psi\left(u_j^i u_j^{i+1}\right) = \begin{cases} 2 & if\ \ j = 2r-4 \\ 3 & if\ \ j = 2r-3, 2r-1 \\ 1 & if\ \ j = 2r-2 \end{cases}$$

$$If\ i \equiv 2\ mod\ 6,\ \psi\left(u_j^i u_j^{i+1}\right) = \begin{cases} 2 & if\ \ j = 2r-4, 2r-1 \\ 1 & if\ \ j = 2r-3, 2r-2 \end{cases}$$

$$If\ i \equiv 3\ mod\ 6,\ \psi\left(u_j^i u_j^{i+1}\right) = \begin{cases} 3 & if\ \ j = 2r-4, 2r-2 \\ 1 & if\ \ j = 2r-3 \\ 2 & if\ \ j = 2r-1 \end{cases}$$

$$If\ i \equiv 4\ mod\ 6,\ \psi\left(u_j^i u_j^{i+1}\right) = \begin{cases} 3 & if\ \ j = 2r-4, 2r-2 \\ 2 & if\ \ j = 2r-3 \\ 1 & if\ \ j = 2r-1 \end{cases}$$

$$If\ i \equiv 5\ mod\ 6,\ \ \psi\left(u_j^i u_j^{i+1}\right) = \begin{cases} 1 & if\ \ j = 2r-4, 2r-1 \\ 2 & if\ \ j = 2r-3, 2r-2 \end{cases}$$

$$If\ i \equiv 0\ mod\ 6,\ \psi\left(u_j^i u_j^{i+1}\right) = \begin{cases} 1 & if\ \ j = 2r-4 \\ 3 & if\ \ j = 2r-3, 2r-1 \\ 2 & if\ \ j = 2r-2 \end{cases}$$

$$\psi\left(u_j^{l+1} u_{j+1}^{l+1}\right) = \begin{cases} 2 & if\ \ j = 2r-4, 2r-3 \\ 1 & if\ \ j = 2r-2 \end{cases}$$

It is easy to verify that ψ is injective edge-coloring of $H^l(r)$. Hence $\chi_i'\left(H^l(r)\right) = 3$.

Case 3. $\boldsymbol{If\ l \equiv 5\ mod\ 6}$

$$\psi\left(u_{2j}^l u_{2j+1}^l\right) = 4,\ \ for\ j \in \{0,1,2, \dots, r-3\},$$

$$\psi\left(u_0^{l+1} u_1^{l+1}\right) = 1,$$

For $j \in \{0,1,2, \dots, 2r-5\}$,

$$\psi\left(u_j^{l+1} u_{j+1}^{l+1}\right) = \begin{cases} 2 & if\ \ j\ \equiv 1,2\ mod\ 4 \\ 1 & if\ \ j\ \equiv 3,0\ mod\ 4 \end{cases}$$

$$\psi\left(u_j^{l-1} u_j^l\right) = \begin{cases} 3 & if\ \ j\ \in \{0,2,4, \dots, 2r-6\} \\ 4 & if\ \ j\ \in \{1,3,5, \dots, 2r-5\} \end{cases}$$

$$\psi\left(u_j^l u_j^{l+1}\right) = \begin{cases} 1 & if\ \ j\ \equiv 0\ mod\ 4 \\ 4 & if\ \ j\ \equiv 1,3\ mod\ 4 \\ 2 & if\ \ j\ \equiv 2\ mod\ 4 \end{cases}$$

If r is odd

$$\psi\left(u_j^0 u_{j+1}^0\right) = \begin{cases} 2 & if\ \ j = 2r-5, 2r-4 \\ 4 & if\ \ j = 2r-3, 2r-2 \end{cases}$$

$$\psi\left(u_j^0 u_j^1\right) = \begin{cases} 2 & if\ j = 2r-4 \\ 3 & if\ j = 2r-3, 2r-1 \\ 4 & if\ j = 2r-2 \end{cases}$$

$If\ j \in \{r-2,\ r-1\}$ and $i \in \{1,2,\dots,l\}$

$$\psi\left(u_{2j}^i u_{2j+1}^i\right) = \begin{cases} 3 & if\ \ i \equiv 1\ mod\ 3 \\ 1 & if\ \ i \equiv 2\ mod\ 3 \\ 2 & if\ \ i \equiv 0\ mod\ 3 \end{cases}$$

For $i \in \{1,2,\dots,l-1\}$, similar to case $l \equiv 3\ mod\ 6$ and r is odd.

$$\psi\left(u_j^l u_j^{l+1}\right) = \begin{cases} 2 & if\ \ j = 2r-4 \\ 1 & if\ \ j = 2r-3, 2r-1 \\ 4 & if\ \ j = 2r-2 \end{cases}$$

$$\psi\left(u_j^{l+1} u_{j+1}^{l+1}\right) = \begin{cases} 2 & if\ \ \ j = 2r-5, 2r-4 \\ 4 & if\ \ \ j = 2r-3, 2r-2 \end{cases}$$

$$\psi\left(u_0^{l+1} u_{2r-1}^{l+1}\right) = 2.$$

It is easy to verify that ψ is injective edge-coloring of $H^l(r)$. Hence $\chi_i'\left(H^l(r)\right) = 4$.

If r is even

$$\psi\left(u_j^0 u_{j+1}^0\right) = \begin{cases} 1 & if\ \ \ j = 2r-5, 2r-4 \\ 4 & if\ \ \ j = 2r-3, 2r-2 \end{cases}$$

$$\psi\left(u_j^0 u_j^1\right) = \begin{cases} 1 & if\ j = 2r-4 \\ 3 & if\ j = 2r-3, 2r-1 \\ 4 & if\ j = 2r-2 \end{cases}$$

For $i \in \{1,2,\dots,l-1\}$

$$If\ j = r-2,\ \psi\left(u_{2j}^i u_{2j+1}^i\right) = \begin{cases} 3 & if\ \ i \equiv 1\ mod\ 3 \\ 2 & if\ \ i \equiv 2\ mod\ 3 \\ 1 & if\ \ i \equiv 0\ mod\ 3 \end{cases}$$

$$If\ j = r-1,\ \psi\left(u_{2j}^i u_{2j+1}^i\right) = \begin{cases} 3 & if\ \ i \equiv 1\ mod\ 3 \\ 1 & if\ \ i \equiv 2\ mod\ 3 \\ 2 & if\ \ i \equiv 0\ mod\ 3 \end{cases}$$

$$\psi\left(u_{2j}^l u_{2j+1}^l\right) = 4, if\ j \in \{r-2,\ r-1\}$$

For $i \in \{1,2,\dots,l-2\}$, similar to case $l \equiv 3\ mod\ 6$ and r is even.

$$\psi\left(u_j^{l-1}u_j^l\right)=\begin{cases}3 & if \quad j=2r-4,2r-2\\ 4 & if \quad j=2r-3,2r-1\end{cases}$$

$$\psi\left(u_j^l u_j^{l+1}\right)=\begin{cases}1 & if \quad j=2r-4\\ 4 & if \quad j=2r-3,2r-1\\ 2 & if \quad j=2r-2\end{cases}$$

$$\psi\left(u_j^{l+1}u_{j+1}^{l+1}\right)=\begin{cases}1 & if \quad j=2r-5,2r-4\\ 2 & if \quad j=2r-3,2r-2\end{cases}$$

$$\psi\left(u_0^{l+1}u_{2r-1}^{l+1}\right)=1$$

It is easy to verify that ψ is injective edge-coloring of $H^l(r)$. Hence $\chi_i'\left(H^l(r)\right)=4$.

Case 4. $\boldsymbol{If\ l\equiv 1\ mod\ 6}$ **and** $\boldsymbol{l\neq 1}$

$\psi\left(u_{2j}^l u_{2j+1}^l\right)=3,\ \ for\ j\in\{0,1,2,\dots,r-3\}$,

$\psi\left(u_0^{l+1}u_1^{l+1}\right)=2,\ \psi\left(u_0^{l+1}u_{2r-1}^{l+1}\right)=2$,

For $j\in\{0,1,2,\dots,2r-5\}$,

$$\psi\left(u_j^{l+1}u_{j+1}^{l+1}\right)=\begin{cases}1 & if\ \ j\ \equiv 1,2\ mod\ 4\\ 2 & if\ \ j\ \equiv 3,0\ mod\ 4\end{cases}$$

$$\psi\left(u_j^{l-1}u_j^l\right)=\begin{cases}1 & if\ \ j\ \equiv 0\ mod\ 4\\ 3 & if\ \ j\ \equiv 1,3\ mod\ 4\\ 2 & if\ \ j\ \equiv 2\ mod\ 4\end{cases}$$

$$\psi\left(u_j^l u_j^{l+1}\right)=\begin{cases}2 & if\ \ j\ \equiv 0\ mod\ 4\\ 3 & if\ \ j\ \equiv 1,3\ mod\ 4\\ 1 & if\ \ j\ \equiv 2\ mod\ 4\end{cases}$$

If r is odd

For $i\in\{1,2,\dots,l-2\}$, similar to case $l\equiv 3\ mod\ 6$ and r is odd.

$$\psi\left(u_j^{l-1}u_j^l\right)=\begin{cases}2 & if\ j=2r-4,2r-2\\ 3 & if\ j=2r-3\\ 4 & if\ j=2r-1\end{cases}$$

$$\psi\left(u_j^l u_j^{l+1}\right)=\begin{cases}4 & if\ j=2r-4,2r-1\\ 3 & if\ j=2r-3\\ 1 & if\ j=2r-2\end{cases}$$

$$\psi\left(u_j^{l+1}u_{j+1}^{l+1}\right)=\begin{cases}4 & if \quad j=2r-5,2r-4\\ 1 & if \quad j=2r-3,2r-2\end{cases}$$

It is easy to verify that ψ is injective edge-coloring of $H^l(r)$. Hence $\chi_i'\left(H^l(r)\right)=4$.

If r is even

$$\psi\left(u_j^0u_{j+1}^0\right)=\begin{cases}1 & if \quad j=2r-5,2r-4\\ 2 & if \quad j=2r-3,2r-2\end{cases}$$

$$\psi\left(u_j^0u_j^1\right)=\begin{cases}1 & if\ j=2r-4\\ 3 & if\ j=2r-3,2r-1\\ 2 & if\ j=2r-2\end{cases}$$

For $i\in\{1,2,\dots,l\}$

$$If\ j=r-2,\ \psi\left(u_{2j}^iu_{2j+1}^i\right)=\begin{cases}3 & if \quad i\equiv 1\ mod\ 3\\ 2 & if \quad i\equiv 2\ mod\ 3\\ 1 & if \quad i\equiv 0\ mod\ 3\end{cases}$$

$$If\ j=r-1,\ \psi\left(u_{2j}^iu_{2j+1}^i\right)=\begin{cases}3 & if \quad i\equiv 1\ mod\ 3\\ 1 & if \quad i\equiv 2\ mod\ 3\\ 2 & if \quad i\equiv 0\ mod\ 3\end{cases}$$

For $i\in\{1,2,\dots,l\}$

$$If\ i\equiv 1\ mod\ 6,\ \psi\left(u_j^iu_j^{i+1}\right)=\begin{cases}2 & if \quad j=2r-4\\ 3 & if \quad j=2r-3,2r-1\\ 1 & if \quad j=2r-2\end{cases}$$

$$If\ i\equiv 2\ mod\ 6,\ \psi\left(u_j^iu_j^{i+1}\right)=\begin{cases}2 & if \quad j=2r-4,2r-1\\ 1 & if \quad j=2r-3,2r-2\end{cases}$$

$$If\ i\equiv 3\ mod\ 6,\ \psi\left(u_j^iu_j^{i+1}\right)=\begin{cases}3 & if \quad j=2r-4,2r-2\\ 1 & if \quad j=2r-3\\ 2 & if \quad j=2r-1\end{cases}$$

$$If\ i\equiv 4\ mod\ 6,\ \psi\left(u_j^iu_j^{i+1}\right)=\begin{cases}3 & if \quad j=2r-4,2r-2\\ 2 & if \quad j=2r-3\\ 1 & if \quad j=2r-1\end{cases}$$

$$If\ i\equiv 5\ mod\ 6,\ \psi\left(u_j^iu_j^{i+1}\right)=\begin{cases}1 & if \quad j=2r-4,2r-1\\ 2 & if \quad j=2r-3,2r-2\end{cases}$$

$$If\ i \equiv 0\ mod\ 6,\ \psi\left(u_j^i u_j^{i+1}\right) = \begin{cases} 1 & if\ \ j = 2r-4 \\ 3 & if\ \ j = 2r-3, 2r-1 \\ 2 & if\ \ j = 2r-2 \end{cases}$$

$$\psi\left(u_j^{l+1} u_{j+1}^{l+1}\right) = \begin{cases} 2 & if\ \ j = 2r-5, 2r-4 \\ 1 & if\ \ j = 2r-3, 2r-2 \end{cases}$$

It is easy to verify that ψ is injective edge-coloring of $H^l(r)$. Hence $\chi_i'\left(H^l(r)\right) = 3$.

If $l \equiv 2\ mod\ 6$ and $l \equiv 0\ mod\ 6$

$$\psi(u_0^0 u_1^0) = 1, \text{For } j \in \{1,2,\dots,2r-5\}, \psi\left(u_j^0 u_{j+1}^0\right) = \begin{cases} 2 & if\ \ j \equiv 1,2\ mod\ 4 \\ 3 & if\ \ j \equiv 3,4\ mod\ 4 \\ 1 & if\ \ j \equiv 5,0\ mod\ 4 \end{cases}$$

$$\psi(u_0^0 u_{2r-1}^0) = 1,$$

For $i \in \{1,2,\dots,l\}$ and $j \in \{0,1,2,\dots,r-3\}$

$$If\ \ i \equiv 1\ mod\ 3,\ \psi\left(u_{2j}^i u_{2j+1}^i\right) = \begin{cases} 3 & if\ \ j \equiv 0\ mod\ 3 \\ 1 & if\ \ j \equiv 1\ mod\ 3 \\ 2 & if\ \ j \equiv 2\ mod\ 3 \end{cases}$$

$$If\ i \equiv 2\ mod\ 3,\ \ \psi\left(u_{2j}^i u_{2j+1}^i\right) = \begin{cases} 2 & if\ \ j \equiv 0\ mod\ 3 \\ 3 & if\ \ j \equiv 1\ mod\ 3 \\ 1 & if\ \ j \equiv 2\ mod\ 3 \end{cases}$$

$$If\ i \equiv 0\ mod\ 3,\ \ \psi\left(u_{2j}^i u_{2j+1}^i\right) = \begin{cases} 1 & if\ \ j \equiv 0\ mod\ 3 \\ 2 & if\ \ j \equiv 1\ mod\ 3 \\ 3 & if\ \ j \equiv 2\ mod\ 3 \end{cases}$$

$$\text{For } j \in \{0,1,2,\dots,2r-5\},\ \psi\left(u_j^0 u_j^1\right) = \begin{cases} 1 & if\ \ j \equiv 0\ mod\ 3 \\ 3 & if\ \ j \equiv 1\ mod\ 3 \\ 2 & if\ \ j \equiv 2\ mod\ 3 \end{cases}$$

For $i \in \{1,2,\dots,l\}$ and $j \in \{0,1,2,\dots,2r-5\}$

$$If\ i \equiv 1\ mod\ 6,\ \psi\left(u_j^i u_j^{i+1}\right) = \begin{cases} 2 & if\ \ j \equiv 0,5\ mod\ 6 \\ 3 & if\ \ j \equiv 1,2\ mod\ 6 \\ 1 & if\ \ j \equiv 3,4\ mod\ 6 \end{cases}$$

$$If\ i \equiv 2\ mod\ 6,\ \ \psi\left(u_j^i u_j^{i+1}\right) = \begin{cases} 2 & if\ \ j \equiv 0,3\ mod\ 6 \\ 1 & if\ \ j \equiv 1,4\ mod\ 6 \\ 3 & if\ \ j \equiv 2,5\ mod\ 6 \end{cases}$$

$$If\ i \equiv 3\ mod\ 6,\ \psi\left(u_j^i u_j^{i+1}\right) = \begin{cases} 3 & if\ \ j \equiv 0,5\ mod\ 6 \\ 1 & if\ \ j \equiv 1,2\ mod\ 6 \\ 2 & if\ \ j \equiv 3,4\ mod\ 6 \end{cases}$$

$$If\ i \equiv 4\ mod\ 6,\ \psi\left(u_j^i u_j^{i+1}\right) = \begin{cases} 3 & if\ \ j \equiv 0,3\ mod\ 6 \\ 2 & if\ \ j \equiv 1,4\ mod\ 6 \\ 1 & if\ \ j \equiv 2,5\ mod\ 6 \end{cases}$$

$$If\ i \equiv 5\ mod\ 6,\ \psi\left(u_j^i u_j^{i+1}\right) = \begin{cases} 1 & if\ \ j \equiv 0,5\ mod\ 6 \\ 2 & if\ \ j \equiv 1,2\ mod\ 6 \\ 3 & if\ \ j \equiv 3,4\ mod\ 6 \end{cases}$$

$$If\ i \equiv 0\ mod\ 6,\ \psi\left(u_j^i u_j^{i+1}\right) = \begin{cases} 1 & if\ \ j \equiv 0,3\ mod\ 6 \\ 3 & if\ \ j \equiv 1,4\ mod\ 6 \\ 2 & if\ \ j \equiv 2,5\ mod\ 6 \end{cases}$$

Case 5. $\boldsymbol{If\ l \equiv 2\ mod\ 6}$

$$\psi\left(u_0^{l+1} u_1^{l+1}\right) = 1,$$

$$For\ j \in \{1,2,\dots,2r-5\},\ \psi\left(u_j^{l+1} u_{j+1}^{l+1}\right) = \begin{cases} 1 & if\ \ j \equiv 1,0\ mod\ 6 \\ 2 & if\ \ j \equiv 2,3\ mod\ 6 \\ 3 & if\ \ j \equiv 4,5\ mod\ 6 \end{cases}$$

Sub Case 5.1. $\boldsymbol{If\ r \equiv 0\ mod\ 3}$

$$\psi\left(u_j^0 u_{j+1}^0\right) = \begin{cases} 2 & if\ \ j = 2r-5, 2r-4 \\ 3 & if\ \ j = 2r-3, 2r-2 \end{cases}$$

$$\psi\left(u_j^0 u_j^1\right) = \begin{cases} 2 & if\ j = 2r-4, 2r-1 \\ 1 & if\ j = 2r-3 \\ 3 & if\ j = 2r-2 \end{cases}$$

For $i \in \{1,2,\dots,l\}$

$$\text{If } j = r-2, \psi\left(u_{2j}^i u_{2j+1}^i\right) = \begin{cases} 1 & if\ \ i \equiv 1\ mod\ 3 \\ 3 & if\ \ i \equiv 2\ mod\ 3 \\ 2 & if\ \ i \equiv 0\ mod\ 3 \end{cases}$$

$$\text{If } j = r-1, \psi\left(u_{2j}^i u_{2j+1}^i\right) = \begin{cases} 2 & if\ \ i \equiv 1\ mod\ 3 \\ 1 & if\ \ i \equiv 2\ mod\ 3 \\ 3 & if\ \ i \equiv 0\ mod\ 3 \end{cases}$$

For $i \in \{0,1,2,\dots,l\}$

$$If\ i \equiv 0\ mod\ 6,\ \psi\left(u_j^i u_j^{i+1}\right) = \begin{cases} 2 & if\ \ j = 2r-4, 2r-1 \\ 1 & if\ \ j = 2r-3 \\ 3 & if\ \ j = 2r-2 \end{cases}$$

$$If\ i \equiv 1\ mod\ 6,\ \psi\left(u_j^i u_j^{i+1}\right) = \begin{cases} 3 & if\ \ j = 2r-4 \\ 1 & if\ \ j = 2r-3, 2r-2 \\ 2 & if\ \ j = 2r-1 \end{cases}$$

$$If\ i \equiv 2\ mod\ 6,\ \ \psi\left(u_j^i u_j^{i+1}\right) = \begin{cases} 3 & if\ \ j = 2r-4, 2r-1 \\ 2 & if\ \ j = 2r-3 \\ 1 & if\ \ j = 2r-1 \end{cases}$$

$$If\ i \equiv 3\ mod\ 6,\ \psi\left(u_j^i u_j^{i+1}\right) = \begin{cases} 1 & if\ \ j = 2r-4 \\ 2 & if\ \ j = 2r-3, 2r-2 \\ 3 & if\ \ j = 2r-1 \end{cases}$$

$$If\ i \equiv 4\ mod\ 6,\ \psi\left(u_j^i u_j^{i+1}\right) = \begin{cases} 1 & if\ \ j = 2r-4, 2r-1 \\ 3 & if\ \ j = 2r-3 \\ 2 & if\ \ j = 2r-2 \end{cases}$$

$$If\ i \equiv 5\ mod\ 6,\ \ \psi\left(u_j^i u_j^{i+1}\right) = \begin{cases} 2 & if\ \ j = 2r-4 \\ 3 & if\ \ j = 2r-3, 2r-2 \\ 1 & if\ \ j = 2r-1 \end{cases}$$

$$\psi\left(u_0^{l+1} u_{2r-1}^{l+1}\right) = 3, \psi\left(u_j^{l+1} u_{j+1}^{l+1}\right) = \begin{cases} 2 & if\ \ j = 2r-4, 2r-3 \\ 3 & if\ \ j = 2r-2 \end{cases}$$

It is easy to verify that ψ is injective edge-coloring of $H^l(r)$. Hence $\chi_i'\left(H^l(r)\right) = 3$.

Sub Case 5.2. $\boldsymbol{If\ r \equiv 1\ mod\ 3}$

$$\psi\left(u_j^0 u_{j+1}^0\right) = \begin{cases} 3 & if\ \ j = 2r-5, 2r-4 \\ 4 & if\ \ j = 2r-3, 2r-2 \end{cases}$$

$$\psi\left(u_j^0 u_j^1\right) = \begin{cases} 3 & if\ j = 2r-4, 2r-1 \\ 2 & if\ j = 2r-3 \\ 4 & if\ j = 2r-2 \end{cases}$$

For $i \in \{1,2, \ldots, l\}$

$$\text{If } j = r-2,\ \psi\left(u_{2j}^i u_{2j+1}^i\right) = \begin{cases} 2 & if\ \ i \equiv 1\ mod\ 3 \\ 1 & if\ \ i \equiv 2\ mod\ 3 \\ 3 & if\ \ i \equiv 0\ mod\ 3 \end{cases}$$

If $j = r-1, \psi\left(u_{2j}^{i}u_{2j+1}^{i}\right) = \begin{cases} 3 & if\ i \equiv 1\ mod\ 3 \\ 2 & if\ i \equiv 2\ mod\ 3 \\ 1 & if\ i \equiv 0\ mod\ 3 \end{cases}$

For $i \in \{1,2,\dots,l-1\}$

$If\ i \equiv 1\ mod\ 6,\ \psi\left(u_j^i u_j^{i+1}\right) = \begin{cases} 1 & if\ j = 2r-4 \\ 2 & if\ j = 2r-3, 2r-2 \\ 3 & if\ j = 2r-1 \end{cases}$

$If\ i \equiv 2\ mod\ 6,\ \psi\left(u_j^i u_j^{i+1}\right) = \begin{cases} 1 & if\ j = 2r-4, 2r-1 \\ 3 & if\ j = 2r-3 \\ 2 & if\ j = 2r-1 \end{cases}$

$If\ i \equiv 3\ mod\ 6,\ \psi\left(u_j^i u_j^{i+1}\right) = \begin{cases} 2 & if\ j = 2r-4 \\ 3 & if\ j = 2r-3, 2r-2 \\ 1 & if\ j = 2r-1 \end{cases}$

$If\ i \equiv 4\ mod\ 6,\ \psi\left(u_j^i u_j^{i+1}\right) = \begin{cases} 2 & if\ j = 2r-4, 2r-1 \\ 1 & if\ j = 2r-3 \\ 3 & if\ j = 2r-2 \end{cases}$

$If\ i \equiv 5\ mod\ 6,\ \psi\left(u_j^i u_j^{i+1}\right) = \begin{cases} 3 & if\ j = 2r-4 \\ 1 & if\ j = 2r-3, 2r-2 \\ 2 & if\ j = 2r-1 \end{cases}$

$If\ i \equiv 0\ mod\ 6,\ \psi\left(u_j^i u_j^{i+1}\right) = \begin{cases} 3 & if\ j = 2r-4, 2r-1 \\ 2 & if\ j = 2r-3 \\ 1 & if\ j = 2r-2 \end{cases}$

$\psi\left(u_0^{l+1}u_{2r-1}^{l+1}\right) = 4,$

$\psi\left(u_j^l u_j^{l+1}\right) = \begin{cases} 1 & if\ j = 2r-4 \\ 3 & if\ j = 2r-3 \\ 2 & if\ j = 2r-2 \\ 4 & if\ j = 2r-1 \end{cases}$

$\psi\left(u_j^{l+1}u_{j+1}^{l+1}\right) = \begin{cases} 2 & if\ j = 2r-5 \\ 3 & if\ j = 2r-4, 2r-3 \\ 4 & if\ j = 2r-2 \end{cases}$

It is easy to verify that ψ is injective edge-coloring of $H^l(r)$. Hence $\chi_i'\left(H^l(r)\right) = 4$.

Sub Case 5.3. $\boldsymbol{If\ r \equiv 2\ mod\ 3}$

$$\psi\left(u_j^0 u_{j+1}^0\right) = \begin{cases} 1 & if \quad j = 2r-5, 2r-4 \\ 4 & if \quad j = 2r-3, 2r-2 \end{cases}$$

$$\psi\left(u_j^0 u_j^1\right) = \begin{cases} 1 & if\ j = 2r-4 \\ 3 & if\ j = 2r-3, 2r-1 \\ 4 & if\ j = 2r-2 \end{cases}$$

For $i \in \{1,2,\dots,l\}$ and $j \in \{r-2, r-1\}$,

$$\psi\left(u_{2j}^i u_{2j+1}^i\right) = \begin{cases} 3 & if \quad i \equiv 1\ mod\ 3 \\ 2 & if \quad i \equiv 2\ mod\ 3 \\ 1 & if \quad i \equiv 0\ mod\ 3 \end{cases}$$

For $i \in \{1,2,\dots,l-1\}$

$$If\ i \equiv 1\ mod\ 6,\ \psi\left(u_j^i u_j^{i+1}\right) = \begin{cases} 2 & if \quad j = 2r-4, 2r-2 \\ 3 & if \quad j = 2r-3, 2r-1 \end{cases}$$

$$If\ i \equiv 2\ mod\ 6,\ \psi\left(u_j^i u_j^{i+1}\right) = \begin{cases} 2 & if \quad j = 2r-4, 2r-2 \\ 1 & if \quad j = 2r-3, 2r-1 \end{cases}$$

$$If\ i \equiv 3\ mod\ 6,\ \psi\left(u_j^i u_j^{i+1}\right) = \begin{cases} 3 & if \quad j = 2r-4, 2r-2 \\ 1 & if \quad j = 2r-3, 2r-1 \end{cases}$$

$$If\ i \equiv 4\ mod\ 6,\ \psi\left(u_j^i u_j^{i+1}\right) = \begin{cases} 3 & if \quad j = 2r-4, 2r-2 \\ 2 & if \quad j = 2r-3, 2r-1 \end{cases}$$

$$If\ i \equiv 5\ mod\ 6,\ \psi\left(u_j^i u_j^{i+1}\right) = \begin{cases} 1 & if \quad j = 2r-4, 2r-2 \\ 2 & if \quad j = 2r-3, 2r-1 \end{cases}$$

$$If\ i \equiv 0\ mod\ 6,\ \psi\left(u_j^i u_j^{i+1}\right) = \begin{cases} 1 & if \quad j = 2r-4, 2r-2 \\ 3 & if \quad j = 2r-3, 2r-1 \end{cases}$$

$$\psi\left(u_0^{l+1} u_{2r-1}^{l+1}\right) = 4,$$

$$\psi\left(u_j^l u_j^{l+1}\right) = \begin{cases} 2 & if \quad j = 2r-4, 2r-2 \\ 1 & if \quad j = 2r-3 \\ 4 & if \quad j = 2r-1 \end{cases}$$

$$\psi\left(u_j^{l+1} u_{j+1}^{l+1}\right) = \begin{cases} 3 & if \quad j = 2r-5 \\ 1 & if \quad j = 2r-4, 2r-3 \\ 4 & if\ j = 2r-2 \end{cases}$$

It is easy to verify that ψ is injective edge-coloring of $H^l(r)$. Hence $\chi_i'\left(H^l(r)\right) = 4$.

Case 6. $\boldsymbol{If\ l \equiv 0\ mod\ 6}$

$$\psi\left(u_0^{l+1}u_1^{l+1}\right) = 3$$

$$For\ j \in \{1,2,\dots,2r-5\},\ \psi\left(u_j^{l+1}u_{j+1}^{l+1}\right) = \begin{cases} 3 & if\ \ j \equiv 1,0\ mod\ 6 \\ 1 & if\ \ j \equiv 2,3\ mod\ 6 \\ 2 & if\ \ j \equiv 4,5\ mod\ 6 \end{cases}$$

Sub Case 6.1. $\boldsymbol{If\ r \equiv 0\ mod\ 3}$

$$\psi\left(u_j^0 u_{j+1}^0\right) = \begin{cases} 2 & if\ \ j = 2r-5, 2r-4 \\ 3 & if\ \ j = 2r-3, 2r-2 \end{cases}$$

For $i \in \{1,2,\dots,l\}$

$$\text{If } j = r-2, \psi\left(u_{2j}^i u_{2j+1}^i\right) = \begin{cases} 1 & if\ \ i \equiv 1\ mod\ 3 \\ 3 & if\ \ i \equiv 2\ mod\ 3 \\ 2 & if\ \ i \equiv 0\ mod\ 3 \end{cases}$$

$$\text{If } j = r-1, \psi\left(u_{2j}^i u_{2j+1}^i\right) = \begin{cases} 2 & if\ \ i \equiv 1\ mod\ 3 \\ 1 & if\ \ i \equiv 2\ mod\ 3 \\ 3 & if\ \ i \equiv 0\ mod\ 3 \end{cases}$$

For $i \in \{0,1,2,\dots,l\}$

$$If\ i \equiv 0\ mod\ 6,\ \psi\left(u_j^i u_j^{i+1}\right) = \begin{cases} 2 & if\ \ j = 2r-4, 2r-1 \\ 1 & if\ \ j = 2r-3 \\ 3 & if\ \ j = 2r-2 \end{cases}$$

$$If\ i \equiv 1\ mod\ 6,\ \psi\left(u_j^i u_j^{i+1}\right) = \begin{cases} 3 & if\ \ j = 2r-4 \\ 1 & if\ \ j = 2r-3, 2r-2 \\ 2 & if\ \ j = 2r-1 \end{cases}$$

$$If\ i \equiv 2\ mod\ 6,\ \psi\left(u_j^i u_j^{i+1}\right) = \begin{cases} 3 & if\ \ j = 2r-4, 2r-1 \\ 2 & if\ \ j = 2r-3 \\ 1 & if\ \ j = 2r-1 \end{cases}$$

$$If\ i \equiv 3\ mod\ 6,\ \psi\left(u_j^i u_j^{i+1}\right) = \begin{cases} 1 & if\ \ j = 2r-4 \\ 2 & if\ \ j = 2r-3, 2r-2 \\ 3 & if\ \ j = 2r-1 \end{cases}$$

$$If\ i \equiv 4\ mod\ 6,\ \psi\left(u_j^i u_j^{i+1}\right) = \begin{cases} 1 & if\ \ j = 2r-4, 2r-1 \\ 3 & if\ \ j = 2r-3 \\ 2 & if\ \ j = 2r-2 \end{cases}$$

$$If\ i \equiv 5\ mod\ 6,\ \ \psi\left(u_j^i u_j^{i+1}\right) = \begin{cases} 2 & if\ \ j = 2r-4 \\ 3 & if\ \ j = 2r-3, 2r-2 \\ 1 & if\ \ j = 2r-1 \end{cases}$$

$$\psi\left(u_0^{l+1} u_{2r-1}^{l+1}\right) = 2$$

$$\psi\left(u_j^{l+1} u_{j+1}^{l+1}\right) = \begin{cases} 3 & if\ \ j = 2r-5 \\ 1 & if\ \ j = 2r-4, 2r-3 \\ 2 & if\ \ j = 2r-2 \end{cases}$$

It is easy to verify that ψ is injective edge-coloring of $H^l(r)$. Hence $\chi_i'\left(H^l(r)\right) = 3$.

Sub Case 6.2. $\boldsymbol{If\ r \equiv 1\ mod\ 3}$

$$\psi\left(u_j^0 u_{j+1}^0\right) = \begin{cases} 3 & if\ \ j = 2r-5, 2r-4 \\ 4 & if\ \ j = 2r-3, 2r-2 \end{cases}$$

$$\psi\left(u_j^0 u_j^1\right) = \begin{cases} 3 & if\ \ j = 2r-4 \\ 1 & if\ \ j = 2r-3 \\ 4 & if\ \ j = 2r-2 \\ 2 & if\ \ j = 2r-1 \end{cases}$$

For $i \in \{1,2, \dots, l\}$

$$\text{If } j = r-2, \psi\left(u_{2j}^i u_{2j+1}^i\right) = \begin{cases} 1 & if\ \ i \equiv 1\ mod\ 3 \\ 2 & if\ \ i \equiv 2\ mod\ 3 \\ 3 & if\ \ i \equiv 0\ mod\ 3 \end{cases}$$

$$\text{If } j = r-1, \psi\left(u_{2j}^i u_{2j+1}^i\right) = \begin{cases} 2 & if\ \ i \equiv 1\ mod\ 3 \\ 3 & if\ \ i \equiv 2\ mod\ 3 \\ 1 & if\ \ i \equiv 0\ mod\ 3 \end{cases}$$

For $i \in \{1,2, \dots, l-1\}$

$$If\ i \equiv 1\ mod\ 6,\ \ \psi\left(u_j^i u_j^{i+1}\right) = \begin{cases} 2 & if\ \ j = 2r-4, 2r-1 \\ 1 & if\ \ j = 2r-3 \\ 3 & if\ \ j = 2r-2 \end{cases}$$

$$If\ i \equiv 2\ mod\ 6,\ \ \psi\left(u_j^i u_j^{i+1}\right) = \begin{cases} 2 & if\ \ j = 2r-4 \\ 3 & if\ \ j = 2r-3, 2r-2 \\ 1 & if\ \ j = 2r-1 \end{cases}$$

$$If\ i \equiv 3\ mod\ 6,\ \ \psi\left(u_j^i u_j^{i+1}\right) = \begin{cases} 1 & if\ \ j = 2r-4, 2r-1 \\ 3 & if\ \ j = 2r-3 \\ 2 & if\ \ j = 2r-2 \end{cases}$$

$$If\ i \equiv 4\ mod\ 6,\ \psi\left(u_j^i u_j^{i+1}\right) = \begin{cases} 1 & if\ \ j = 2r-4 \\ 2 & if\ \ j = 2r-3, 2r-2 \\ 3 & if\ \ j = 2r-1 \end{cases}$$

$$If\ i \equiv 5\ mod\ 6,\ \ \psi\left(u_j^i u_j^{i+1}\right) = \begin{cases} 3 & if\ \ j = 2r-4, 2r-1 \\ 2 & if\ \ j = 2r-3 \\ 1 & if\ \ j = 2r-2 \end{cases}$$

$$If\ i \equiv 0\ mod\ 6,\ \psi\left(u_j^i u_j^{i+1}\right) = \begin{cases} 3 & if\ \ j = 2r-4 \\ 1 & if\ \ j = 2r-3, 2r-2 \\ 2 & if\ \ j = 2r-1 \end{cases}$$

$$\psi\left(u_0^{l+1} u_{2r-1}^{l+1}\right) = 2,\ \psi\left(u_j^l u_j^{l+1}\right) = \begin{cases} 3 & if\ \ j = 2r-4 \\ 4 & if\ \ j = 2r-3 \\ 1 & if\ \ j = 2r-2 \\ 2 & if\ \ j = 2r-1 \end{cases}$$

$$\psi\left(u_j^{l+1} u_{j+1}^{l+1}\right) = \begin{cases} 1 & if\ \ j = 2r-5 \\ 4 & if\ \ j = 2r-4, 2r-3 \\ 2 & if\ \ j = 2r-2 \end{cases}$$

It is easy to check that ψ is injective edge-coloring of $H^l(r)$. Hence $\chi_i'\left(H^l(r)\right) = 4$.

Sub Case 6.3. $\boldsymbol{If\ r \equiv 2\ mod\ 3}$

$$\psi\left(u_j^0 u_{j+1}^0\right) = \begin{cases} 1 & if\ \ j = 2r-5, 2r-4 \\ 4 & if\ \ j = 2r-3, 2r-2 \end{cases}$$

$$\psi\left(u_j^0 u_j^1\right) = \begin{cases} 1 & if\ \ j = 2r-4 \\ 3 & if\ \ j = 2r-3 \\ 4 & if\ \ j = 2r-2 \\ 2 & if\ \ j = 2r-1 \end{cases}$$

For $i \in \{1,2,\dots,l\}$

$$\text{If } j = r-2, \psi\left(u_{2j}^i u_{2j+1}^i\right) = \begin{cases} 3 & if\ \ i \equiv 1\ mod\ 3 \\ 2 & if\ \ i \equiv 2\ mod\ 3 \\ 1 & if\ \ i \equiv 0\ mod\ 3 \end{cases}$$

$$\text{If } j = r-1, \psi\left(u_{2j}^i u_{2j+1}^i\right) = \begin{cases} 2 & if\ \ i \equiv 1\ mod\ 3 \\ 3 & if\ \ i \equiv 2\ mod\ 3 \\ 1 & if\ \ i \equiv 0\ mod\ 3 \end{cases}$$

For $i \in \{1,2,\dots,l-1\}$

$$If\ i \equiv 1\ mod\ 6,\ \psi\left(u_j^i u_j^{i+1}\right) = \begin{cases} 2 & if\ \ j = 2r-4, 2r-1 \\ 3 & if\ \ j = 2r-3, 2r-2 \end{cases}$$

$$If\ i \equiv 2\ mod\ 6,\ \psi\left(u_j^i u_j^{i+1}\right) = \begin{cases} 2 & if\ \ j = 2r-4, \\ 1 & if\ \ j = 2r-3, 2r-1 \\ 3 & if\ \ j = 2r-2 \end{cases}$$

$$If\ i \equiv 3\ mod\ 6,\ \psi\left(u_j^i u_j^{i+1}\right) = \begin{cases} 3 & if\ \ j = 2r-4 \\ 1 & if\ \ j = 2r-3, 2r-1 \\ 2 & if\ \ j = 2r-2 \end{cases}$$

$$If\ i \equiv 4\ mod\ 6,\ \psi\left(u_j^i u_j^{i+1}\right) = \begin{cases} 3 & if\ \ j = 2r-4, 2r-1 \\ 2 & if\ \ j = 2r-3, 2r-2 \end{cases}$$

$$If\ i \equiv 5\ mod\ 6,\ \ \psi\left(u_j^i u_j^{i+1}\right) = \begin{cases} 1 & if\ \ j = 2r-4, 2r-2 \\ 2 & if\ \ j = 2r-3 \\ 3 & if\ \ j = 2r-1 \end{cases}$$

$$If\ i \equiv 0\ mod\ 6,\ \psi\left(u_j^i u_j^{i+1}\right) = \begin{cases} 1 & if\ \ j = 2r-4, 2r-2 \\ 3 & if\ \ j = 2r-3 \\ 2 & if\ \ j = 2r-1 \end{cases}$$

$$\psi\left(u_0^{l+1} u_{2r-1}^{l+1}\right) = 4,$$

$$\psi\left(u_j^l u_j^{l+1}\right) = \begin{cases} 1 & if\ \ j = 2r-4, 2r-2 \\ 3 & if\ \ j = 2r-3 \\ 4 & if\ \ j = 2r-1 \end{cases}$$

$$\psi\left(u_j^{l+1} u_{j+1}^{l+1}\right) = \begin{cases} 2 & if\ \ j = 2r-5 \\ 3 & if\ \ j = 2r-4, 2r-3 \\ 4 & if\ \ j = 2r-2 \end{cases}$$

It is easy to verify that ψ is injective edge-coloring of $H^l(r)$. Hence $\chi_i'\left(H^l(r)\right) = 4$.

3. Conclusion

In this paper, I investigated the injective edge-coloring numbers of H-graphs and generalized H-graphs. To derive similar results for other graph families is an open area of research.

Acknowledgement

The author expresses his sincere thanks to the referee for his/ her careful reading and suggestions that helped to improve this paper.

References

1. Bertossi A.A, Bonuccelli M.A, Code assignment for hidden terminal interference avoidance in multihop packet radio networks, IEEE/ACM Trans. Networking, 3 (1995), 441–449.
2. Bondy.J.A and Murthy. U.S.R, Graph Theory and its Application, (North - Holland),Newyork (1976).
3. Bu Y, Chen W, Injective edge-coloring of planar graphs with girth at least 6, Journal of Zhejiang Normal University, 43 (2020), 19–25 (In Chinese).
4. Bu Y, Qi C, Zhu J, Injective edge-coloring of planar graphs, Adv. Math., 6 (2020), 675–684(In Chinese).
5. Bu Y, Qi C, Injective edge-coloring of sparse graphs, Discrete Mathematics, Algorithms and Applications, 10 (2018), 1850022.
6. Cardoso D. M, Cerdeira J. O, Cruz J. P, Dominic C, Injective edge-coloring of graphs, Filomat, 33 (2019), 6411–6423.
7. Daouya Laıche and Eric Sopena, Packing coloring of some classes of cubic graph, Australasian journal of combinatorics 72(2) (2018), 376–404.
8. Ferdjallah B, Kerdjoudj S, Raspaud A, Injective edge-coloring of sparse graphs, arXiv:1907.0983v2 [math.CO], 2019.
9. Hahn G, Kratochvil J, Sira J, Sotteau D, On the injective chromatic number of graphs, Discrete Math., 256 (2002), 179–192.
10. Kostochka A, Raspaud A, Xu J, Injective edge-coloring of graphs with given maximum degree, Eur. J. Combin., 96 (2021), 103355.
11. Yue J, Zhang S, Zhang X, Note on the perfect EIC-graphs, Appl. Math. Comput., 289 (2016), 481–485.

MULTIVARIATE ANALYSIS AND MODELING THE EFFECT OF THE GDP OF NIGERIA ON THE PETROLEUM PRODUCT PRICES (1987-2018)

[1]Elekanachi, Maraizu Stella, [2]Wonu, Nduka & [3]Onu, Obineke Henry

[1,2,3] *Department of Mathematics/Statistics,*

Ignatius Ajuru University of Education, Port Harcourt, Nigeria

Corresponding Author email: ndukawonu@gmail.com

Abstract:

The study presented multivariate analysis and modeling of the effect of the GDP of Nigeria on the Nigerian petroleum product prices from 1987 to 2018. The petroleum products considered as the response variables were the Premium Motor Spirit (PMS(Y1), Automotive Gas Oil (AGO(Y2)) and Dual Purpose Kerosene (DPK(Y3)) while the predictors were GDP(Z1), Total Reserve(Z2), External Debt(Z3), Gross National Expenditure(Z4) and GDP/Capita(Z5). These predictors were studied in pairs on the responses and also studied jointly with all the five predictors on the responses. Comparisons were made among the pairs, also, each pair was compared with the joint analysis. SPSS software was used in the analysis in which Pillai's Trace, Wilks' Lambda, F-value, P-value, coefficient of determination and sum of square errors were applied to determine the contributions of each predictor variable in the models built, to the petroleum product prices. Correlation and covariance analysis were also applied to know the joint effects of the variables. It was observed that PMS was greatly affected by the economic policies of Nigeria, same to the AGO and then DPK. PMS is insignificantly impacted in an economy with two indicators where GNE is involved. PMS and AGO proved better than DPK in the economy of Nigeria. The relationship between GDP on Total reserve or External debt is positive. That is to say, any increase in these variables will result to an increase in the petroleum product prices. Correlation and Covariance analysis revealed that the analysis between GNE and External debt proved to be the worst pair. The analysis on all the five predictors, GNE and External Debt, Total Reserve and External Debt, Total Reserve and GNE and Total Reserve and GDP had no negative correlation, while GDP and GNE had negative correlations between AGO and DPK and AGO and PMS, also, GDP and GDP/Capita and GDP and Total Reserve recorded negative correlation respectively between PMS and AGO and AGO and PMS.

Keywords: *Petroleum products prices, GDP, GNE, Total Reserve, External Debt, economy*

1. INTRODUCTION

The petroleum products are mainly used industrially for the production of goods and services, such products are also used in our homes for many purposes, such as cooking (Dual Purpose Kerosene DPK) and (Automotive Gas Oil AGO), in Vehicles and Generators (Premium Motor Spirit PMS) etc. The importance of crude oil to Nigerian economy cannot be over emphasized, because it has the highest share in the economy of Nigeria as seen in Amagoh et al (2014) and Francis (2012). Eregha et al (2016) stated that petroleum sector accounts for over 90% of the foreign exchange earnings and gives jobs to Nigerians. See CBN (2010). The National Petroleum Corporation (NNPC) established on first of April, 1977 was given the mandate of the exploration

of oil in Nigeria and was charged with the powers of refining, transporting, and marketing the products of the crude oil exploration. The activities of NNPC and its subsidiaries were regulated by the Department of Petroleum Resources (DPR), it ensures compliance with the regulations of the industry and process applications for permits, licenses and leases. Crude oil has become one of the strongest indicators of worldwide economic activities according to Amagoh et al (2014), this was as a result of its ability in the supply of energy demand in the world. Prices of oil are usually not fixed and it is always dependent on the share of the cost of oil in the general GDP and the level of the countries' dependence on the product consumption on a domestic basis and its alternatives in obtaining the product.

Onu (2020) stated that PMS is highly affected by the economic development of Nigeria than the AGO and the DPK. Also, that PMS performs poorly in an economy paired where GNE is involved. The subsidy in PMS reduces the positive effects of PMS on the economy, thereby making AGO and DPK to perform optimally in some quarters.

Aliyu (2004) argued that the increase in price of the crude oil is considered positive for countries exporting oil and negative for countries importing oil and the reverse should be expected when the oil price decreases, all things being equal. But in Nigeria today, the masses suffer in both ways because if the price of crude oil is increased in the international market, Nigeria as an oil exporting country benefits from the high cost, but pays high to import the finished products from foreign countries, thereby making the end product of crude oil PMS, DPK, AGO etc, to be sold with high prices in our flow stations. Since the discovery of oil in Oloibiri in Bayelsa State, Nigeria in 1956 according to Monday et al (2016), the Gross Domestic Product of the country have been highly dependent on the petroleum products, thereby making Agriculture which was the main stay of the countries' economy to be under founded and attention been shifted to the petroleum products. Many researchers have studied the effect of price shock on the Gross Domestic Product GDP. Some of these studies include; macroeconomic implications of oil price shocks on macroeconomic performance in Nigeria, petroleum product prices and inflationary dynamics in Nigeria, relationship between energy pricing and finance, petroleum product pricing and complementary policies; experience of 65 under developed countries, and impact of oil price on Nigerian economy and On the pairwise multivariate analysis of Nigerian economy and the petroleum products prices. Some of these researches conducted in Nigeria did not take into consideration the actual areas of the Nigerian economy, while some of the researches were conducted outside Nigeria, where the economy of Nigeria was not considered. Amagoh et al (2014) who considered some other aspects of the Nigerian economy like GDP, Total reserve, external debt, Gross national income, Gross national expenditure and GDP per capita on the prices of the petroleum products, did not consider pairing the predictors on the response variables and compare the result with what was obtained when all the five predictors which are Gross Domestic Product(Z1), TOTAL RESERVE(Z2), EXTERNAL DEBT(Z3), GROSS NATIONAL EXPENDITURE(Z4) and GDP/CAPITA(Z5) were used together on the response variables. Here we will consider the effect of GDP(Z1) and EXTERNAL DEBT(Z3) on the response variables, GDP(Z1) and TOTAL RESERVE(Z2) on the response variables, GDP(Z1) and GROSS NATIONAL EXPENDITURE(Z4) on the response variables, GDP(Z1) and GDP/CAPITA(Z5), GDP/CAPITA(Z5) and TOTAL RESERVE(Z2), TOTAL RESERVE(Z2) and GROSS NATIONAL EXPENDITURE(Z4), TOTAL RESERVE(Z2) and EXTERNAL DEBT(Z3), GROSS NATIONAL EXPENDITURE(Z4) and EXTERNAL DEBT(Z3), EXTERNAL DEBT(Z3) and GDP/CAPITA(Z5) and GROSS NATIONAL

EXPENDITURE(Z4) and GDP/CAPITA(Z5), finally consider the three, PMS, AGO and DPK on the five economics variables from 1987 to 2018. We then compare the effects of each pair on the economy when the other variable is not significant or classified as error, may be due to unavailability of data. We compare each pair with the three responses and draw conclusion. Also Onu (2020) considered the pairwise multivariate analysis of Nigerian economy and petroleum products prices, here, he studied the effects of the petroleum products prices on the paired economic variables, but the study did not consider comparing the paired analysis with the analysis of all the five economic variables, it is against this backdrop this work was presented.

The study is aimed at determining the effect of petroleum prices (PMS, AGO and DPK) on some economic variables in pair when the other is insignificant or unavailable in other to determine the overall impact of these pairs on the Nigerian economy and compare the result with what is obtained when all the five predictors are considered. The study will consider the data of petroleum product prices as response variables from 1998 to 2018 on the economic variables such as GDP, Total reserve, External Debt, Gross national expenditure and GDP per capita. The petroleum products considered in this study are the premium motor spirit (PMS), popularly called fuel, the Dual Purpose Kerosene (DPK) simply called Kerosene, and the Automotive Gas Oil (AGO). Ten different multivariate multiple linear regressions with two predictors shall be analyzed and one multivariate multiple linear regression with five predictors shall also be considered.

2. MATERIALS AND METHODS

We designed this study to analyze the effects of the petroleum products' prices on the economy of Nigeria using multivariate settings. Analyzing the data by the use of Ordinary Least Square (OLS), Pillai's trace, Wilks' Lambda statistic, F-statistic, P-test statistic, covariance approach, correlation approach and coefficient of determinant were considered, whose methods are shown in the following sections. The analysis will be carried out using SPSS multivariate Software package.

The secondary data used in this research was an annual data obtained from National bureau of Statistics 2017, National bulletin, Amagoh et al (2014) and it spanned through 1987-2018, making 32 years' period covered in the research.

The multivariate multiple linear regression is one with more than one response variables and more than one predictor as seen in Richard and Dean (2002).

The multivariate processes are expressed as seen in Ilesanmi and Olurankinse (2010) and Amagoh et al (2014) as

$$Y_{nxm} = \begin{pmatrix} y_{11} & \cdots & y_{1m} \\ \vdots & \ddots & \vdots \\ y_{n1} & \cdots & y_{nm} \end{pmatrix} \quad (1)$$

Where Y_{nxm} represents the responses

The predictors can be given as

$$X_{nxm} = \begin{pmatrix} x_{10} & \cdots & x_{1m} \\ \vdots & \ddots & \vdots \\ x_{n1} & \cdots & x_{nm} \end{pmatrix} \quad (2)$$

With the parameters given as

$$\underline{\hat{\beta}}_{rxm} = \begin{pmatrix} \beta_{10} & \cdots & \beta_{1m} \\ \vdots & \ddots & \vdots \\ \beta_{r1} & \cdots & \beta_{rm} \end{pmatrix} \quad (3)$$

And the stochastic disturbance known as the error that follows normal with mean zero and constant variance, is given as

$$e_{rxm} = \begin{pmatrix} e_{11} & \cdots & e_{1m} \\ \vdots & \ddots & \vdots \\ e_{n1} & \cdots & e_{nm} \end{pmatrix} \quad (4)$$

The economic model used in this study is given as

$$Y_{n\times m} = X_{(n\times(r+1))}\beta_{(r+1)X1)} + e_{n\times m} \quad (5)$$

Which can be reduced to

$$Y_{ij} = \beta_{ij}x_{ij} + e_i,\ i = 1, 2,\ \ldots,\ m \text{ and } j = 1, 2,\ \ldots,\ m \quad (6)$$

Where $E(e_{(i)}) = 0_{n\times 1}$ and $cov(e_{(i)}, e_{(j)}) = \delta_{ij}I$.

With the outcome of the response Y given and the predictors x_i as full rank, the least square method is applied to estimate $\hat{\beta}_{(i)}$ and this is done particularly from the observations $Y_{(i)}$on the least square given as

$$\underline{\hat{\beta}}_{(i)} = (x'x)^{-1}x'Y_{(i)} \quad (7)$$

Where $x'$is the transpose of x, which implies that if x is $n \times m$ then x' will be

$m \times n$. The reason for obtaining $x'x$ is to make the matrix a nonsingular matrix. We then obtain $x'Y_{(i)}$ by multiplying the transpose of x by the matrix of the predictor. The SPSS multiple regression is applied to this study. We then test for the significance of the variables and apply MANOVA in the study.

The model to be used can be expressed as

$$Y = \beta 0 + \beta 1Z1 + \beta 2Z2 + e \quad (8)$$

Where any of Z2, Z3, Z4 or Z5 can replace Z1 in a paired model, while in the full model of the five economic variables it can be written as

$$Yi=\beta 0+\beta 1Z1 +\beta 2Z2+. \ . \ .+\beta 5Z5+e \quad (9)$$

The covariance of two random variables X_i and X_j, is defined as

$$cov(X_i, X_j) = E(x_i - u_i)(x_j - u_j) \quad (10)$$

Where $u_i = E(x_i)$, $u_j = E(x_j)$and E denotes the expectation. If $i = j$ it is observed that the covariance of the variable $x_i$on itself and that of $x_j$on itself is known simply as the variance, hence, needless to define variances and covariance in an independent manner in the case of multivariate analysis.

The variances and covariance can be arranged in the symmetric matrix given as

$$\boldsymbol{\varepsilon}=\begin{pmatrix} \delta_1^2 & \delta_{12} & \cdots & \delta_{1q} \\ \delta_{21} & \delta_2^2 & \cdots & \delta_{2q} \\ \vdots & \vdots & \vdots & \vdots \\ \delta_{q1} & \delta_{q2} & \cdots & \delta_{qq}^2 \end{pmatrix} \quad (11)$$

Which can be estimated as

$$S = \frac{1}{n-1}\sum_{i=1}^{n}(x_i - \bar{x})(x_i - \bar{x})^T \quad (12)$$

Where $x_i^T = (x_{i1}, x_{i2}, \ldots, x_{iq})$ is the vector of numeric observations for the ith individual and

$\bar{X} = \frac{\sum_{i=1}^{n} x_i}{n}$ is the mean vector of observations and the diagonal of S contains the sample variances of each variable which is denoted as S_i^2. In a multivariate data, having q observed variables, indicates that we will have q variances and $\frac{q(q-1)}{2}$ covariance, also,

The correlation between two variables are estimated using the formula as seen

$$\rho_{ij} = \frac{\delta_{ij}}{\delta_i \delta_j} \quad (13)$$

Where $\delta_i = \sqrt{\delta_i^2}$

The Pearson's correlation coefficient denoted by R is given in multivariate settings as

$$R = D^{-1/2} S D^{-1/2} \quad (14)$$

Where $D^{-1/2} = diag(1/S_1, 1/S_2, \ldots 1/S_q)$ and $S_i = \sqrt{S_i^2}$ is the sample standard deviation of the variable.

Pillai' trace and Wilks' Lambda approaches

The Pillai's trace $= tr[B(B+W)^{-1}]$ (15)

And Wilks' lambda statistic $\Lambda^* = \frac{|W|}{|B+W|}$ (16)

Where B is the Residual sum of square error given as

$$B = \sum_{i=1}^{n} m(\bar{X}_i - \bar{X})(\bar{X}_i - \bar{X})' \quad (17)$$

And W is the sum of square treatment given as

$$W = \sum_{i=1}^{n}\sum_{j=1}^{m}(X_{ij} - \bar{X})(X_{ij} - \bar{X})' \quad (18)$$

Sum of square total (B+W)= $\sum_{i=1}^{n} m(\bar{X}_i - \bar{X})(\bar{X}_i - \bar{X})' + \sum_{i=1}^{n}\sum_{j=1}^{m}(X_{ij} - \bar{X})(X_{ij} - \bar{X})'$ (19)

A larger value of the Pillai's trace, the more the effects contributes to the model and also, a smaller the value of Wilkis' Lambda, the better the effects contributes to the model. The two statistics are all positive-valued statistics and Wilks' Lambda lies between 0 and 1.

The analysis in this study made use of sum of square type III error imbedded in the SPSS software used in the analysis. Type III error just like type I and II, is correctly accepting or rejecting the null hypothesis for the wrong question or data. Since no research is 100% correct, there may be errors, may be type I, II, III, etc. We tried as much to minimize the error by ensuring that the study was properly designed and that the data is not a faulty data.

3. RESULTS

Multivariate Analysis of PMS(Y1), AGO(Y2), DPK(Y3) on paired variables

The SPSS result is as shown below

MULTIVARIATE ANALYSIS OF PMS (Y1), AGO (Y2), DPK (Y3) ON GDP (Z1), AND EXTERNAL DEBT (Z3)

General Linear Model

Table 1 (Multivariate Tests[a] for paired analysis GDPZ1 and External Debt Z3)

Effect		Value	F	Sig.
Intercept	Pillai's Trace	.933	125.797[b]	.000
	Wilks' Lambda	.067	125.797[b]	.000
GDPZ1	Pillai's Trace	.984	541.444[b]	.000
	Wilks' Lambda	.016	541.444[b]	.000
				.
EXTTERNALDEBTZ3	Pillai's Trace	.058	.554[b]	.650
	Wilks' Lambda	.942	.554[b]	.650

a. Design: Intercept + GDPZ1 + EXTTERNALDEBTZ3

Table 2 (Tests of Between-Subjects Effects for paired analysis GDPZ1 and External Debt Z3)

Source	Dependent Variable	Type III Sum of Squares	df	Mean Square	F
Corrected Model	PMSY1	63111.090[a]	2	31555.545	322.985
	DPKT3	12594.432[b]	2	6297.216	23.123
	AGOY2	116575.025[c]	2	58287.512	216.906
Intercept	PMSY1	13783.578	1	13783.578	141.081
	DPKT3	1031.670	1	1031.670	3.788
	AGOY2	27088.386	1	27088.386	100.804
GDPZ1	PMSY1	63048.413	1	63048.413	645.329
	DPKT3	12472.456	1	12472.456	45.799
	AGOY2	116156.491	1	116156.491	432.254
EXTTERNALDEBTZ3	PMSY1	70.292	1	70.292	.719
	DPKT3	333.566	1	333.566	1.225

	AGOY2	2.849	1	2.849	.011
Error	PMSY1	2833.291	29	97.700	
	DPKT3	7897.592	29	272.331	
	AGOY2	7792.956	29	268.723	
Total	PMSY1	137514.013	32		
	DPKT3	49541.563	32		
	AGOY2	245935.623	32		
Corrected Total	PMSY1	65944.381	31		
	DPKT3	20492.024	31		
	AGOY2	124367.981	31		

a. R Squared = .957 (Adjusted R Squared = .954)

b. R Squared = .615 (Adjusted R Squared = .588)
c. R Squared = .937 (Adjusted R Squared = .933)

MULTIVARIATE ANALYSIS OF PMS(Y1), AGO(Y2), DPK(Y3) ON THE FIVE VARIABLES

MULTIVARIATE ANALYSIS OF PMS(Y1), AGO(Y2), DPK(Y3) ON GDP (Z1), TOTAL RESERVE (Z2), EXTERNAL DEBT (Z3), GROSS NATIONAL EXPENDITURE (Z4) AND GDP/CAPITA (Z5)

General Linear Model

Table 3 (Multivariate Tests[a] for combined analysis of the five variables)

Effect		Value	F	Sig.
Intercept	Pillai's Trace	.848	44.712[b]	.000
	Wilks' Lambda	.152	44.712[b]	.000
GDPZ1	Pillai's Trace	.588	11.426[b]	.000
	Wilks' Lambda	.412	11.426[b]	.000
TOTALRESERVEZ2	Pillai's Trace	.341	4.146[b]	.017
	Wilks' Lambda	.659	4.146[b]	.017
EXTERNALDEBTZ3	Pillai's Trace	.272	2.996[b]	.051
	Wilks' Lambda	.728	2.996[b]	.051
GROSSNATIONALEXPENDITUREZ4	Pillai's Trace	.586	11.323[b]	.000
	Wilks' Lambda	.414	11.323[b]	.000

GDPPERCAPITAZ5	Pillai's Trace	.301	3.448[b]	.032
	Wilks' Lambda	.699	3.448[b]	.032

a. Design: Intercept + GDPZ1 + TOTALRESERVEZ2 + EXTERNALDEBTZ3 GROSSNATIONALEXPENDITUREZ4 + GDPPERCAPITAZ5

Table 4 (Tests of Between-Subjects Effects for combined analysis)

Source	Dependent Variable	Type III Sum of Squares	df	Mean Square	F
Corrected Model	PMSY1	64099.662[a]	5	12819.932	180.688
	AGOY2	121388.788[b]	5	24277.758	211.877
	DPKY3	17913.181[c]	5	3582.636	36.120
Intercept	PMSY1	1736.747	1	1736.747	24.478
	AGOY2	11550.339	1	11550.339	100.802
	DPKY3	36.689	1	36.689	.370
GDPZ1	PMSY1	307.956	1	307.956	4.340
	AGOY2	3326.139	1	3326.139	29.028
	DPKY3	843.599	1	843.599	8.505
TOTALRESERVEZ2	PMSY1	495.379	1	495.379	6.982
	AGOY2	216.674	1	216.674	1.891
	DPKY3	903.844	1	903.844	9.113
EXTERNALDEBTZ3	PMSY1	402.698	1	402.698	5.676
	AGOY2	353.483	1	353.483	3.085
	DPKY3	.899	1	.899	.009
GROSSNATIONALEXPENDITUREZ4	PMSY1	136.467	1	136.467	1.923
	AGOY2	3609.769	1	3609.769	31.503
	DPKY3	259.495	1	259.495	2.616
GDPPERCAPITAZ5	PMSY1	77.236	1	77.236	1.089
	AGOY2	64.995	1	64.995	.567
	DPKY3	494.308	1	494.308	4.984
Error	PMSY1	1844.718	26	70.951	
	AGOY2	2979.193	26	114.584	
	DPKY3	2578.844	26	99.186	

Total	PMSY1	137514.013	32		
	AGOY2	245935.623	32		
	DPKY3	49541.563	32		
Corrected Total	PMSY1	65944.381	31		
	AGOY2	124367.981	31		
	DPKY3	20492.024	31		

a. R Squared = .972 (Adjusted R Squared = .967)
b. R Squared = .976 (Adjusted R Squared = .971)
c. R Squared = .874 (Adjusted R Squared = .850)

4. DISCUSSION OF RESULTS

Finding for PMS(Y1), AGO(Y2), DPK(Y3) ON GDP(Z1) AND EXTERNAL DEBT(Z3)

The analysis revealed that Nigeria economy has higher contribution to the prices of PMS than the AGO(Y2) and then the DPK(Y3) for this model. The intercepts of the model of PMS(Y1), AGO(Y2) and DPK(Y3) are negative. The AGO(Y2) has the highest intercept followed by the PMS(Y1). Generally, it was revealed that in the analysis of the multivariate test, the contribution of the GDP(Z1) to PMS(Y1), AGO(Y2) and DPK(Y3) is higher than the contribution of the intercept and also higher than the contribution of External Debt(Z3) which is shown by the F-value, P-value, Pillai's trace and Wilks' lambda values. The PMS(Y1) is majorly affected by the economy of Nigeria than AGO(Y2) and AGO(Y2) is affected by more than DPK(Y3) when the GDP(Z1) and External Debt(Z3) are used as the indicator of the Nigerian economy.

Findings for PMS(Y1), AGO(Y2), DPK(Y3) ON GDP(Z1) AND TOYAL RESERVE(Z2)

The multivariate test reveals that GDP(Z1) contributes more to the prices of these petroleum products under study than the Total Reserve(Z2). The test of between-subject effects reveals that PMS(Y1) is highly influenced by the Nigeria economic polices followed by the AGO(Y2) and then the DPK(Y3) when GDP(Y1) and Total Reserve(Z2) are used as indicator. In the estimation of parameters of the model, it was revealed that all the intercept for PMS(Y1), AGO(Y2) and DPK(Y3) models are negative. The correlation between AGO(Y2) and DPK(Y3) is higher than any other joint effect in the study, showing that the joint effect of the two responses will be greatly affected by the economic policies of Nigeria. The joint effect of AGO(Y2) and PMS(Y1) gave negative value, implying that, their joint effect may be negatively affected by the economic policies of Nigeria.

Findings for PMS(Y1), AGO(Y2), DPK(Y3) ON GDP(Z1) AND GROSS NATIONAL EXPENDITURE GNE(Z4)

The multivariate test reveals that the GDP(Z1) provides the highest contribution to Nigerian's economic growth and has the highest impact in the regulation of the Nation's petroleum products price than the GNE(Z4). All the variables under study are significant in the analysis. These are revealed by the values of Pillai's trace and Wilks' lambda. In the test of between-subject effects, it was revealed that AGO(Y2) is seriously affected by the economy of Nigeria when the indicators of the economy are GDP(Z1) and GNE(Z4) than PMS(Y1) as revealed by the value of R^2in the corrected model. The estimation of parameters also shows that the intercepts are all negative which could mean the negative effect of the instability in prices of these petroleum

products to the poor masses in Nigeria. In the correlation analysis, it was revealed that the relationship between PMS(Y1) and DPK(Y3) is higher than others, while AGO(Y2) and DPK(Y3) and AGO(Y2) and PMS(Y1) have negative relationships.

Findings for PMS(Y1), AGO(Y2), DPK(Y3) ON GDP(Z1) AND GDP/CAPITA(Z5)

Multivariate test shows that GDP(Z1) contributes more to the regulation of the petroleum products prices than the GDP/CAPITA(Z5), but the GDP(Z1) and GDP/CAPITA(Z5) are significant in the analysis as shown in the F-value, P-value, Pillai's trace and Wilks' lambda statistic. The test of between-subject effects shows that PMS(Y1) is highly affected by the economic policies of Nigeria than AGO(Y2) and DPK(Y3) which is revealed by the F-value in the corrected model and the intercepts followed by AGO(Y2) and then DPK(Y3), but same is not true for GDP(Z1) and GDP/CAPITA(Z5), where the opposite is witnessed. The mean square error revealed that PMS(Y1) is generally the highest to be affected by the Nigerian economic policies followed by DPK(Y3) in this model under study. R^2revealed that the model of PMS(Y1) is better in analyzing the economy of Nigeria followed by that of AGO(Y2) and DPK(Y3). The estimation of parameters shows that the intercepts for PMS(Y1) and AGO(Y2) are negative showing how their negative impact of their instability in price will be on the poor masses and DPK(Y3) has a positive intercept which reveals the positive impact its price has been on the masses, may be, this could be as a result of the relative stability of the price of DPK(Y3) in Nigerian Filling Stations. The correlation between PMS(Y1) and DPK(Y3) recorded the highest value which suggests that their joint effect will be better than the joint effect of the others. PMS(Y1) and AGO(Y2) has a negative relationship.

Findings for PMS(Y1), AGO(Y2), DPK(Y3) ON GDP/CAPITA(Z5) AND TOTAL RESERVE(Z2)

This test reveals that GDP/CAPITA(Z5) contributes more to Nigerian economy than Total Reserve(Z2) and all the factors are significant in the analysis as revealed by the F-value, Pillai's and Wilks' statistic and the P-value. In the test of between-subject effects, it was revealed that PMS(Y1) proves to be better than AGO(Y2) , DPK(Y3) for both corrected model, intercept model, model of GDP/CAPITA(Z5) and Total Reserve(Z2), this is as revealed by the F-value, mean square errors and R^2 for model having GDP/CAPITA(Z5) and Total Reserve(Z2) as the indicators of the economy. Parameter estimate shows that the intercept for PMS(Y1) and AGO(Y2) are negative while DPK(Y3) is positive. Correlation shows that AGO(Y2) and DPK(Y3) are jointly affected in a maximum level, followed by PMS(Y1) and DPK(Y3), there is no negative relationship in the correlation in the analysis of GDP/CAPITA(Z5) and Total Reserve(Z2) because, increase in the prices of the petroleum products under study is favored by Total Reserve(Z2) and the GDP/CAPITAL(Z5).

Findings for PMS(Y1), AGO(Y2), DPK(Y3) ON GDP/CAPITA(Z5) AND TOTAL RESERVE(Z2)

This test reveals that GDP/CAPITA(Z5) contributes more to Nigerian economy than Total Reserve(Z2) and all the factors are significant in the analysis as revealed by the F-value, Pillai's and Wilks' statistic and the P-value. In the test of between-subject effects, it was revealed that PMS(Y1) proves to be better than AGO(Y2) , DPK(Y3) for both corrected model, intercept model, model of GDP/CAPITA(Z5) and Total Reserve(Z2), this is as revealed by the F-value, mean square errors and R^2 for model having GDP/CAPITA(Z5) and Total Reserve(Z2) as the

indicators of the economy. Parameter estimate shows that the intercept for PMS(Y1) and AGO(Y2) are negative while DPK(Y3) is positive. Correlation shows that AGO(Y2) and DPK(Y3) have the highest joint contribution followed by PMS(Y1) and DPK(Y3), there is no negative relationship in the correlation in the analysis of GDP/CAPITA(Z5) and Total Reserve(Z2) because, increase in the prices of the petroleum products under study is favored by Total Reserve(Z2) and the GDP/CAPITAL(Z5).

Findings for PMS(Y1), AGO(Y2), DPK(Y3) ON TOTAL RESERVE(Z2) AND EXTERNAL DEBT (Z3)

The Total Reserve(Z2) favors the fluctuations of the prices of the petroleum products than the External Debt(Z3) this is revealed by the F-value, P-value, Pillai's trace and Wilks' lambda value. In the test of between-subject effects, the PMS(Y1) is affected more than AGO(Y2) and DPK(Y3) by the economic policies of Nigeria for the corrected model, while for model of Total Reserve(Z2), it shows that the prices of DPK(Y3) is favored by the Total Reserve(Z2), the prices of PMS(Y1) is favored by the External Debt(Z3) in the model of External Debt(Z3). R^2reveals that PMS(Y1) generally, is affected more than the other two, followed by the AGO(Y2) by the growth of Nigerian economy. The intercepts are all positive this is because, the increase in prices of the petroleum products is resulted by the increase in the Total Reserve(Z2) and decrease in the External Debt(Z3) of Nigeria, hence reducing inflation and making the country stable economically. The correlations are all positive in this analysis.

Findings for PMS(Y1), AGO(Y2), DPK(Y3) ON GROSS NATIONAL EXPENDITURE(Z4) AND EXTERNAL DEBT (Z3)

The multivariate test reveals that the GNE(Z4) contributes more to the economy of Nigeria than External Debt(Z3), this is evident from F-value, Pillai's trace and Wilks' lambda values. The test of between-subject effects shows that PMS(Y1) is affected more by the Nation's economic growth for corrected model, intercept model and GNE(Z4) model, but AGO(Y2) is also affected more by the External Debt(Z3). All the intercepts are positive and the correlation are also positive.

Findings for PMS(Y1), AGO(Y2), DPK(Y3) ON EXTERNAL DEBT (Z3) AND GDP/CAPITA(Z5)

The multivariate test reveals that GDP/CAPITAL(Z5) contributes more to the economy of Nigeria than the External Debt(Z3). The intercept model and the model of GDP/CAPITAL(Z5) are significant while the model of External Debt(Z3) is not. AGO(Y2) is affected more than the other two followed by the PMS(Y1) by the economy of Nigeria. All the parameters including the intercepts are negative, except that of GDP/CAPITA(Z5) on PMS(Y1) and GDP/CAPITA(Z5) on AGO(Y2). All the correlations are positive and the highest correlation is between DPK(Y3) and PMS(Y1) followed by DPK(Y3) and AGO(Y2).

Findings for PMS(Y1), AGO(Y2), DPK(Y3) ON GROSS NATIONAL EXPENDITURE (Z4) AND GDP/CAPITA(Z5)

The multivariate test reveals that GDP/CAPITAL(Z5) contributes more than the GNE(Z4) in the economy of Nigeria, but all the economic variables are significant in the analysis. AGO(Y2) is affected more than the other two in the economy having GDP/CAPITA(Z5) and GNE(Z4) as

indicator. This is also true from the value of $R^2$for test of between-subject effects. All the intercepts are negative in the analysis, also, all the correlations showed positive relationships.

Findings for PMS(Y1), AGO(Y2), DPK(Y3) ON Z1, Z2, Z3, Z4, AND Z5

In the multivariate test for all the five economic variables, it was revealed that the intercept, GDP(Z1) and GNE(Z4) are significant in the combined analysis. In the test of between-subject effects, it was revealed that AGO(Y2) is affected more than the other two, followed by the DPK(Y3) and this is true for intercept model, GDP(Z1) model, Total Reserve(Z2) model and GNE(Z4) model but for External Debt(Z3) and GDP/CAPITA(Z5) the PMS(Y1) is affected more than the other two. The PMS(Y1) model still recorded the smallest mean square error, where AGO(Y2) shows slight increase in R^2 than the PMS(Y1). The PMS(Y1) and AGO(Y2) has negative intercept while DPK(Y3) has positive intercept. The PMS(Y1) and AGO(Y2) has negative correlation, where the rest have positive correlation.

5. CONCLUSION

Based on the findings so far, we conclude that PMS is greatly affected by the economic policies of Nigeria, followed by the AGO and then DPK. PMS is insignificantly affected in an economy with two indicators where GNE is involved. PMS and AGO proved stronger than DPK in the economy of Nigeria. The negative values obtained in the intercept of the petroleum products especially the PMS signifies the negative impact of the increase in prices of the products have on the poor masses. The subsidy on PMS makes the product weaker in its performance to the economy of the Nation. The parameters of the models both for paired models and the full model, showed low values as the gradients of the economic variables to the economy of Nigeria using the three petroleum products as the responses. This tell us that each of the five economic variables may not marginally have significant impact to the prices of petroleum products, unless in combined form. It is because of this reason that the R^2 value showed that the combined analysis was better than each of the paired analysis. The paired analysis is better if there are no resource or no data on all the economic variables, others can be used as error. Also if you want to obtain the individual contributions and their joint effects as revealed by the analysis of correlation, the paired analysis mostly had higher values than the combined model. We also conclude that GDP plays major role in the regulation of the prices of the petroleum products than any other economic variables. The relationship between GDP to any of Total reserve and External debt is positive because the increase in the prices of the petroleum products results in decrease in the external debt, and increase in total reserve.

REFERENCES

1. Akinleye S.O. & Ekpo S. (2013). Oil price shocks and macroeconomic performance in Nigeria, *economía mexicana nueva época*, 2, 2013,565-624.

2. Akinmade, T. N. (2003). Privatization: Bridging Hope Back. The Nigerian Tell Magazine, Vol. 2, p.48.

3. Aliyu,S.U. (2009). Impact of Oil Price Shock And Exchange Rate Volatility On Economic Growth In Nigeria: An Empirical Investigation, Associate Professor of Economics At Bayero University Kano Research Department of The Central Bank of Nigeria

4. Amagoh, M. N., Odoh, C. M, & Okuh, B. A. (2014). Modeling petroleum product prices and the Nigerian economy; IOSR *Journal of mathematics (IOSR-JM),* 10, 72-79.

5. Arinze P.E. (2011). The impact of oil price on the Nigerian economy, JORIND,

6. Ayadi, O.F. (2005). Oil Price Fluctuations and The Nigerian Economy. OPEC Review: 199-217

7. Bobai F. D. (2012). An Analysis of the Relationship between Petroleum Prices and Inflation in Nigeria. *International Journal of Business and Commerce*, 1(12): 1-7.

8. Central Bank of Nigeria (2017). Annual report.

9. Edame, G. E., Effiong, C. E., Adaba, G. A & Uwoghiren, B. O., 2014. The nexus between energy pricing, investment financing and economic growth in Nigeria. Mediterranean Journal of Social Sciences MCSER Publishing, Rome Italy, 5(4).

10. François, L & Mignon, V., (2008). The influence of oil prices on economic activity and other macroeconomic and financial variables. CEPII Research Centre.

11. Eson, P. (2002). Political Economy of Oil Extraction in Nigeria. In Boiling Point – A Committee for the Development of Human Rights (CDHR) Publication on the Crisis in the Oil Producing Communities in Nigeria, Raji, W., A. Ale and E. Akinsola (Eds.), Frankad Publishers, Lagos, Nigeria

12. Eregha, B, Ekundayo Mesagan, & Ayoola, O. (2015), petroleum products prices and inflationary dynamics in Nigeria.

13. Kojima, K., (2013). Petroleum product pricing and complementary policies: Experience of 65 Developing Countries since 2009. Policy Research Working Paper 6396, World Bank.

14. Labys W.C. (2006). Globalization, Oil Price Volatility, and the U.S. Economy. Regional Research Institute, Natural Resource Economics Program, West Virginia University Morgantown, WV, 26506-6108.

15. Mba-Afolabi, J. (1999). The Oil Price of Hike Blunder, Newswatch, January 18, pp. 8 – 16.

16. Monday J. U, Ekeuware M. C and Muritala B. R. (2016), Downstream oil deregulation and Nigeria economy.

17. Nwosu, C.P. (2009). Import of Fuel Prices on Inflation: Evidences from Nigeria. Research Department, Central Bank of Nigeria, http://ssm.com/abstract=1365820.

18. Odidison, O. (2003). Fuel Price Hike: OPS Union React. The Nigerian Business Times, p.17.

Ogunbodede, E., Ilesanmi, A. & Olurankinse, F. (2010). Petroleum Motor Spirit (PMS) Pricing Crisis and the Nigerian Public Passenger Transportation System", Journal of Social Sciences, 5,113 – 121

19. Olusegun,O.A. (2008). Oil Price Shock And Nigerian Economy: A Forecasty Orlu Error Decomposition Analysis. *Journal Of Economic Theory 2 (4*): 124-130.

20. Onu O. H. (2020); On the pair-wise multivariate analysis of Nigerian economy and the petroleum products prices. *International Journal of Applied Science and Mathematical Theory,* 6(3), 8-19.

21. Orlu, R. N. (2017). The impact of domestic pricing of petrol on economic growth of Nigeria (1970-2013). *Global Journal of Social Sciences*. 16

22. Raymond Li (2010). The Relationship Among Petroleum Prices. International Conference on Applied Economics-ICOAE, P. 459.

23. Regnier, E. (2007). Oil and energy price volatility. *Energy Economics*, 29(3), 405–427.

Data of petroleum products prices and real economy used in this research is as shown below.

Year	PMS	AGO	DPK	Z1	Z2	Z3	Z4	Z5
1987	0.5	0.4	0.3	2.74E+10	1.5E+09	2.22E+10	2.24E+10	303.66
1988	0.5	0.4	0.3	3.02E+10	9.33E+08	2.9E+10	2.25E+10	325.2
1989	0.6	0.5	0.4	3.23E+10	2.04E+09	2.96E+10	2.26E+10	339.82
1990	0.6	0.5	0.4	3.5E+10	4.13E+09	3.01E+10	2.2E+10	358.55
1991	0.7	0.5	0.5	3.66E+10	4.68E+09	3.34E+10	2.43E+09	366.46
1992	0.7	0.55	0.5	3.77E+10	1.2E+09	3.35E+10	2.57E+10	368.1
1993	3.25	3	2.75	3.85E+10	1.64E+09	2.9E+10	3.21E+10	367.28
1994	11	9	6	3.86E+10	1.65E+09	3.07E+10	2.2E+10	359.03
1995	11	9	6	3.95E+10	1.71E+09	3.31E+10	2.34E+10	359.43
1996	11	9	6	4.62E+10	4.33E+09	3.41E+10	2.75E+10	366.22
1997	11	9	6	4.24E+10	7.78E+09	3.14E+10	2.8E+10	367.46
1998	11	9	6	4.32E+10	7.3E+09	2.85E+10	3.36E+10	365.75
1999	20	19	17	4.36E+10	5.65E+09	3.03E+10	3.36E+10	361.2
2000	22	21	17	4.6E+10	1.01E+10	2.91E+10	3.62E+10	371.77
2001	22	21	17	4.74E+10	1.06E+10	3.14E+10	3.59E+10	374.17
2002	26	26	24	4.81E+10	7.57E+09	3.1E+10	4.29E+10	370.81
2003	39.5	41.5	41	5.31E+10	7.42E+09	3.05E+10	5.95E+10	399.06
2004	48	48	48	5.87E+10	1.73E+10	3.46E+10	6.61E+09	430.58
2005	50	60	50	6.19E+10	2.86E+10	3.78E+10	7.65E+10	442.72
2006	65	60	50	6.57E+10	4.27E+10	2.21E+10	9.49E+10	458.63
2007	65	60	50	7E+10	5.19E+10	7.69E+09	1.25E+11	476.21
2008	70	80	70	7.42E+10	5.36E+10	8.53E+09	1.41E+11	492.34

2009	65	110	95	7.94E+10	4.55E+10	1.13E+10	1.82E+11	513.77
2010	65	140	50	8.56E+10	3.59E+10	7.71E+09	1.55E+11	540.21
2011	65	150	50	9.13E+10	3.63E+10	7.88E+09	1.84E+11	561.9
2012	97	155	50	9.28E+10	3.92E+10	6.9E+11	1.5E+13	690.5
2013	97	155	50	9.55E+10	3.02E+10	9E+14	2.78E+13	712.91
2014	97	155	50	1.01E+11	3.72E+10	1.02E+14	8.46E+13	768.13
2015	97	155	50	1.1E+11	3.88E+10	1.21E+14	1.03E+14	801.49
2016	145	155	50	1.15E+11	4.03E+10	2.68E+14	1.92E+14	846.92
2017	145	155	50	1.2E+11	4.33E+10	2.17E+14	3.14E+14	892.87
2018	145	155	50	1.27E+11	5.72E+10	2.29E+14	5.03E+14	928.13

Source: National bureau of Statistics 2017, National bulletin, Amagoh et al (2014)

Appendix

Table 5 (Parameter Estimates for paired analysis, GDPZ1 and External Debt Z3)

Dependent Variable	Parameter	B	T	Sig.
PMSY1	Intercept	-50.429	-11.878	.000
	GDPZ1	1.533E-9	25.403	.000
	EXTTERNALDEBTZ3	2.801E-20	.848	.403
DPKT3	Intercept	-13.796	-1.946	.061
	GDPZ1	6.817E-10	6.767	.000
	EXTTERNALDEBTZ3	6.102E-20	1.107	.278
AGOY2	Intercept	-70.695	-10.040	.000
	GDPZ1	2.080E-9	20.791	.000
	EXTTERNALDEBTZ3	5.639E-21	.103	.919

Table 6 (Parameter Estimates for combined analysis)

Dependent Variable	Parameter	B	t	Sig.
PMSY1	Intercept	-40.887	-4.948	.000
	GDPZ1	7.537E-10	2.083	.047
	TOTALRESERVEZ2	5.183E-10	2.642	.014
	EXTERNALDEBTZ3	3.431E-14	2.382	.025
	GROSSNATIONALEXPENDITUREZ4	3.446E-14	1.387	.177
	GDPPERCAPITAZ5	.055	1.043	.306
AGOY2	Intercept	-105.443	-10.040	.000
	GDPZ1	2.477E-9	5.388	.000
	TOTALRESERVEZ2	-3.428E-10	-1.375	.181

	EXTERNALDEBTZ3	-3.214E-14	-1.756	.091
	GROSSNATIONALEXPENDITUREZ4	-1.772E-13	-5.613	.000
	GDPPERCAPITAZ5	.050	.753	.458
DPKY3	Intercept	5.943	.608	.548
	GDPZ1	1.247E-9	2.916	.007
	TOTALRESERVEZ2	7.001E-10	3.019	.006
	EXTERNALDEBTZ3	-1.621E-15	-.095	.925
	GROSSNATIONALEXPENDITUREZ4	-4.751E-14	-1.617	.118
	GDPPERCAPITAZ5	-.139	-2.232	.034

Table 7 (Residual SSCP Matrix for combined analysis)

		PMSY1	AGOY2	DPKY3
Covariance	PMSY1	70.951	-3.031	36.816
	AGOY2	-3.031	114.584	7.398
	DPKY3	36.816	7.398	99.186
Correlation	PMSY1	1.000	-.034	.439
	AGOY2	-.034	1.000	.069
	DPKY3	.439	.069	1.000

SOLVING SYSTEM OF INTEGRO-DIFFERENTIAL EQUATIONS USING A NEW HYBRID SEMI-ANALYTICAL METHOD

[1]George Albert Toma & [1]Shaza Alturky

[1]Department of Mathematics,

Aleppo University, Aleppo, Syria

Email: george.toma.1987@gmail.com, shazaalturkey@gmail.com

Abstract

This paper presents a new hybrid method that combines Kharrat-Toma transform technique with the homotopy perturbation method for the solutions of linear and nonlinear initial value problems represented by integro-differential equations systems with initial conditions. Where, the advantages of this hybrid approach are rapid convergence to an approximate or exact solution, reduces the computational steps and integrals which making it a highly efficient and applicable method compared with the classical methods. Therefore, this proposed new hybrid approach (Kharrat-Toma transform and homotopy perturbation method) can be apply to find the analytical solutions of integro-differential equations systems arising in many applications. To show the accuracy and effectiveness of the presented technique several examples are introduced.

Keywords*: Homotopy perturbation method, Kharrat-Toma transform, System of Integro-differential equations.*

INTRODUCTION

Integro-differential equations system arises in many fields of engineering, science and mathematical physics applications. Therefore, the researchers were interested in these types of equations, but sometimes it is difficult to solve it by traditional methods, so the researchers and academicians suggested new hybrid methods that are more efficient than classical methods. There are various analytical and numerical methods were used for these types of problems. Bakodah et.al [1] proposed method on the discrete Adomian decomposition method to solve Volterra integro-differential equations and Fredholm integro-differential equations. In [2] the Petrov-Galerkin method has been discussed for solving Integro-differential equations system. Jafarzadeh and Keramati presented numerical method based on Taylor polynomial for solving system of higher order linear integro differential equations [3]. Hesameddini and Rahimi introduced a new numerical scheme includes reconstruction of variational iteration method with Laplace transform to handle the systems of integro-differential equations [4]. Sinc-Derivative collocation method was used in [5] to solve second-order integro-differential boundary value problems.

In [6], Issa et.al, applied a collocation method using sinc functions and Chebyshev wavelet method to approximate the solution of systems of Volterra integro-differential equations. Hamaydi and Qatanania [7] employed the variational iteration method and the Taylor expansion to solve Volterra equation. Biazar and Ebrahimi [8] introduced an extension of Chebeyshev wavelets method to solve integro-differential equations systems. Moreover, many numerical methods were used for integro-differential equations systems, such as single term Walsh series [9], rationalized Haar functions [10], power series [11], differential transform [12], finite difference approximation method [13], homotopy perturbation method [14].

A new hybrid scheme based on Kharrat-Toma transform with homotopy perturbation method is suggested in this paper to find solutions of integro-differential equations systems. The proposed hybrid approach finds an infinite series solution, which convergence to an exact or approximate solution.

The article is ordered as follows: in Section 2, the Kharrat-Toma transform method is presented. The new hybrid method and methodology is outlined in Section 3. In Section 4, the proposed method is implemented for three numerical examples. Finally, conclusions are showed in Section 5.

KHARRAT-TOMA TRANSFORM METHOD:

The new Kharrat-Toma integral transform method is presented by Kharrat and Toma (2020) to solve initial or boundary value problems.

Definition: [15] The Kharrat-Toma integral transform technique of a function $f(x)$ is described as follows:

$$B\left[f(x)\right]=G(S)=s^3\int_0^{\infty} f(x)\,e^{\frac{-x}{s^2}}dx \quad , \quad x\geq 0$$

The inverse Kharrat-Toma integral transform is defined as:

$$f(x)=B^{-1}\left[G(S)\right]=B^{-1}\left[s^3\int_0^{\infty} f(x)\,e^{\frac{-x}{s^2}}dx\right]$$

The B^{-1} will be the inverse of the B integral transform. Where

$$B\left[f^{(n)}(x)\right]=\frac{1}{s^{2n}}G(s)-\sum_{k=0}^{n-1}s^{-2n+2k+5}f^{(k)}(0) \quad ; n\geq 1$$

Methodology

The methodology of the proposed hybrid method to solve system of linear and nonlinear integro-differential equations is illustrated in this section.

Consider the system of integro-differential equations as follows:

$$\begin{cases} f_1^{(n)}(x)=\psi_1\left(x,f_2(x),...,f_2^{(n)}(x),f_3(x),...,f_3^{(n)}(x),f_m(x),...,f_m^{(n)}(x)\right)+\int_0^x K_1\left(x,t,f_1(t),...,f_1^{(n)}(t),...,f_m(t),...,f_m^{(n)}(t)\right)dt \\ f_2^{(n)}(x)=\psi_2\left(x,f_1(x),...,f_1^{(n)}(x),f_3(x),...,f_3^{(n)}(x),f_m(x),...,f_m^{(n)}(x)\right)+\int_0^x K_2\left(x,t,f_1(t),...,f_1^{(n)}(t),...,f_m(t),...,f_m^{(n)}(t)\right)dt \\ \vdots \\ f_m^{(n)}(x)=\psi_m\left(x,f_1(x),...,f_1^{(n)}(x),f_2(x),...,f_2^{(n)}(x),f_{m-1}(x),...,f_{m-1}^{(n)}(x)\right)+\int_0^x K_m\left(x,t,f_1(t),...,f_1^{(n)}(t),...,f_m(t),...,f_m^{(n)}(t)\right)dt \end{cases} \quad (1)$$

With initial conditions

$$f_m^{(n)}(0)=\alpha_{n,m} \quad , \quad \alpha_{n,m}=const \quad , \quad n=0,1,...,a-1 \quad , \quad m=1,2,...,b$$

Taking the Kharrat-Toma transform on (1), yields

$$\begin{cases} \frac{1}{s^{2n}}B(f_1)-\sum_{k=0}^{n-1}s^{-2n+2k+5}f_1^{(k)}(0)=B\left[\psi_1\left(x,f_2(x),...,f_2^{(n)}(x),f_3(x),...,f_3^{(n)}(x),f_m(x),...,f_m^{(n)}(x)\right)\right] \\ \qquad +B\left[\int_0^x K_1\left(x,t,f_1(t),...,f_1^{(n)}(t),...,f_m(t),...,f_m^{(n)}(t)\right)dt\right] \\ \frac{1}{s^{2n}}B(f_2)-\sum_{k=0}^{n-1}s^{-2n+2k+5}f_2^{(k)}(0)=B\left[\psi_2\left(x,f_1(x),...,f_1^{(n)}(x),f_3(x),...,f_3^{(n)}(x),f_m(x),...,f_m^{(n)}(x)\right)\right] \\ \qquad +B\left[\int_0^x K_2\left(x,t,f_1(t),...,f_1^{(n)}(t),...,f_m(t),...,f_m^{(n)}(t)\right)dt\right] \\ \vdots \\ \frac{1}{s^{2n}}B(f_m)-\sum_{k=0}^{n-1}s^{-2n+2k+5}f_m^{(k)}(0)=B\left[\psi_m\left(x,f_1(x),...,f_1^{(n)}(x),f_2(x),...,f_2^{(n)}(x),f_{m-1}(x),...,f_{m-1}^{(n)}(x)\right)\right] \\ \qquad +B\left[\int_0^x K_m\left(x,t,f_1(t),...,f_1^{(n)}(t),...,f_m(t),...,f_m^{(n)}(t)\right)dt\right] \end{cases} \quad (2)$$

Then

$$
\begin{cases}
B\left(f_1\right)=\sum_{k=0}^{n-1} s^{2k+5} f_1{}^{(k)}(0)+s^{2n}B\left[\psi_1\left(x,f_2(x),...,f_2{}^{(n)}(x),f_3(x),...,f_3{}^{(n)}(x),f_m(x),...,f_m{}^{(n)}(x)\right)\right] \\
\qquad\qquad +s^{2n}B\left[\int_0^x K_1\left(x,t,f_1(t),...,f_1{}^{(n)}(t),...,f_m(t),...,f_m{}^{(n)}(t)\right)dt\right] \\
B\left(f_2\right)=\sum_{k=0}^{n-1} s^{2k+5} f_2{}^{(k)}(0)+s^{2n}B\left[\psi_2\left(x,f_1(x),...,f_1{}^{(n)}(x),f_3(x),...,f_3{}^{(n)}(x),f_m(x),...,f_m{}^{(n)}(x)\right)\right] \\
\qquad\qquad +s^{2n}B\left[\int_0^x K_2\left(x,t,f_1(t),...,f_1{}^{(n)}(t),...,f_m(t),...,f_m{}^{(n)}(t)\right)dt\right] \\
\vdots \\
B\left(f_m\right)=\sum_{k=0}^{n-1} s^{2k+5} f_m{}^{(k)}(0)+s^{2n}B\left[\psi_m\left(x,f_1(x),...,f_1{}^{(n)}(x),f_2(x),...,f_2{}^{(n)}(x),f_{m-1}(x),...,f_{m-1}{}^{(n)}(x)\right)\right] \\
\qquad\qquad +s^{2n}B\left[\int_0^x K_m\left(x,t,f_1(t),...,f_1{}^{(n)}(t),...,f_m(t),...,f_m{}^{(n)}(t)\right)dt\right]
\end{cases} \tag{3}
$$

The homotopy of (3) can be written as:

$$
\begin{cases}
B\left(f_1\right)=\sum_{k=0}^{n-1} s^{2k+5} f_1{}^{(k)}(0)+p\,s^{2n}B\left[\psi_1\left(x,f_2(x),...,f_2{}^{(n)}(x),f_3(x),...,f_3{}^{(n)}(x),f_m(x),...,f_m{}^{(n)}(x)\right)\right] \\
\qquad\qquad +p\,s^{2n}B\left[\int_0^x K_1\left(x,t,f_1(t),...,f_1{}^{(n)}(t),...,f_m(t),...,f_m{}^{(n)}(t)\right)dt\right] \\
B\left(f_2\right)=\sum_{k=0}^{n-1} s^{2k+5} f_2{}^{(k)}(0)+p\,s^{2n}B\left[\psi_2\left(x,f_1(x),...,f_1{}^{(n)}(x),f_3(x),...,f_3{}^{(n)}(x),f_m(x),...,f_m{}^{(n)}(x)\right)\right] \\
\qquad\qquad +p\,s^{2n}B\left[\int_0^x K_2\left(x,t,f_1(t),...,f_1{}^{(n)}(t),...,f_m(t),...,f_m{}^{(n)}(t)\right)dt\right] \\
\vdots \\
B\left(f_m\right)=\sum_{k=0}^{n-1} s^{2k+5} f_m{}^{(k)}(0)+p\,s^{2n}B\left[\psi_m\left(x,f_1(x),...,f_1{}^{(n)}(x),f_2(x),...,f_2{}^{(n)}(x),f_{m-1}(x),...,f_{m-1}{}^{(n)}(x)\right)\right] \\
\qquad\qquad +p\,s^{2n}B\left[\int_0^x K_m\left(x,t,f_1(t),...,f_1{}^{(n)}(t),...,f_m(t),...,f_m{}^{(n)}(t)\right)dt\right]
\end{cases} \tag{4}
$$

Where $p\in[0,1]$ is an embedding parameter.

According to the homotopy perturbation method HPM the solution of (4) can be written as a power series in p

$$f_m = \sum_{i=0}^{\infty} p^i f_{m_i} \tag{5}$$

Substituting (5) into (4), and comparing the coefficients of terms with identical powers of *p* and taking the inverse Kharrat-Toma transform, gives

Setting $p = 1$, we get the approximate solution of (1)

$$f_m(x) = \sum_{i=0}^{\infty} f_{m_i}(x)$$

Numerical Examlpes

In this part, we will implement the proposed hybrid approach for three integro-differential equations systems to test the power and efficiency of this new hybrid technique.

Example .1

Consider the nonlinear integro-differential equation system of the form:

$$\begin{cases} u'(x) = 2x + \dfrac{x^4}{6} + \dfrac{2x^6}{15} + \displaystyle\int_0^x (x - 2t)\left(u^2(t) + v(t)\right)dt \\ v'(x) = -2x - \dfrac{x^4}{6} + \dfrac{2x^6}{15} + \displaystyle\int_0^x (x - 2t)\left(u(t) + v^2(t)\right)dt \end{cases} \tag{6}$$

With initial conditions

$u(0) = 1 \ , \ v(0) = 1$

Taking the Kharrat-Toma transform on (6), finds

$$\begin{cases} \dfrac{1}{s^2} B(u) - s^3 u(0) = B\left[2x + \dfrac{x^4}{6} + \dfrac{2x^6}{15}\right] + B\left[\displaystyle\int_0^x (x - 2t)\left(u^2(t) + v(t)\right)dt\right] \\ \dfrac{1}{s^2} B(v) - s^3 v(0) = B\left[-2x - \dfrac{x^4}{6} + \dfrac{2x^6}{15}\right] + B\left[\displaystyle\int_0^x (x - 2t)\left(u(t) + v^2(t)\right)dt\right] \end{cases} \tag{7}$$

Then we have

$$\begin{cases} B\left(u\right)=s^5+s^2B\left[2x+\dfrac{x^4}{6}+\dfrac{2x^6}{15}\right]+s^2B\left[\displaystyle\int_0^x\left(x-2t\right)\left(u^2(t)+v(t)\right)dt\right] \\ B\left(v\right)=s^5+s^2B\left[-2x-\dfrac{x^4}{6}+\dfrac{2x^6}{15}\right]+s^2B\left[\displaystyle\int_0^x\left(x-2t\right)\left(u(t)+v^2(t)\right)dt\right] \end{cases} \tag{8}$$

Now, constructing the homotopy on (8) as follows

$$\begin{cases} B\left(u\right)=s^5+s^2B\left[2x+\dfrac{x^4}{6}+\dfrac{2x^6}{15}\right]+ps^2B\left[\displaystyle\int_0^x\left(x-2t\right)\left(u^2(t)+v(t)\right)dt\right] \\ B\left(v\right)=s^5+s^2B\left[-2x-\dfrac{x^4}{6}+\dfrac{2x^6}{15}\right]+ps^2B\left[\displaystyle\int_0^x\left(x-2t\right)\left(u(t)+v^2(t)\right)dt\right] \end{cases} \tag{9}$$

Substituting (5) into (9), we get

$$\begin{cases} B\left(\displaystyle\sum_{i=0}^{\infty}p^i u_i\right)=s^5+s^2B\left[2x+\dfrac{x^4}{6}+\dfrac{2x^6}{15}\right]+ps^2B\left[\displaystyle\int_0^x\left(x-2t\right)\left(\left(\sum_{i=0}^{\infty}p^i u_i(t)\right)^2+\sum_{i=0}^{\infty}p^i v_i(t)\right)dt\right] \\ B\left(\displaystyle\sum_{i=0}^{\infty}p^i v_i\right)=s^5+s^2B\left[-2x-\dfrac{x^4}{6}+\dfrac{2x^6}{15}\right]+ps^2B\left[\displaystyle\int_0^x\left(x-2t\right)\left(\sum_{i=0}^{\infty}p^i u_i(t)+\left(\sum_{i=0}^{\infty}p^i v_i(t)\right)^2\right)dt\right] \end{cases} \tag{10}$$

Comparing coefficients of terms with identical powers of p in (10), leads to

$$p^0:\begin{cases} B\left[u_0\right]=s^5+s^2B\left[2x+\dfrac{x^4}{6}+\dfrac{2x^6}{15}\right] \\ B\left[v_0\right]=s^5+s^2B\left[-2x-\dfrac{x^4}{6}+\dfrac{2x^6}{15}\right] \end{cases} \tag{11}$$

$$p^1:\begin{cases} B\left[u_1\right]=s^2B\left[\displaystyle\int_0^x\left(x-2t\right)\left(\left(u_0(t)\right)^2+v_0(t)\right)dt\right] \\ B\left[v_1\right]=s^2B\left[\displaystyle\int_0^x\left(x-2t\right)\left(u_0(t)+\left(v_0(t)\right)^2\right)dt\right] \end{cases} \tag{12}$$

Taking the inverse Kharrat-Toma transform of Equations. (11) and (12), yields

$$\begin{cases} u_0 = 1 + x^2 + \dfrac{x^5}{30} + \dfrac{2x^7}{105} \\ v_0 = 1 - x^2 - \dfrac{x^5}{30} + \dfrac{2x^7}{105} \end{cases}$$

$$\begin{cases} u_1 = -\dfrac{x^5}{30} - \dfrac{2x^7}{105} - \dfrac{x^8}{2016} - \dfrac{13x^{10}}{10800} - \dfrac{x^{12}}{3850} - \dfrac{x^{13}}{154440} - \dfrac{4x^{15}}{716625} - \dfrac{x^{17}}{803250} \\ v_0 = \dfrac{x^5}{30} - \dfrac{2x^7}{105} + \dfrac{x^8}{2016} - \dfrac{13x^{10}}{10800} + \dfrac{x^{12}}{3850} - \dfrac{x^{13}}{154440} + \dfrac{4x^{15}}{716625} - \dfrac{x^{17}}{803250} \end{cases}$$

Table 1. shows the comparison of absolute errors results by taking two terms $u_0 + u_1$ and $v_0 + v_1$ of the proposed hybrid method.

Where the exact solution of Eqn. (6) is

$u(x) = 1 + x^2$, $v(x) = 1 - x^2$

TABLE 1: The comparison of absolute errors for Example 1

x	Error of proposed hybrid method (n=2) u_0+u_1	Error of proposed hybrid method (n=2) v_0+v_1
0	0	0
0.1	5.08100 e -12	4.84020 e -12
0.2	1.39417 e -09	1.14763 e -09
0.3	3.97915 e -08	2.55740 e -08
0.4	4.55704 e -07	2.03182 e -07
0.5	3.17750 e -06	8.24916 e -07
0.6	1.61865 e -05	1.61245 e -06
0.7	6.62842 e -05	1.85040 e -06
0.8	2.30897 e -04	2.83648 e -05
0.9	7.09592 e -04	1.33526 e -04
1	1.97278 e -03	4.50070 e -04

Example .2

Consider the system of nonlinear integro-differential equation

$$\begin{cases} u''(x) = 1 - \dfrac{x^3}{3} - \dfrac{1}{2}v'^2(x) + \dfrac{1}{2}\displaystyle\int_0^x \left(u^2(t) + v^2(t)\right)dt \\ v''(x) = -1 + x^2 - x\,u(x) + \dfrac{1}{4}\displaystyle\int_0^x \left(u^2(t) - v^2(t)\right)dt \end{cases} \tag{13}$$

With initial conditions

$u(0) = 1$, $u'(0) = 2,$, $v(0) = -1$, $v'(0) = 0$

Taking the Kharrat-Toma transform on (13), yields

$$\begin{cases} \dfrac{1}{s^4}B(u) - s\,u(0) - s^3u'(0) = B\left[1 - \dfrac{x^3}{3}\right] + B\left[-\dfrac{1}{2}v'^2(x) + \dfrac{1}{2}\displaystyle\int_0^x \left(u^2(t) + v^2(t)\right)dt\right] \\ \dfrac{1}{s^4}B(v) - s\,v(0) - s^3v'(0) = B\left[-1 + x^2\right] + B\left[-x\,u(x) + \dfrac{1}{4}\displaystyle\int_0^x \left(u^2(t) - v^2(t)\right)dt\right] \end{cases} \tag{14}$$

Then we have

$$\begin{cases} B(u) = s^5 + 2s^7 + s^4B\left[1 - \dfrac{x^3}{3}\right] + s^4B\left[-\dfrac{1}{2}v'^2(x) + \dfrac{1}{2}\displaystyle\int_0^x \left(u^2(t) + v^2(t)\right)dt\right] \\ B(v) = -s^5 + s^4B\left[-1 + x^2\right] + s^4B\left[-x\,u(x) + \dfrac{1}{4}\displaystyle\int_0^x \left(u^2(t) - v^2(t)\right)dt\right] \end{cases} \tag{15}$$

Now, constructing the homotopy on (15) as follows

$$\begin{cases} B(u) = s^5 + 2s^7 + p\,s^4B\left[1 - \dfrac{x^3}{3}\right] + p\,s^4B\left[-\dfrac{1}{2}v'^2(x) + \dfrac{1}{2}\displaystyle\int_0^x \left(u^2(t) + v^2(t)\right)dt\right] \\ B(v) = -s^5 + p\,s^4B\left[-1 + x^2\right] + p\,s^4B\left[-x\,u(x) + \dfrac{1}{4}\displaystyle\int_0^x \left(u^2(t) - v^2(t)\right)dt\right] \end{cases} \tag{16}$$

Substituting (5) into (16), we get

$$\begin{cases} B\left(\displaystyle\sum_{i=0}^{\infty} p^i u_i\right) = s^5 + 2s^7 + p\,s^4B\left[1 - \dfrac{x^3}{3}\right] + p\,s^4B\left[-\dfrac{1}{2}\left(\displaystyle\sum_{i=0}^{\infty} p^i v_i'(x)\right)^2 + \dfrac{1}{2}\displaystyle\int_0^x \left(\left(\sum_{i=0}^{\infty} p^i u_i(t)\right)^2 + \left(\sum_{i=0}^{\infty} p^i v_i(t)\right)^2\right)dt\right] \\ B\left(\displaystyle\sum_{i=0}^{\infty} p^i v_i\right) = -s^5 + p\,s^4B\left[-1 + x^2\right] + p\,s^4B\left[-x\displaystyle\sum_{i=0}^{\infty} p^i u_i(x) + \dfrac{1}{4}\displaystyle\int_0^x \left(\left(\sum_{i=0}^{\infty} p^i u_i(t)\right)^2 - \left(\sum_{i=0}^{\infty} p^i v_i(t)\right)^2\right)dt\right] \end{cases} \tag{17}$$

Comparing coefficients of terms with identical powers of *p* in (17) and taking the inverse Kharrat-Toma transform of equations results, yields

$$\begin{cases} u_0 = 1 + 2x + \dfrac{x^2}{2} - \dfrac{x^6}{60} \\ v_0 = -1 - \dfrac{x^2}{2} + \dfrac{x^4}{12} \end{cases}$$

$$\begin{cases} u_1 = \dfrac{x^3}{6} + \dfrac{x^4}{24} + \dfrac{x^5}{20} + \dfrac{7x^6}{360} + \dfrac{x^7}{1260} - \dfrac{x^8}{960} - \dfrac{x^9}{6720} - \dfrac{x^{10}}{86400} + \dfrac{x^{11}}{285120} + \dfrac{x^{13}}{12355200} \\ v_1 = -\dfrac{x^3}{6} - \dfrac{x^4}{8} - \dfrac{x^5}{120} + \dfrac{x^6}{240} + \dfrac{x^7}{5040} + \dfrac{11x^8}{40320} + \dfrac{x^9}{120960} - \dfrac{x^{10}}{172800} - \dfrac{x^{11}}{570240} + \dfrac{x^{13}}{24710400} \end{cases}$$

Table 2. shows the comparison of absolute errors results by taking two terms $u_0 + u_1$ and $v_0 + v_1$ of the proposed hybrid method.

Where the exact solution of Eqn. (13) is

$u(x) = x + e^x$, $v(x) = x - e^x$

TABLE 2: The comparison of absolute errors for Example 2

x	Error of proposed hybrid method (n=2) u_0+u_1	Error of proposed hybrid method (n=2) v_0+v_1
0	0	0
0.1	2.68180 e -07	5.52251 e -09
0.2	9.16053 e -06	3.61242 e -07
0.3	7.39692 e -05	4.15692 e -06
0.4	3.30191 e -04	2.36034 e -05
0.5	1.06355 e -03	9.10839 e -05
0.6	2.78356 e -03	2.75379 e -04
0.7	6.30713 e -03	7.03698 e -04
0.8	1.28500 e -02	1.59025 e -03
0.9	2.41216 e -02	3.27218 e -03
1	4.24245 e -02	6.25383 e -03

Example .3

Consider the system of integro-differential equation

$$\begin{cases} u''(x) = -1 - x + \cosh x - \dfrac{\sin^3 x}{3} - \sinh x + e^x + \displaystyle\int_0^x \left(\left(e^{-t} \right) u(t) + \left(\sin^2 t \right) v(t) \right) dt \\ v''(x) = -3 + x^2 - \dfrac{2x^3}{3} - 2(x-1)e^x + \displaystyle\int_0^x \left(\left(x^2 - t^2 \right) u(t) + (x-t) v(t) \right) dt \end{cases} \tag{18}$$

With initial conditions

$u(0) = 2$, $u'(0) = 1$, , $v(0) = 1$, $v'(0) = 0$

And the same technique as example .1 and .2, we get

$$\begin{cases} u_0 = 2 + x + \dfrac{x^2}{2} - \dfrac{x^3}{6} + \dfrac{x^4}{12} - \dfrac{x^5}{60} + \dfrac{x^6}{360} + \dfrac{x^7}{252} + \dfrac{x^8}{20160} - \dfrac{13x^9}{25920} + \dfrac{x^{10}}{1814400} + \dfrac{41x^{11}}{997920} \\ v_0 = 1 - \dfrac{x^2}{2} - \dfrac{x^5}{15} - \dfrac{x^6}{120} - \dfrac{x^7}{630} - \dfrac{x^8}{4032} - \dfrac{x^9}{30240} - \dfrac{x^{10}}{259200} - \dfrac{x^{11}}{2494800} \end{cases}$$

$$\begin{cases} u_1 = \dfrac{x^3}{3} - \dfrac{x^4}{24} + \dfrac{x^5}{40} - \dfrac{x^6}{240} - \dfrac{x^7}{504} - \dfrac{29x^8}{40320} + \dfrac{227x^9}{362880} - \dfrac{491x^{10}}{3628800} - \dfrac{563x^{11}}{19958400} + \dfrac{259x^{12}}{17107200} + \dfrac{359x^{13}}{141523200} - \dfrac{51221x^{14}}{43589145600} + \ldots \\ v_1 = \dfrac{x^4}{24} + \dfrac{x^5}{15} + \dfrac{x^6}{144} + \dfrac{x^7}{630} - \dfrac{x^8}{4032} + \dfrac{x^9}{22680} - \dfrac{17x^{10}}{1814400} + \dfrac{x^{11}}{1663200} + \dfrac{x^{12}}{1368576} + \dfrac{x^{13}}{222393600} - \dfrac{41x^{14}}{889574400} + \ldots \end{cases}$$

Table 3. shows the comparison of absolute errors results by taking two terms $u_0 + u_1$ and $v_0 + v_1$ of the proposed hybrid method.

Where the exact solution of Eqn. (18) is

$u(x) = e^x + 1$, $v(x) = \cos x$

TABLE 3: The comparison of absolute errors for Example 3

x	Error of proposed hybrid method (n=2) u_0+u_1	Error of proposed hybrid method (n=2) v_0+v_1
0	0	0
0.1	1.86384 e -09	2.71720 e -11
0.2	1.56480 e -07	1.28777 e -09
0.3	1.67907 e -06	3.40049 e -08
0.4	8.88811 e -06	3.39780 e -07
0.5	3.20504 e -05	2.02536 e -06
0.6	9.07880 e -05	8.71294 e -06
0.7	2.18214 e -04	2.99323 e -05
0.8	4.66190 e -04	8.72269 e -05
0.9	9.12492 e -04	2.24188 e -04
1	1.67100 e -03	5.21873 e -04

CONCLUSIONS

In conclusion, a new hybrid method to solve systems of integro-differential equations is suggested. The presented method is depended on the hybridization between Kharrat-Toma transform with the homotopy perturbation method. The new hybrid approach is easy to apply and reduce the computational steps compared to other traditional methods. Thus, the new hybrid method can be applied to solve several integro-differential equations systems arising in many applications.

REFERENCES

1. Bakodah H. O, Al-Mazmumy M, Almuhalbedi S. O. "Solving System of Integro Differential Equations using Discrete Adomian Decomposition Method". Journal of Taibah University for Science, Taylor & Francis, 13: 805-812, 2019.
2. Rabbani M. "Existence of Solution and Solving the Integro-Differential Equations System by the multi-wavelet Petrov-Galerkin Method". Int. J. Nonlinear Anal. Appl. 7: 207-218, 2008.

3. Jafarzadeh Y, Keramati B. "Numerical Method for a system of integro-differential equations and convergence analysis by Taylor Collocation". Ain Shams Engineering Journal, 9: 1433-1438, 2018.
4. Hesameddini E, Rahimi A. "A New Numerical Scheme for Solving Systems of Integro-differential equations", Computational Methods for Differential Equations, 2: 108-119, 2013.
5. Abdella K, Ross G. "Solving Integro-Differential Boundary Value Problems Using Sinc-Derivative Collocation", Mathematics, MDPI, PP:1-13, 2020.
6. Issa A, Qatanani N, Daraghmeh A. "Approximate Techniques for Solving Linear of Volterra Integro-Differential Equations", Journal of Applied Mathematics, Hindawi, PP:1-13, 2008.
7. Hamaydi J, Qatannani N. "Computational Methods for Solving Linear fuzzy Volterra integral equation", Journal of Applied Mathematics, Hindawi, PP:1-12, 2017.
8. Biazar J, Ebrahimi H. "A Strong Method for Solving Systems of Integro-Differential Equations", Applied Mathematics , Scientific Research, 2: 1105-1113, 2011.
9. Sekar R, Murugesan K. "System of linear second order Volterra integro-differential equations using single term walsh series technique", Applied Mathematics and Computation, 273:484-492, 2016.
10. Maleknejad K, Mirzaee F, Sezerb M. "Solving Linear integro-differential equations system by using rational Haar functions method", Applied Mathematics and Computation, 2:317-328, 2004.
11. Gachpazan M. "Numerical scheme to solve integro-differential equations system", Journal of Advanced Research in Scientific Computing, Vol. 1, No. 1, 2009.
12. Arikolgu A, Ozkol I. "Solutions of integral and integro-differential equations systems by using differential transform method", Computers and Mathematics with Applications, 9:2411-2417, 2008.
13. Jangveladze T, Kiguradze Z, Neta B. "Finite difference approximation of a nonlinear integro-differential system", Applied Mathematics and Computations, 215: 615-628, 2009.
14. Biazar J, Ghazvini, Eslami M. "He's homotopy perturbation method for systems of integro-differential equations", Chaos Solitons and Fractals, 39:1253-1258, 2009.
15. Kharrat B. N, Toma A. G, "A New Integral Transform: Kharrat-Toma Transform and Its Properties", World Applied Science Journal, 38(5):436-443, 2020.

A NEW APPROACH TO CONSTRUCT (K, N) THRESHOLD SECRET SHARING SCHEMES BASED ON FINITE FIELD EXTENSION

[1]*Vanashree Gupta* & [2]*Smita* Bedekar

Interdisciplinary School of Scientific Computing,
Savitribai Phule Pune University, Pune , Maharashtra, India
Email: [1]vanashreegupta@gmail.com ,[2]smitab@unipune.ac.in

Abstract
With increase in use of internet there is need to keep passwords, secret keys, important information secret. One way to do this is encryption. But it also need key which should be kept secure. Sometimes key is secure. But what will happens if the key is lost, forgotten etc. This problem can be solved using secret sharing. Instead of sharing whole secret, it is divided into pieces and distributed to finite set of pieces and some subset of pieces called access structure of scheme, which can recover secret. Here we propose a new way to construct threshold secret sharing schemes based on finite field extension using Blakley's secret sharing as a base. It is useful in many cryptographic applications and security. Because of finite fields the size of numbers stays within a specified range, doesn't matter how many operations we apply on number.

Keywords: *Finite Field extension, Secret Sharing Scheme, Blakley's secret sharing, Access structure, Security*

1. Introduction
A secret sharing is useful in hiding information among certain pieces called shares\shadows and distributed to those many people. This is called share distribution. When particular subset of pieces called access structure joined together will get the complete secret. This is called secret recovery. There are lots of studies about secret sharing schemes. Shamir's secret sharing [1] which is polynomial interpolation based, Blakley's Secret Sharing [2] is hyperplane based, Asmuth Bloom Secret Sharing [3][23] based on Chinese remainder theorem, Mignotte Secret Sharing [5] based on Chinese remainder theorem [4] . Beimel [7] gave detail study about construction of secret sharing schemes. Shalini et al [23] proposed secret sharing scheme based on elliptic curve and gave a comparative analysis of secret sharing schemes with special reference to e-commerce applications. [8] explains about various multifarious secret sharing schemes, their applications and the comparison based on various extended capabilities.In [25] an alternative way to Shamir's secret sharing scheme lagrange interpolation over finite field is proposed.

Here we proposed a new way to construct a threshold secret sharing scheme. We use Blakley's secret sharing as a base and same technique of finite field can be used to construct new scheme using Shamir's secret sharing as base.

1.1 Our Contribution

In this work, we provide a brief overview of existing threshold secret sharing schemes Shamir's secret sharing [1] and Blakley's Secret Sharing [2] .The proposed secret sharing is based on finite field extension and Blakley secret sharing. Based on different parameters the proposed method is compared with existing ones. Here we also claim that same finite field extension method can be used over Shamir's secret sharing to improve the results.

1.2 Organization

The rest of the paper is organized as follows: Section 2 covers required background and preliminaries. Section 3 gives an idea of proposed method. Section 4 is about analysis and discussion of proposed scheme. Section 5 concludes with final remarks.

2. Background & Preliminaries

A secret sharing scheme is a method in which a dealer distributes shares to participants such that only authorized subsets of participants can reconstruct secret [7].

2.1 Threshold secret sharing scheme

In secret sharing there is one dealer and n players. The dealer distributes shares to each player in such a way that any group of t (for threshold) or more players can together reconstruct the secret but no group of fewer than t players can(perfect) . Such a system is called a (t,n) - threshold scheme [19].

2.2 Shamir's secret sharing scheme [1]

Adi- Shamir idea for secret scheme was 2 points can define a line, 3 points can define a parabola, 4 points a cubic curve and so forth [22]. k points are sufficient to define a polynomial of degree(k-1). Shamir's secret sharing is linear approach based on Lagrange's polynomial interpolation. The correctness and privacy of Shamir's scheme is due to this [7]. It has two parameters: *t*, the threshold and *n*, the number of participants / players. The main idea of the scheme is that *t* points are sufficient to define a polynomial of degree *t* -1.

Given (t,n) secret sharing with k as secret and n shareholders { P_1,P_2,P_3, …..,P_n}. Using t-1 degree random polynomial with random coefficient.

Step 1: Polynomial construction

$f(x)=a_0+a_1x+a_2x^2+\ldots\ldots+a_{t-1}x^{t-1}(\text{mod } p)$

Step 2: Share distribution

$\text{Share}_i(s)=(x_i,f(x_i))$

Step 3: Secret recovery

Using Lagrange Interpolation formula, the polynomial f(x) can be written in the form

$$f(x) = \sum_{i=0}^{t-1} f(x_i) * L_i(x)$$

where $L_i(x)$ is the Lagrange Polynomial.

$$L_i(x) = \prod_{j=0, j \neq i}^{t-1} \frac{x - x_j}{x_i - x_j}$$

$L_i(x)$ has value 1 at x_i, and 0 at every other x_j .

This scheme have some limitations like computationally hard, larger the share size, more memory is required which lowers the efficiency etc [25].

2.3 Blakley's secret sharing scheme [2]

As per [2][16] Blakley is based on hyper plane geometry.To solve a (t, n) threshold secret sharing scheme problem,each of the participant is given a hyper-plane equation in a t dimensional space over a finite field such that each hyper plane passes through a certain point. When t participants come together, they can solve the system of equations to find the secret.The point of intersection of the hyper planes is the secret in t dimensional space.An affine hyper plane in a t-dimensional space with coordinates in a field F can be described by a linear equation of the following form:

$a_1 x_1 + a_2 x_2 + ... + a_t x_t = b$

Reconstruction or recovery of original secret is simply by solving a linear system of equations.By finding the inter-section of any t of these hyper planes will get intersection point(secret). The secret can be any of the coordinates of the intersection point or any function of the coordinates. The most common application of Blakley's scheme is in distributing a key between different participants and reconstructing the key based on each share. Due to large space states this method is not efficient enough.

3. MATHEMATICAL FORMULATION OF THE PROBLEM

Assume the number of elements of field extension be $q = p^m$ (p is prime and $m \in Z+$). We choose the secret and IDs of participants from the following set.

$Mq = \{u \mid 0 \leq u \leq q\ 1, u \in Z\}$……(1)

One way to define Galois field or Finite fields is to transform the selected integers to the polynomials of (GF(q))[x] by Algorithm 1 as follows :

Algorithm 1.

Input: $u \in Mq$

Output: $v \in GF(q)$ or F(q) [Finite fields are also called as Galois fields].

Step 1: u is transformed into vectors of length with respect to base .

Step 2: All these vectors can be written as a polynomial in $F_q[x]$.

Example 1. Consider $7 \in M_8 \Rightarrow 7 = (111)_2 = \theta^2 + \theta + 1 \in GF(8)$, where θ is a primitive element of GF(8).

Example 2. Consider $5 \in M_9 \Rightarrow 5 = (12)_3 = \theta + 2 \in GF(9)$, where θ is a primitive

element of GF(9).

Then obtained polynomials can be transformed to integers by Algorithm 2 as follows:

Algorithm 2.

Input: $v \in GF(q)$

Output: $u \in Mq$

Step 1: v is transformed into vectors of length m with respect to base p.

Step 2: These vectors are written with respect to base 10.

Example 3. Let $\theta^2+\theta+1 \in GF(8) \Rightarrow \theta^2+\theta+1 = (111)_2 = 7 \in M_8$, where θ is a primitive element (root) of GF(8).

Example 4. Let $2\theta + 1 \in GF(9) \Rightarrow 5 = (21)_3 = 7 \in M_9$, where θ is a primitive element of GF(9).

3.1 Proposed Scheme using Blakley's secret sharing scheme as base

Consider the finite field F_q is the secret space. Here we are proposing a (k,n) threshold scheme based on Blakley's method i.e. at least k participants out of n will recover the secret.

Steps for Share Distribution :

1) Choose any vector $x=(x_1,x_2,x_3,\ldots x_m) \in Mq$ whose first coordinate (here x_1) is the secret.

2) Consider n vectors of length m to find the secret pieces for all n participants.

3) Let these be A_{u1} , A_{u2} , A_{u3} ,…., A_{un} .

4) Then calculate the secret pieces for each n participants such that

$Y_{u\,1} = A_{u1} \,.\, x^T$

$Y_{u\,2} = A_{u2} \,.\, x^T$

$Y_{u\,3} = A_{u3} \,.\, x^T$

…..

$Y_{u\,n} = A_{un} \,.\, x^T$

5) Transform values of $Y_{u\,i}$ $(1 \leq i \leq n)$ to the elements of Fq .

Steps for Secret Recovery:

Assume that $u_1,u_2,u_3,\ldots,u_k$ participants can recover the secret.Here it is the following linear equation system.

$Y = A \cdot x^T$

$$\begin{pmatrix} A_{u1} \\ A_{u2} \\ A_{u3} \\ \ldots\ldots \\ A_{uk} \end{pmatrix} \cdot \begin{pmatrix} x_1 \\ x_2 \\ x_3 \\ \ldots\ldots \\ x_k \end{pmatrix} = \begin{pmatrix} Y_{u1} \\ Y_{u2} \\ Y_{u3} \\ \ldots\ldots \\ Y_{uk} \end{pmatrix}$$

The secret can be reached by solving above system of equation.

If the matrix A is non-singular, then the secret can be recovered. Otherwise it cannot be recovered.

Example 5. Let F_8 be the secret space, the number of participants n= 5, the threshold value k=3 and the secret s = 4. Construct a secret sharing scheme based on F_8 with these parameters by using Blakley's method.

Consider the polynomial $f(x) = x^3+x^2+1$ which is irreducible over F_2. Let Θ be a root of f. We know that if $f \in F_2[x]$ is an irreducible polynomial over F_2 degree , then by adjoining a root of f to F_2, we get a finite field with 2^d elements[24].

Assume θ to be a root of irreducible polynomial f(x). The elements of F_8 are as following.

$F_8 = \{ 0, 1, \theta, \theta+1, \theta^2, \theta^2+1, \theta^2+\theta, \theta^2+\theta+1\}$

$\theta^1 = \theta$

$\theta^2 = \theta^2$

$\theta^3 = \theta^2+1$

$\theta^4=\theta^2+\theta+1$

$\theta^5=\theta+1$

$\theta^6=\theta^2+\theta$

$\theta^{7=} \theta^0 =1$

The transformation between M_8 and F_8 is as follows.

$0 \longrightarrow 0$

$1 \longrightarrow 1$

$2 \longrightarrow \theta$

$3 \longrightarrow \theta + 1$

$4 \longrightarrow \theta^2$

$5 \longrightarrow \theta^2 + 1$

$6 \longrightarrow \theta^2 + \theta$

$7 \longrightarrow \theta^2 + \theta + 1$

We choose the vector $(5, 2, 3) \in M_8$ whose first coordinate $x_1=5$ is the secret.

Since the scheme will be (3, 5)-threshold scheme, we consider the five vectors as the participants.

Let us these vectors be

$A_{u1} = (0, 2, 2)$

$A_{u2} = (1, 3, 3)$

$A_{u3} = (1, 5, 5)$

$A_{u4} = (0, 3, 2)$

$A_{u5} = (5, 2, 5)$

These vectors correspond to the following vectors in $F_8[x]$.

$A_{u1}' = (0, \theta, \theta)$

$A_{u2}' = (1, \theta + 1, \theta + 1)$

$A_{u3}' = (1, \theta^2 + 1, \theta^2 + 1)$

$A_{u4}' = (0, \theta + 1, \theta)$

$A_{u5}' = (\theta^2 + 1, \theta, \theta^2 + 1)$

Now we calculate the secret pieces as below.

$Y_{u\,1} = (0, \theta, \theta) .(\theta^2 + 1, \theta, \theta+1)^T = \theta$

$Y_{u2} = (1, \theta + 1, \theta + 1) .(\theta^2 + 1, \theta, \theta+1)^T$

$= \theta^2+\theta=\theta^6$

$Y_{u3} = (1, \theta^2 + 1, \theta^2 + 1) \cdot(\theta^2 + 1, \theta, \theta+1)^T = 0$

$Y_{u4} = (0, \theta + 1, \theta) (\theta^2 + 1, \theta, \theta+1)^T = 0$

$Y_{u5} = (\theta^2 + 1, \theta, \theta^2 + 1) .(\theta^2 + 1, \theta, \theta+1)^T = 0$

When three participants combine their shares the secret will be recovered since the scheme is a (3, 5)-threshold scheme. Assume that the participants with number 2, 4, 5 can recover the secret.

$$\left(\begin{array}{ccc|c} 1 & \theta^5 & \theta^5 & \theta^6 \\ 0 & \theta^5 & \theta & 0 \\ \theta^3 & \theta & \theta^3 & 0 \end{array}\right) \xrightarrow[l_3 \to \theta^4 l_3 + l_1]{l_2 \to \theta^2 l_2}$$

$$\left(\begin{array}{ccc|c} 1 & \theta^5 & \theta^5 & \theta^6 \\ 0 & 1 & \theta^3 & 0 \\ 0 & 0 & \theta & \theta^6 \end{array}\right) \xrightarrow{l_3 \to \theta^6 l_3}$$

$$\left(\begin{array}{ccc|c} 1 & \theta^5 & \theta^5 & \theta^6 \\ 0 & 1 & \theta^3 & 0 \\ 0 & 0 & 1 & \theta^5 \end{array}\right) \xrightarrow{l_2 \to l_2 + \theta^3 l_3}$$

$$\left(\begin{array}{ccc|c} 1 & \theta^5 & \theta^5 & \theta^6 \\ 0 & 1 & 0 & \theta \\ 0 & 0 & 1 & \theta^5 \end{array}\right) \xrightarrow{l_1 \to l_1 + \theta^5 l_2 + \theta^5 l_3}$$

$$\left(\begin{array}{ccc|c} 1 & 0 & 0 & \theta^3 \\ 0 & 1 & 0 & \theta \\ 0 & 0 & 1 & \theta^5 \end{array}\right)$$

$x_1 = \theta^3 = \theta^2 + 1 \Rightarrow x_1 = 5 \in M_8$

$x_2 = \theta \Rightarrow x_2 = 2 \in M_8$

$x_3 = \theta^5 = \theta + 1 \Rightarrow x_3 = 3 \in M_8$

$x = (5, 2, 3)$

It is seen that the secret $s = x_1 = 5$ recovered.

4. Analysis & Discussion

4.1 Security Analysis

In the proposed sharing algorithm the secret is split into shares and it is reconstructed by collecting pieces. Secret is computed by doing computations in field extension. To do so a new approach in the elements of the field extension is used. The secret can be reached every element of field extension F_q ($q = p^m$) can be uniquely expressed l in θ over Fp . So, this scheme is very strong and reliable.

4.2 Performance Analysis

The access structure of this scheme consists of the *k* elements. So the performance of the system will increase.

4.3 Comparative study analysis

Table I shows comparative summary between Shamir, Blakley, Mignotte, Asmuth- Bloom and proposed secret sharing scheme.

Table I. Comparison of different threshold secret sharing schemes [25][8]

Parameters	**Secret Sharing Scheme**				
	Shamir[1]	**Blakley**[2]	**Mignotte**[5]	**Asmuth-Bloom**[3]	**Proposed**
Techniques used	Polynomial interpolation	Vector space (Hyper plane)	Chinese reminder theorem	Chinese reminder theorem	Vector space and finite fields
Perfect	Yes	No	No	No	Yes
Ideal	Yes	No	No	No	Yes
Multiple secret sharing	No	No	No	No	No
Threshold	Yes	Yes	Yes	Yes	Yes
Verifiable	No	No	No	No	No
Proactive	No	No	No	No	No
Security	Low	Low	Low	Low	High

5. Conclusion

Here we proposed a new approach of threshold secret sharing over finite field extension based on Blakely secret sharing. Due to the finite fields the security of the scheme is increased. This scheme is reliable. Using this technique of finite field extension we can create a secret sharing scheme over finite field extension based on Shamir secret sharing in similar fashion. This method has lots of application in image secret sharing.

REFERENCES

[1] A.Shamir, "How to Share a Secret", Communications of the ACM, vol.22, no.11, 1979.

[2] G. Blakely, "Safeguarding cryptographic keys", Proceedings of the AFIPS 1979 National Computer Conference, vol. 48, Arlington, VA, June 1997, pp. 313–317.

[3] C. Asmuth and J. Bloom, "A modular approach to key safeguarding", IEEE Transactions on Information Theory, Vol. 29, Issue 2, pp.208–210, March 1983.

[4] Kamer Kaya and Ali Aydn Selcuk, "Threshold cryptography based on Asmuth Bloom secret sharing", Information Sciences, 2000, 177.

[5] M. Mignotte, "How to Share a Secret, Cryptography", Lecture notes in Computer Science, Springer-Verlag, Germany, pp 371-375, 1983.

[6] Cheng Gu and Chin-Chen Chang," A Construction for Secret Sharing Scheme with General Access Structure", Journal of Information Hiding and Multimedia Signal Processing Ubiquitous International Volume 4-No.1, January 2013 2013 ISSN 2073-4212

[7] Amos Beimel, "Secret Sharing Schemes: A Survey", IWCC 2011, LNCS 6639, pp. 11-46, 2011, Springer-Verlag Berlin Heidelberg 2011.

[8] Sonali Patil, Prashant Deshmukh, "An Explication of Multifarious Secret Sharing Schemes", International Journal of Computer Applications (0975 – 8887) Volume 46– No.19, May 2012.

[9] D. R. Stinson, "Cryptography: Theory and Practice",CRC Press, Boca Raton 1995.

[10] E. D. Karnin, J. W. Greene, and M. E. Hellman, " On secret sharing systems ," vol. IT-29, no. 1, pp. 35–41, Jan. 1983.

[11] P. Giblin," Primes and Programming: An introduction to Number Theory with Computing" , Cambridge University Press/New York, pp. 79-82, 1993.

[12] Levent Ertaul, William Marques Baptista ,"Storing Credit Card Information Securely using Shamir Secret Sharing in a Multi-Provider Cloud "

[13] J. Kleinberg and É. Tardos , " Algorithm Design", Pearson Education /Boston, 1st ed., pp. 234-242, 2006.

[14] P. Choudhary," A Practical Approach to : Linear Algebra", Oxford Book Company /India, 1st Ed, 2009.

[15] A Sreekumar, "Secret sharing schemes using visual cryptography,Ph.D. thesis, Cochin University of Science and Technology, 2009.

[16] V Binu, "Secret Sharing Schemes with Extended Capabilities and Applications", Ph.D. thesis, Cochin University of Science and Technology, 2016.

[17] Janhavi Sirdeshpande, Sonali Patil , "Amended Biometric Authentication using Secret Sharing ", International Journal of Computer Applications (0975 – 8887) Volume 98 – No.21, July 2014

[18]https://ericrafaloff.com/shamirs-secret- sharing-scheme/

[19]https://en.wikipedia.org/wiki/Secret_sharing

[20] Neelam Yadav, Kanina Dhiraj Kumar, Ravi Yadav,"Key Sharing Schemes Using Visual Cryptography ", International Journal of New Innovations in Engineering and Technology (IJNIET) Vol. 1 Issue 4 April 2013 ISSN: 2319-6319

[21] T-79.159 Cryptography and Data Security, 24.03.2004 Lecture 9: Secret Sharing, Threshold Cryptography, MPC, Helger Lipmaa

[22]https://en.wikipedia.org/wiki/Shamir%27s_Secret_Sharing

[23]Shalini I S, Mohan Naik R, S V Sathyanarayana ,"A comparative analysis of Secret Sharing Schemes with special reference to e-commerce applications", International Conference on Emerging Research in Electronics, Computer Science and Technology (ICERECT), 2015

[24]Selda Calkavur , Fatih Molla ,"The Blakely based secret sharing approach", Sigma Journal of Engineering and Natural Sciences,37 (2), 2019, pp.489-494

[25]Vanashree Gupta,Smita Bedekar,"Alternative to Shamir's Secret Sharing Scheme Lagrange Interpolation over Finite Field",International Journal of Technical Research & Science (IJTRS) ,V6-I3-002 , March 2021, ISSN: 2454-2024 , https://doi.org/10.30780/IJTRS.V06.I03.002

DATA AGGREGATION IN WIRELESS SENSOR NETWORKS: EMERGING RESEARCH AREAS

Ajobiewe, Damilola Nnamaka

Department of Computer Science,
Federal College of Education (Special) Oyo, Nigeria.
ajobiewe.dn@fcesoyo.edu.ng
https://orcid.org/0000-0001-6734-3858

Abstract

Wireless Sensor Networks (WSNs) generate an immense measure of explicit data usage. Such data, which is an exorbitant issue, should be prepared and then transmitted to the base station. Efficient data handling and energy monitoring are primary challenges. since WSN hubs are asset-compelled. The point of wireless sensor networks is not confined to data collection in the present climate. Yet the retrieval of beneficial data still depends on it. The term used for the retrieval of beneficial data is data aggregation. In social affairs, data aggregation helps to collect data in energy-efficient ways to elongate the network's duration. The majority of the detected data by the sensors were seen to be excessive. On the off chance that data repetition can be reduced, it will prompt the organization's extended lifetime and decreased inertness at that point. This paper explains a wide methodological analysis of literature on data aggregation in WSNs. Review of various strategies to reduce data repetition, and specifically through aggregation, as well as scientific categorization of data aggregation, challenges, and broken-down aggregation methods proposed over the last ten (10) years, are discussed.

Keywords: *Data Aggregation, Wireless Sensor Network, Security, Network Lifespan, Energy Efficiency.*

Introduction

Wireless sensor networks (WSNs) consist of a wide-ranging amount of sensor nodes for particular applications distributed in the area of concern, which is typically tiny nodes with networking, connectivity, and sensing capacities. These sensor nodes are identified by (Pourpeighambar et al., 2011; Randhawa & Jain, 2017; Tan & Körpeoğlu, 2003); as well as detailing how they interact through short-range radio signals and work to complete shared tasks. WSNs are critical in a variety of network areas, including environmental control, military applications, health-care applications, industrial process management, home intelligence, safety as well as surveillance, and so on. Therefore, by finding several routes between source and destination, a protocol for routing that remains effective per resources, data aggregation, and energy consumption must be defined. (Tan & Körpeo'lu, 2003). Security concerns, energy usage, latency, data confidentiality, honesty, in addition, once the sensor node is deployed in a hostile environment, data aggregation is crucial (Massad et al., 2008). A study of various data aggregation approaches, the impact of data aggregation within WSN, data aggregation methods, data aggregation security issues in WSN data aggregation are discussed. The article also includes a methodical literature review to assess and identify research problems in the area of data aggregation within WSNs centered on current studies. According to the article, energy

savings, as well as latency, are the two most significant variables that influence the efficiency of data aggregation techniques for wireless sensor networks. The latency is associated with aggregating data from local sources and delay is the process of keeping data back across intermediate nodes to merge that to data by distant sources. When evaluating the factors, the two root positioning models are used (energy savings and delay). The two models are defined by the event radius (ER) model with each random source model (Rajagopalan & Varshney, 2006). Important energy benefits are feasible with data aggregation where the origins are grouped around each other or placed arbitrarily, according to the modeling. The benefits are greatest because there are a lot of outlets and they're both close but further away from the base station (Al-Humidi & Chowdhary, 2019; Gatani et al., 2006; Renjith & Baburaj, 2016).

The Literature Review

Chatterjea and Havinga (2003b) suggested Clustered Diffusion with Dynamic Data Aggregation (CLUDDA), using diffusion through a clustering-based data-centric strategy that utilizes in-arrange preparation to maximize data. The grouping strategy is combined with coordinated distribution in this technique. Another curiosity message configuration is defined, in which the inquiry comprehension data is sent along with the query. This instrument is used so that a node may decode the new condition's fluctuating structure query. Intrigue proliferation and data engendering are the two steps of the measurement. When one method fails, it employs an effort to repair the machine in order to restore it. If the field of necessary data sources shifts, so does the data aggregation focus. This technique eliminates unnecessary handling and increases idleness while still requiring a large amount of memory to store intrigue changes and inquiry responses (Chatterjea & Havinga, 2003a). For the most part, this approach is secondary to the fundamental naming system. To reduce data fragmentation induced by spatial similarities between clusters, a range of researchers have proposed using clustering procedure for Decentralized Optimal Compression (DOC) and perhaps a time to reduce coding technique. To lower the cost of intra-cluster contact, the suggested algorithm decides the best proportion allocation inside each cluster. Although an intra-cluster coding procedure was proposed for performing Slepian–Wolf technique within a particular cluster, Wang, Li, et al. (2007) claimed that the technique, while improving communication cost and compression ratio, failed to account for energy consumption.

Zhou et al. (2008) in this study, the authors centered on data aggregation problems of energy-constrained sensor networks. The authors performed research on data aggregation algorithms for wireless sensor networks. Using multiple algorithms, try comparing different output metrics such as lifespan, data precision, and latency. Finally, possible research avenues were discussed.

Chen et al. (2008); (Zheng et al., 2010) cluster-based data aggregation was investigated, and a circulated data aggregation mechanism was proposed. Their main aim was to resolve the Clustered Slepian–Wolf Coding (CSWC) difficulty and optimize compression gain by using the most disjoint cluster possible to cover the network. Jung et al. (2011) suggested a hybrid data aggregation approach known as mixed clustering-based data aggregation to help with complicated aggregation by combining multiple clustering methods at once. The evaluation method for an appropriate clustering strategy is dependent on the network's status. During the

initialization process of this proposed strategy, between the sink node as well as the other network nodes, tree topology is formed. In the next step, cluster head dynamic selection algorithms were being used. In a way, depending on the network status, this hybrid approach provides both dynamic and static clustering. Maraiya et al. (2011a) proposed an Efficient Cluster-head Selection Scheme for Data Aggregation (ECHSSDA), employs a paradigm of cluster-head selection and without depending upon latency as a metric, cluster formation will increase network lifespan and energy efficiency. This technique reduces clustering overhead by choosing a cluster head and a subordinate cluster-head. When a cluster head is overburdened with tasks like sending, receiving, and computations, it may lose control. As a result, anytime a cluster-head dies or fails, a new election is held to choose a new cluster-head, and re-clustering is done to eliminate hot spots. However, the notion of an affiliate cluster-head, who might take responsibility for cluster-head if its energy level fell beyond a certain threshold, might be used to reduce overhead. The cluster setup process, wherein clusters are created, and cluster steady phase is the two phases of the proposed algorithm. The cluster-head is activated in the second step to gather incoming data packets, compile results and send a message to its base station. This technique enhances energy performance then streamlines the cluster choice procedure. A Two-Tier Cluster-Based Data Aggregation (TTCDA) architecture was suggested, which uses temporal and spatial similarity to apply discretely as well as separable aggregation for data packets given by each node (Mantri et al., 2012). The TTCDA is in control of cluster creation, inter-cluster and intra-cluster aggregation are two types of aggregation. Tier 2 then combines the aggregated into one packet depending on the software parameters, utilizing division or additive functionality. However, taking into account node versatility and heterogeneity will strengthen this strategy much further. In the second step, the sensor nodes use additive and divisible aggregation functions in an absolute routine configuration to send transmissions to the cluster head over short distances. The cluster head is assigned to a group based on the nearest distance to both the sink as well as the total packet count. Data packets are collected differently at periodic intervals from a transmitted broadcast message in intra-cluster aggregation. Each cluster head acts as an individual node in the third step. Reduced packet count in data aggregation is the end product at the sink.

Yuea et al. (2012) suggested an Energy-Efficient then Balanced Cluster-Based Data Aggregation Algorithm (EEBCDA) to see if there is an ideal balanced load distributor approach across the whole network where one-hop contact is used to transfer data from cluster-head to base station, eliminating energy dissipation by decreased intra-cluster communication. Any swim-lane remains separated into a set of quadrilateral sections referred to as grids, and each swim-lane is divided into one-of-a-kind sizes of rectangular areas referred to as swim lanes. The network division step is a part of the network structuring process. Each grid elects a cluster-head node with the most electricity. Grids that are further apart from the base station become longer and contain more nodes. The amount of energy used is balanced in this process, since a cluster-head that absorbs more power, more sensor nodes will participate in cluster-head voting. According to Al-Karaki et al. (2009), this approach increases network lifespan and has a stable energy consumption, but in remote grids, latency is higher.

Grouping nodes and clusters for green knowledge aggregation (GCEDA) were introduced by Mantri et al. (2013), in which nodes are clustered mainly based on accessible facts. Despite the higher latency, transmitting costs were lowered. To pass aggregated data to a distant sink, the cluster head employs divisible and additive knowledge aggregation characteristics. Each cluster-head calculates the connection between nodes that are one hop apart. The suggested method divides the whole routing protocol into three stages. Clusters are randomly formed throughout the first section, cluster forming. Based on Euclidean distance and maximal electricity, the cluster-head is chosen. Nodes with similar statistics are discovered and grouped in the intra-cluster section, and then a few aggregation functions are used to depend on the data. Both cluster heads serve as supply nodes in the inter-cluster segment, sending the aggregated records to the base station. Cluster head grouping reduces resource consumption and increases community reliability without sacrificing node heterogeneity or data quality (Mantri et al., 2013).

Sinha and Lobiyal (2013) proposed an energy-efficient data aggregation approach focused on divergence, wherein sensors having sensed the very same thing were first grouped according to certain distinct clusters. The least divergent clusters would be eventually merged since these residual un-clustered sensors approximate their separation throughout comparison to nearby clusters. The route from root to sink is determined by the node's highest utilizable residual capacity. It was discovered that it had a longer total node life.

The algorithm has two stages: preliminary clustering and final clustering. The nodes that sense the same data are placed in separate clusters in the first step. In the second stage, the residual sensors calculate the deviation from nearest neighbors and join each cluster with the least divergence. The sensed data is mapped in the range [0...1] using a window function. After taking into consideration the latency constraint, this approach is used to increase convergence speeds, aggregation rates, packet size losses, transmission cost, and network lifespan. This approach may be enhanced still further by accounting for node heterogeneity and energy-rich multiple sinks.

To boost energy performance in a cluster-based duty-cycled WSN, Rout and Ghosh (2014) suggested an energy-efficient adaptive knowledge aggregation with group coding (ADANC) (at the bottleneck zone) via hoping away some individual nodes from the clustered head that serve as network decoder nodes while others serve in place of simple spread nodes in the cluster. It's a low-power, cluster-based data aggregation system that divides sensor nodes into two types: simple relay nodes and group coder nodes. Data aggregation is solely the responsibility of the stage of document correlation. Network compression is used where the sum of knowledge similarity issues in the obtained packets is limited. In any case, conventional data aggregation is complete, whereas the data correlation problem is serious. With the obligation interval, energy demand is often minimized at the node level. This method is used to reduce transmission costs and thereby reduce power consumption; however, network latency is not taken into account.

As a result, Banerjee and Bhattacharyya (2014) introduced a fairly balanced distribution-based data aggregation process, wherein fluffy reasoning is often used to choose the cluster head and

disperse the same amount of burden through bunches to maximize data transmission. It was planned to develop an energy-efficient routing algorithm that would minimize the overall number of packets transmitted and re-clustering at each round while maintaining network service efficiency. The primary aim of this suggested solution is to resolve the problem of community heads' energy spillage, which arises as a consequence of lopsided burden conveyance. The suggested process is divided into three phases, each of which is divided into three adjusts. The CSMA/CD technique is used to frame bunches during the initial arrangement period. In the standard setup stage, any node transmits its energy status data to the group head, which is also sent to the sink or base station as the case maybe.

Jesus et al. (2014), reported a critical overview of the impact of distributed aggregation algorithms, defining the various forms of aggregation techniques. To reduce the data transmission scale, Xu et al. (2015) proposed an improved data aggregation method focused on signal processing (HDACS), which allows for the complex set of multiple compression levels based on the scale of clusters at various tiers of the data aggregation tree. Rather than setting up the strongest node as the drain, a structure of multi-stage clusters remains built for intermediate data processing. In contrast to other compressive sensing methods, it decreases the data extent in knowledge exchange. The underlying domain is restored using a DCT-based algorithm. The value is often defined by the number of processors as well as the volume of radio energy used. The proposed approach was validated using real-world data and simulated datasets in Sidnetswan's simulation platform.

By focusing on energy consumption, for heterogeneous networks, Mantri et al. (2015) proposed a bandwidth-efficient cluster-based data aggregation (BECDA) method. To provide a solution to the inefficient data collection of the in-network method, an optimized approach of intra- and inter-cluster aggregation at different rates of data generation on randomly distributed nodes was created.

This procedure employs the concept of data link inside the parcel to add aggregation capability to data produced by sensor hubs. Any node may produce erratic data that varies from 0 to 1 by using arbitrary power. Standard hub (20 J), advance hub (30 J), and superhub (40 J) are the three types of nodes, each with a different energy level (40 J). It is created the variable traffic measure. CH is the node in the network of a homogeneous network by far the most energy of both the cluster participants and the most neighbor nodes. This approach decreases data transmission rates, electricity use, and correspondence costs. In either scenario, it results in a decrease in throughput.

Distributed and efficient data aggregation scheduling, proposed by Gao et al. (2019), is a modern approach for scheduling distributed and efficient data aggregation over multi-channel connections (DEDAS-MC). DEDAS-MC lowers latency by transmitting aggregated data to a sink over several channels. DEDAS-MC is a sensor scheduling algorithm that minimizes data aggregation latency and prevents interruptions on a given tree. After that, a distributed algorithm for constructing low-latency data aggregation trees is suggested using the Markov approximation technique. The study centered on the data aggregation latency problem. Two variables determine the latency of data aggregation. Due to the presence of interference,

collision-free scheduling is crucial for reducing data aggregation latency. In addition, the tree structure has a major impact on data aggregation latency.

In the area of data aggregation, new research is constantly emerging. However, a systematic literature review is needed to assess and integrate the current studies in this area.

Data Aggregation designed for Wireless Sensor Networks: Security Concerns

In a wireless sensor network, confidentiality and honesty remain the two types of security that are necessary for data aggregation. Data protection, or shielding critical data transfer against passive attacks such as eavesdropping, is the most fundamental security issue. Since the wireless channel is susceptible to eavesdropping via a cryptographic system, data confidentiality is predominantly used in a hostile setting (Maraiya et al., 2011b). Data integrity is the next protection problem. Integrity tends to deter malicious sensor sources including aggregator nodes from compromising the final aggregation value significantly. A sensor node in a sensor network may be easily compromised, changing or discarding messages. There are two strategies for protecting data aggregation: both hop-by-hop encryption nor end-to-end encryption use the same strategy.

Data Aggregation Classification

In this paper, data aggregation overview involved lifetime of the network, data accuracy, energy efficiency, latency, and data aggregation rate as suggested by (Dagar & Mahajan, 2013; Li et al., 2011)

(a) Energy Efficiency: each sensor will use the same amount of energy during each data collection round, but sensor nodes use different quantities of energy for data transmission. A data aggregation procedure in WSNs remains energy efficient if it has the greatest versatility when using the least amount of energy. Energy efficiency is described as the ratio of the amount of data efficiently transmitted in a sensor network to the total energy required to transmit that data.

Energy efficiency is calculated using Equation 1.

$$\sum_{i=1}^{n}\left(\frac{Total\ number\ of\ successfull\ data\ transferred\ in\ a\ sensor\ network}{Total\ amount\ of\ energy\ consumed\ to\ transfer\ data}\right) \quad (1)$$

In a sensor network, *n* represents the number of sensor nodes, and *i* represents the number of iterations.

(b) Network Lifespan represents the amount of data aggregation rounds performed before the first sensor node's energy is drained. In other terms, it is described as the period (number of rounds) before the first sensor node or group of sensor nodes in the network runs out of energy (battery power) or network disconnection due to the failure of one or more sensors, as (Equation 2):

$$NS_n^n = \min_{v \in V} NS_v \quad (2)$$

Where the network lifetime NS_n^n terminates as soon as the first node fails and NS_v is the lifespan of node *v, V* is the node-set without the sink node.

(c) Data Accuracy: Depending on the application for which the sensor network is designed,data accuracy is defined in different ways. The close approximation of goal location at the sink, for example, determines data precision in the target localization dilemma. Data consistency is characterized as the proportion of correctly transferred data to total data submitted (Equation 3).

$$Data\ Accuracy = \frac{Sum\ of\ data\ transferred\ successfull}{Total\ sum\ of\ data\ sent} \quad (3)$$

(d) Latency: the duration between the data packets received at the sink and the data packets produced at the source nodes is referred to as latency. To put it another way, latency refers to the period it takes a sensor node to send and receive results. As shown in (4)

$$Latency_i = \sum_{i=1}^{n} (Time\ taken\ to\ receive\ data - Time\ of\ sending\ data) \quad (4)$$

(e) In WSNs, data aggregation rate is the method of gathering and integrating valuable knowledge in a specific area of interest. Data aggregation is characterized in terms of data aggregation rate and can be called a fundamental processing technique to minimize energy usage and conserve limited resources. The data collection frequency is described as the proportion of successfully aggregated data to the total amount of data sensed (Equation 5).

$$Data\ Aggregation\ Rate = \frac{Sum\ of\ the\ successfull\ data\ aggregated}{Total\ sum\ of\ Sensed\ data} \times \frac{100}{1} \quad (5)$$

Present State of Data Aggregation Strategies in WSNs

For aggregating valuable data in WSNs, the Data Aggregation Technique (DAT) is important (Krishnamachari et al., 2002). Data is stored at intermediate nodes in this system to conserve resources and reduce processing time. Since it seeks to minimize energy usage at any node, this method, therefore, extends the network lifespan. Lossy aggregation including packet size reduction as well as lossless data aggregation without packet size reduction are the remaining two methods for in-network aggregation. Data is collected from different source nodes and then a category feature such as number (), count (), limit (), and minimum () is added to the gathered data in lossy aggregation (). Since only the measured value of the aggregate feature is introduced into the packet after compression, rather than submitting the whole packet of each node, the size of the packet is minimized in this technique. Consider a forest fire monitoring device, where a simple average or maximum temperature reading is needed. Lossy aggregation is expected in such applications since it reacts to the base station in a timely fashion. Each packet is combined into a single packet without being compressed in lossless aggregation.

Data Aggregation Methodology

Data aggregation methodologies include clustered, tree-based, cluster-based approaches, and in-network aggregation, as seen in Figure 1.

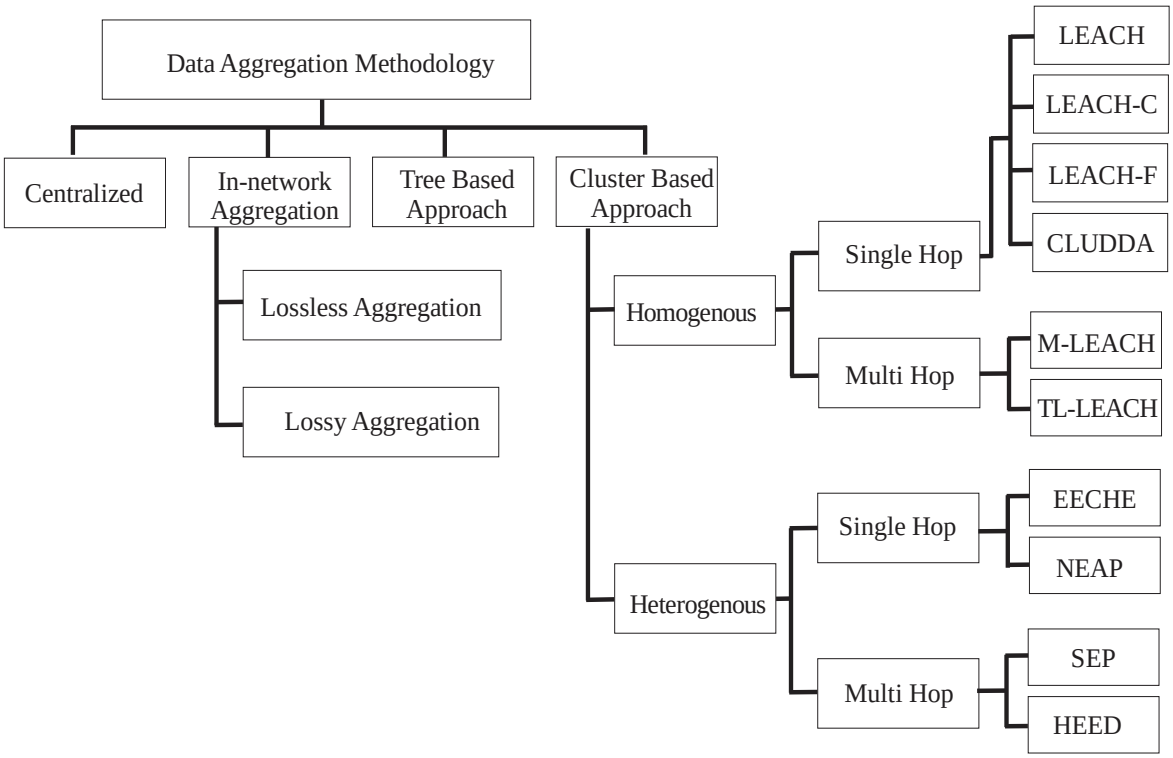

Figure 1: Data Aggregation Methodologies

Source: Author's construct (2020)

The data aggregation process is carried out using a specific routing protocol. The goal is to collect data to reduce energy consumption. As a consequence, sensor nodes will route packets based on data packet content and choose the next hop to make network aggregation easier. Routing protocols are divided by network configuration, which is why they are focused on careful considerations (Krishnamachari et al., 2002).

Tree-Based Approach

The tree-based method requires building an aggregation tree to describe aggregation. The tree is a limited spanning tree in which the sink node acts as the foundation and the root node serves as the leaves. The leaves node sends data to the drain, which is the root node (base station). Wireless sensor networks, as we already know, are vulnerable to failure. If a data packet is lost at any level of the tree, the data is lost not just for that level, but also for all subtrees that are connected to it. This method can be used to create the best aggregation techniques. Madden et al. (2005), created the Tiny Aggregation (TAG) approach, which is a data-centric protocol. The operation of TAG is split into two phases: spread and set. First, an aggregation tree, which is usually a minimum spanning tree, is constructed. The root node serves as the base station, while the leaf nodes serve as the source nodes and the intermediate nodes serve as the parent nodes

in this tree. In a route discovered between leaf node and base station, the leaf nodes give their sensed node to their parent node.

Cluster-Based Approach

It is impractical for sensors to relay data directly to the sink in energy-constrained sensor networks of significant scale in such scenarios. Cluster-based approaches are hierarchical. The whole network is split into many clusters in the cluster-based method. A cluster-head is chosen from among cluster representatives for each cluster. Cluster-heads serve as aggregators, combining data obtained from cluster participants on a local level and transmitting the result to the base station (sink). Several cluster-based network organization and data-aggregation protocols for wireless sensor networks have recently been suggested. Figure 1 illustrates the organization of a sensor network focused on clusters. Long-range transmissions or multi-hopping via other cluster heads enable the cluster heads to interact directly with the drain. The maximum lifetime data aggregation (MLDA) algorithm was suggested, which finds data gathering schedules based on sensor node and base-station position, data packet size, and sensor node capacity. For each round, data-gathering schedule determines how data packets are gathered from sensors and sent to the base station. A plan is basically a set of aggregation trees. Dagar and Mahajan (2013), suggested a heuristic-greedy clustering-related MLDA based on the MLDA algorithm in (Dagar & Mahajan, 2013). They split the network into clusters and related to each cluster as a super-sensor in this way. They then calculate the super-sensors' maximum lifetime schedule and use it to create aggregation trees for the sensors. A two-phase clustering (TPC) scheme is presented by (Wang, Li, et al., 2007; Wang, Zheng, et al., 2007). Step I of this scheme generates clusters with both a cluster-head, but each node inside the cluster links directly to the cluster-head. Move 1 necessitates dispersed cluster-head rotating dependent on the residual energy level of sensor nodes, reducing sensor period volatility and conserving energy by eliminating unnecessary cluster-head rotation. In phase 2, each node in the cluster searches for a data relay position, which is a neighbor who is nearby to the cluster-head and creates a data relay link. Sensor nodes in a cluster now transmit data to the cluster-head through a direct connection or a data relay channel, which is a much more energy-efficient scheme. The data relay point aggregates data before sending it to another data relay point or cluster-head. TPC phase II may create an unwanted data relay connection between neighbors in the case of a high network density, causing sensors to close together to feel the same data, causing a loss of energy. Using this form, the field of concern is separated into a set of clusters. Each cluster chooses a cluster head, whom sole task is to compile the data. Instead of sending data to the base station directly, each node detects the required phenomenon and reports it to the cluster's CH. As a result, it saves a significant amount of electricity in a network.

Data Aggregation Progression

The evolution of data aggregation strategies (DATs) in WSNs from 2002 to 2019 is seen. In the year 2002, network lifetime and network density data aggregation approaches based on network lifetime and resources were presented. Clustered diffusion with Dynamic Data Aggregation (CLUDDA) and dynamic data aggregation technique was proposed in 2003 as diffusion and clustering dependent data-centric technique focusing on network lifetime

(Chatterjea & Havinga, 2003). In 2006, a safe pattern-based data aggregation methodology focusing on security and bandwidth was proposed. In 2007, a sparse data aggregation method was proposed, focusing on expense and failure likelihood (Wang et al., 2007).

In the year 2008, a linear distribution-based data aggregation methodology focusing on energy was proposed (Zhou et al., 2008). In addition, parameters-based, energy-oriented distributed and scalable, and dynamic (Zheng et al., 2010) data aggregation strategies were proposed in 2010, with a focus on connectivity expense, network lifetime, energy, aggregation time, latency, and aggregation rate. During this time, researchers sought to optimize the global compression advantage (Zheng et al., 2010).

In 2011, an effective cluster-head selection scheme for data aggregation (ECHSSDA) was introduced, which uses a model of cluster-head selection and cluster creation, estimation, adaptive clustering, and multi-source temporal dependent data aggregation techniques, with a focus on communication redundancy, network lifetime, resources, packet transmission, error rate, and success rate without co-location, with an emphasis on transmission redundancy, network lifetime, energy, packet transmission, error rate, and success rate without (Jung et al., 2011; Maraiya et al., 2011a). In 2012, recoverable hidden two-tier clustering-based mechanisms and tree-based data aggregation methods were discussed, with a focus on connectivity overhead, expense, packet utilization, energy consumption, and energy expense utilizing temporal and spatial correlation (Mantri et al., 2012). Also, in 2012, EEBCDA (energy efficient and balanced cluster-primarily based data aggregation algorithm) was suggested. This approach extends the existence of the network and reduces electricity demand; however, it increases latency in far-flung grids (Yuea et al., 2012). In 2013, data aggregation strategies that centered on network lifespan, energy usage delivery ratio, aggregate ratio, network reliability, and node density were presented (Mantri et al., 2013; Sinha & Lobiyal, 2013). Researchers proposed an energy-efficient adaptive knowledge aggregation utilizing population coding (ADANC), shortest path-dependent, semantic correlation tree (SCT) based adaptive, enhanced distributed, and latency related data aggregation strategies in 2014, network lifetime, propagation overhead, energy consumption, data efficiency, and aggregation latency are all variables to remember. (Banerjee & Bhattacharyya, 2014; Jesus et al., 2014; Rout & Ghosh, 2014). In 2015, Data aggregation strategies focused on bandwidth-efficient cluster-based, delay-aware, confidence management, multi-criterion decision-making, and learning automata were suggested, with a focus on bandwidth, latency, packet distribution ratio, energy usage, network lifespan, aggregation expense, protection, connectivity overhead, and privacy-preserving effectiveness (Mantri et al., 2015; Xu et al., 2015).

In 2016, Atoui et al. (2016), presented a scheme whereby data is filtered using fitting functions at the first level, and if the data's norm value is within a threshold value, it's sent to the aggregator for second-level aggregation. As a result, in Khriji et al. (2018), differential data from sensors reduces the transmission of unnecessary data over successive cycles are used. Aggregators are fixed in this system, while algorithms are dispersed in a cluster network.

Also, in 2019, Kumar and Kim (2019) employ multi-channel TDMA scheduling techniques to decrease collusion and minimize latency, as well as a meta-heuristic approach for energy

reduction. The network type is the tree, the aggregator is fixed, and the node type is homogeneous. Unlike Kumar and Kim (2019), Sarangi and Bhattacharya (2019) used cluster generation based on a neural network with ant colony optimization. In this system, aggregators are mobilized using distributed methods, and the deployment model is the cluster.

Yadav and Yadav (2019) The aggregator nodes, which are also homogeneous model types, utilize a linear classifier svm - based to identify and eliminate redundant input. With a distributed algorithm, the aggregators are fixed.

The topic of data aggregation latency was a focus for researchers in 2019. Two factors, according to studies, affect data aggregation latency. For instance, reducing data aggregation latency due to disruption needs efficient collision-free scheduling. Second, data aggregation latency is highly influenced by the tree structure (Gao et al., 2019).

Conclusion

This paper focuses on data aggregation, data aggregation advancements, different methods of data aggregation strategies, and a review of data aggregation techniques with and without wireless sensor networks. Rajagopalan and Varshney, as well as Jesus et al., have previously identified data aggregation research issues. This paper utilizes a systemic research method to survey the most recent field study in WSN data aggregation up to 2019. Data aggregation mechanisms and subtypes are thoroughly examined. The data aggregation strategies are compared based on important aspects of data aggregation, as well as the researcher's intent, commitment to science, and various data aggregation algorithms like adaptive, cluster, hidden, resources, latency, network lifetime, network density, nature-inspired optimized, QoS, scheduling, tree, predictor, structure-free real-time, evolutionary game, and a. The majority of the study focused on energy-based data aggregation, with data aggregation with prediction, structure-free real-time, evolutionary game, and hybrid data aggregation techniques still in the early stages of development. Cluster-based data aggregation is the most researched area of WSN after energy-based data aggregation. Data aggregation study was also found to be more widespread in 2011 than in 2002 and 2005, according to the literature. Moreover, during this period, research on data aggregation in WSN concentrated on energy as a QoS parameter, ignoring the fact that reliability and congestion control as QoS parameters still need a considerable amount of work.

References

1. Al-Humidi, N., & Chowdhary, V. (2019). Lightweight Data Transmission Scheme Based onData Aggregation Technique in Wireless Sensor Networks. Proceedings of International Conference on Communication and Information Processing (ICCIP),

2. Al-Karaki, J. N., Ul-Mustafa, R., & Kamal, A. E. (2009). Data aggregation and routing in wireless sensor networks: Optimal and heuristic algorithms. *Computer Networks*, *53*(7), 945-960.

3. Atoui, I., Ahmad, A., Medlej, M., Makhoul, A., Tawbe, S., & Hijazi, A. (2016). Tree-based data aggregation approach in wireless sensor network using fitting functions. 2016

Sixth international conference on digital information processing and communications (ICDIPC),

4. Banerjee, R., & Bhattacharyya, C. K. (2014). Cluster based routing algorithm with evenly load distribution for large scale networks. 2014 International Conference on Computer Communication and Informatics,

5. Chatterjea, S., & Havinga, P. (2003a). CLUDDA-Clustered diffusion with dynamic data aggregation. Ajaccio, Corsica, France: Cabernet Radicals Workshop,

6. Chatterjea, S., & Havinga, P. (2003b). A dynamic data aggregation scheme for wireless sensor networks. *Proc. Program for Research on Integrated Systems and Circuits*.

7. Chen, H., Mineno, H., & Mizuno, T. (2008). Adaptive data aggregation scheme in clustered wireless sensor networks. *Computer Communications*, *31*(15), 3579-3585.

8. Dagar, M., & Mahajan, S. (2013). Data aggregation in wireless sensor network: a survey. *International Journal of Information and Computation Technology*, *3*(3), 167-174.

9. Gao, Y., Li, X., Li, J., & Gao, Y. (2019). Distributed and efficient minimum-latency data aggregation scheduling for multichannel wireless sensor networks. *IEEE Internet of Things Journal*, *6*(5), 8482-8495.

10. Gatani, L., Re, G. L., & Ortolani, M. (2006). Robust and efficient data gathering for wireless sensor networks. Proceedings of the 39th Annual Hawaii International Conference on System Sciences (HICSS'06),

11. Jesus, P., Baquero, C., & Almeida, P. S. (2014). A survey of distributed data aggregation algorithms. *IEEE Communications Surveys & Tutorials*, *17*(1), 381-404.

12. Jung, W.-S., Lim, K.-W., Ko, Y.-B., & Park, S.-J. (2011). Efficient clustering-based data aggregation techniques for wireless sensor networks. *Wireless Networks*, *17*(5), 1387-1400.

13. Khriji, S., Raventos, G. V., Kammoun, I., & Kanoun, O. (2018). Redundancy elimination for data aggregation in wireless sensor networks. 2018 15th International Multi-Conference on Systems, Signals & Devices (SSD),

14. Krishnamachari, L., Estrin, D., & Wicker, S. (2002). The impact of data aggregation in wireless sensor networks. Proceedings 22nd international conference on distributed computing systems workshops,

15. Kumar, S., & Kim, H. (2019). Energy efficient scheduling in wireless sensor networks for periodic data gathering. *IEEE access*, *7*, 11410-11426.

16. Li, H., Lin, K., & Li, K. (2011). Energy-efficient and high-accuracy secure data aggregation in wireless sensor networks. *Computer Communications*, *34*(4), 591-597.

17. Madden, S. R., Franklin, M. J., Hellerstein, J. M., & Hong, W. (2005). TinyDB: An acquisitional query processing system for sensor networks. *ACM Transactions on database systems (TODS)*, *30*(1), 122-173.

18. Mantri, D., Prasad, N. R., & Prasad, R. (2013). Grouping of clusters for efficient data aggregation (GCEDA) in wireless sensor network. 2013 3rd IEEE International Advance Computing Conference (IACC),

19. Mantri, D., Prasad, N. R., Prasad, R., & Ohmori, S. (2012). Two tier cluster based data aggregation (TTCDA) in wireless sensor network. 2012 IEEE International Conference on Advanced Networks and Telecommunciations Systems (ANTS),

20. Mantri, D. S., Prasad, N. R., & Prasad, R. (2015). Bandwidth efficient cluster-based data aggregation for Wireless Sensor Network. *Computers & Electrical Engineering*, *41*, 256-264.

21. Maraiya, K., Kant, K., & Gupta, N. (2011a). Efficient cluster head selection scheme for data aggregation in wireless sensor network. *International Journal of Computer Applications*, *23*(9), 10-18.

22. Maraiya, K., Kant, K., & Gupta, N. (2011b). Wireless sensor network: a review on data aggregation. *International Journal of Scientific & Engineering Research*, *2*(4), 1-6.

23. Massad, Y., Goyeneche, M., Astrain, J., & Villadangos, J. (2008). Data aggregation in wireless sensor networks. 2008 3rd International Conference on Information and Communication Technologies: From Theory to Applications,

24. Pourpeighambar, S. B., Aminian, M., & Sabaei, M. (2011). Energy efficient data aggregation of moving object in wireless sensor networks. 2011 Australasian Telecommunication Networks and Applications Conference (ATNAC),

25. Rajagopalan, R., & Varshney, P. K. (2006). Data aggregation techniques in sensor networks: A survey.

26. Randhawa, S., & Jain, S. (2017). Data aggregation in wireless sensor networks: Previous research, current status and future directions. *Wireless Personal Communications*, *97*(3), 3355-3425.

27. Renjith, P., & Baburaj, E. (2016). EASDAG–Energy Aware Secure Data Aggregation in Wireless Sensor Networks. *Asian Journal of Research in Social Sciences and Humanities*, *6*(11), 1273-1286.

28. Rout, R. R., & Ghosh, S. K. (2014). Adaptive data aggregation and energy efficiency using network coding in a clustered wireless sensor network: An analytical approach. *Computer Communications*, *40*, 65-75.

29. Sarangi, K., & Bhattacharya, I. (2019). A study on data aggregation techniques in wireless sensor network in static and dynamic scenarios. *Innovations in systems and software engineering*, *15*(1), 3-16.

30. Sinha, A., & Lobiyal, D. K. (2013). Performance evaluation of data aggregation for cluster-based wireless sensor network. *Human-Centric Computing and Information Sciences*, *3*(1), 1-17.

31. Tan, H. Ö., & Körpeoğlu, I. (2003). Power efficient data gathering and aggregation in wireless sensor networks. *ACM Sigmod Record*, *32*(4), 66-71.

32. Wang, P., Li, C., & Zheng, J. (2007). Distributed data aggregation using clustered slepian-wolf coding in wireless sensor networks. 2007 IEEE International Conference on Communications,

33. Wang, P., Zheng, J., & Li, C. (2007). Data aggregation using distributed lossy source coding in wireless sensor networks. IEEE GLOBECOM 2007-IEEE Global Telecommunications Conference,

34. Xu, X., Ansari, R., Khokhar, A., & Vasilakos, A. V. (2015). Hierarchical data aggregation using compressive sensing (HDACS) in WSNs. *ACM Transactions on Sensor Networks (TOSN)*, *11*(3), 1-25.

35. Yadav, S., & Yadav, R. S. (2019). Redundancy elimination during data aggregation in wireless sensor networks for IoT systems. In *Recent trends in communication, computing, and electronics* (pp. 195-205). Springer.

36. Yuea, J., Zhang, W., Xiao, W., Tang, D., & Tang, J. (2012). Energy efficient and balanced cluster-based data aggregation algorithm for wireless sensor networks. *Procedia Engineering*, *29*, 2009-2015.

37. Zheng, J., Wang, P., & Li, C. (2010). Distributed data aggregation using Slepian–Wolf coding in cluster-based wireless sensor networks. *IEEE Transactions on Vehicular Technology*, *59*(5), 2564-2574.

38. Zhou, Y., Fang, Y., & Zhang, Y. (2008). Securing wireless sensor networks: a survey. *IEEE Communications Surveys & Tutorials*, *10*(3), 6-28.

FIXED POINT THEOREMS IN REVISED FUZZY METRIC SPACES

[1]Dr. A. Muraliraj & [2]R. Thangathamizh

[1]Assistant Professor, PG & Research Department of Mathematics,
Urumu Dhanalakshmi College, Bharathidasan University, Trichy, India.
Email id: karguzali@gmail.com.
[2]Research Scholar, PG & Research Department of Mathematics
Urumu Dhanalakshmi College, Bharathidasan University, Trichy, India.
Email id: thamizh1418@gmail.com.

Abstract

In this paper, we examine the existence of fixed point results for Banach and Edelstein contraction theorems in Revised fuzzy metric spaces with the assistance of Grabiec. Thus, we create a new path in Revised fuzzy theory to obtain fixed point results. We hope that this paper creates a new way to come up with several fixed point results in the Revised fuzzy metric spaces.

Keywords: *Revised fuzzy metric space, continuous t-conorm, banach contraction, Edelstein contraction, fixed point*

INTRODUCTION

Zadeh designed the hypothesis of fuzzy sets in 1965 [11]. The class of elements with grade of membership deals in fuzzy metric space was presented at first by Kramosil and Michalek [7]. Later on, George and Veeramani [3] gave the altered idea of fuzzy metric spaces because of Kramosil and Michalek [7] and examined a Hausdorff geography of fuzzy metric spaces. As of late, Gregori et al. [5] gave many fascinating instances of fuzzy metrics with regards to the feeling of George and Veeramani [3] and have additionally applied these fuzzy measurements to shading picture handling. In 1977 B. E. Rhoades [10] established the various definitions of contractive mappings, which are very import results for the researchers. Later M. Grabiec [5] and Goebel [4] introduce the existence of fixed points in fuzzy metric space in 1988 and existence of fixed point in metric space. As late of many authors have examined the concept of fuzzy metric space in various aspects.

Alexander Sostak [1] described the concept of "George-Veeramani Fuzzy Metrics Revised". Later on Olga Grigorenko [9], Juan jose Minana, Alexander Sostak, Oscar Valero introduced "On t-conorm based Fuzzy (Pseudo) metrics". In 2020, Alexander Sostak and Tarkan Öner [2] initiate the concept of On Metric-Type Spaces supported Extended t-Conorms. In 2021, Muraliraj.M

& Thangathamizh.R [8] firstly introduced the existence of fixed point theorems in Revised fuzzy metric space [8] in 2021.

2. PRELIMINARIES

To initiate the concept of Revised fuzzy metric space, which was introduced by Alexander Sostak [1] in 2018 is recalled here.

Definition 2.1: [1]

A binary operation $\oplus: [0,1] \times [0,1] \to [0,1]$ is a t-conorm if it satisfies the following conditions:

a) $\oplus$ is associative andcommutative,
b) $\oplus$ is continuous,
c) $a \oplus 0 = a$ for all $a \in [0,1]$,
d) $a \oplus b \leq c \oplus d$ whenever $a \leq c$ and $b \leq d$

for all $a, b, c, d \in [0,1]$.

Examples 2.2: [2]

i.Lukasievicz t-conorm: $a \oplus b = max\{a, b\}$
ii.Product t-conorm: $a \oplus b = a + b - ab$
iii.Minimum t-conorm: $a \oplus b = min(a + b, 1)$

Definition 2.3: [1]

A Revised fuzzy metric space is an ordered triple $(X, \mu, \oplus)$ such that X is a nonempty set, $\oplus$ is a continuous t-conorm and μ is a Revised fuzzy set on $X \times X \times (0, \infty) \to [0,1]$ satisfies the following conditions:

$\forall x, y, z \in X \; and \; s, t > 0$
(RGV1) $\mu(x, y, t) < 1, \forall t > 0$
(RGV2) $\mu(x, y, t) = 0$ if and only if $x = y, t > 0$
(RGV3) $\mu(x, y, t) = \mu(y, x, t)$
(RGV4) $\mu(x, z, t + s) \leq \mu(x, y, t) \oplus \mu(y, z, s)$
(RGV5) $\mu(x, y, -): (0, \infty) \to [0,1)$ is continuous.
Then μ is called a Revised fuzzy metric on X.

Example 2.4: [1]

Let (X, d) be a metric space. Define $a \oplus b = max\{a, b\}$ for all $a, b \in [0,1]$, and define $\mu : X \times X \times (0, \infty) \to [0,1]$ as

$$\mu(x, y, t) = \frac{d(x, y)}{t + d(x, y)}$$

$\forall x, y, z \in X \; and \; t > 0$. Then $(X, \mu, \oplus)$ is a Revised fuzzy metric space.

Definition 2.5: [1]

Let $(X, \mu, \oplus)$ be a Revised fuzzy metric space, for $t > 0$ the open ball $B(x, r, t)$ with a centre $x \in X$ and a radius $0 < r < 1$ is defined by

$$B(x, r, t) = \{y \in X : \mu(x, y, t) < r\}.$$

A subset $A \subset X$ is called open if for each $x \in A$, there exist $t > 0$ and

$0 < r < 1$ such that $B(x, r, t) \subset A$. Let τ denote the family of all open subsets of X. Then τ is topology on X, called the topology induced by the Revised fuzzy metric μ.

We call this fuzzy metric induced by the metric d as the standard Revised fuzzy metric.

Definition 2.6: [8]

Let $(X, \mu, \oplus)$ be a Revised fuzzy metric space,

1. A sequence $\{x_n\}$ in X is said to be convergent to a point $x \in X$ if $lim_{n\to\infty}\mu(x, y, t) = 0 \; for \; all \; t > 0$.
2. A sequence $\{x_n\}$ in X is called a Cauchy sequence, if for each $0 < \epsilon < 1$ and $t > 0$, there exists $n_0 \in \mathbb{N}$ such that $\mu(x_n, x_m, t) < \epsilon$ for each $n, m \geq n_0$
3. A Revised fuzzy metric space in which every Cauchy sequence is convergent is said to be complete.
4. A Revised fuzzy metric space in which every sequence has a convergent subsequence is said to be compact.

Lemma 2.7: [8]
Let $(X, \mu, \oplus)$ be a Revised fuzzy metric space. For all $u, v \in X, \mu(u, v, -)$ is non-increasing function.

MAIN RESULT

Theorem 3.1: (Banach Contraction Theorem in Revised Fuzzy metric)

Let $(\Sigma, \mu, \oplus)$ be a complete Revised fuzzy metric space. Let $F : \Sigma \to \Sigma$ be a function satisfying,

$$\mu(F\zeta, F\eta, \lambda) \leq \mu(\zeta, \eta, \lambda) \qquad (3.1)$$

for all $\zeta, \eta \in \Sigma$. $0 < k < 1$. Then z has unique fixed point.

Proof:

Let $\zeta \in \Sigma \; and \; \{\zeta_n\} = f^n(a)$ $(n \in \mathbb{N})$.

By Mathematical induction, we obtain

$$\mu(\zeta_n, \zeta_{n+p}, \lambda) \leq \mu(\zeta, \zeta_1, \frac{\lambda}{k^n}) \tag{3.2}$$

for all $n > 0$ and $\lambda > 0$. Thus for any non-negative integer p, we have

$$\mu(\zeta_n, \zeta_{n+p}, \lambda) \leq \mu(\zeta, \zeta_{n+1`}, \frac{\lambda}{p}) \oplus \cdots (p - times) \cdots \oplus \mu(\zeta_{n+p-1}, \zeta_{n+p`}, \frac{\lambda}{p})$$

$$\leq \mu(\zeta, \zeta_{n+1`}, \frac{\lambda}{pk^n}) \oplus \cdots (p - times) \cdots \oplus \mu(\zeta, \zeta_1, \frac{\lambda}{pk^{n+p-1}})$$

by (3.2) and the definition of Revised fuzzy metric space conditions,

we get

$$lim_{n\to\infty}\, \mu(\zeta_n, \zeta_{n+p}, \lambda) \leq 0 \oplus \cdots (p - times) \cdots \oplus 0 = 0$$

Therefore, $\{\zeta_n\}$ is Cauchy sequence and it is convergent to a limit, let the limit point is η. Thus, we get

$$\mu(F\eta, \eta, \lambda) \leq \mu(F\eta, F\zeta_n, \frac{\lambda}{2}) \oplus \mu(\zeta_{n+1}, \eta, \frac{\lambda}{2})$$

$$\leq \mu\left(\eta, \zeta_n, \frac{\lambda}{2k}\right) \oplus \mu\left(\zeta_{n+1}, \eta, \frac{\lambda}{2}\right) \to 0 \oplus 0 = 0$$

Since we see that $\mu(\zeta, \eta, \lambda) = 0 \ iff \ \zeta = \eta$

We get $F\eta = \eta$, which is the fixed point of Revised fuzzy metric space. To show the uniqueness, let us assume that $F\omega = \omega$ for some $\omega \in \Sigma$

$$0 \leq \mu(\zeta, \omega, \lambda) = \mu(F\eta, F\omega F\omega, \lambda) \leq \mu\left(\zeta, \omega, \frac{\lambda}{K}\right) = \mu(F\zeta, F\omega, \frac{\lambda}{K}) \leq \mu(\eta, \omega, \frac{\lambda}{K^2})$$

$$\leq \cdots \leq \mu(\zeta, \omega, \frac{\lambda}{K^n}) \to 0 \ as \ n \to \infty$$

From the definition of Revised fuzzy metric space, We get $\eta = \omega$.

Therefore z has a unique fixed point.

Lemma 3.2:

Let $(\Sigma, \mu, \oplus)$ be a complete Revised fuzzy metric space. Then,

(a) If $lim_{n\to\infty}\, \zeta_n = \zeta \ and \ lim_{n\to\infty}\, \eta_n = \eta$, then

$$\mu(\zeta, \eta, \lambda - \epsilon) \geq lim_{n\to\infty}\, sup\, \mu(\zeta_n, \eta_n, \lambda)$$

(b) If $lim_{n\to\infty}\, \zeta_n = \zeta \ and \ lim_{n\to\infty}\, \eta_n = \eta$, then

$$\mu(\zeta,\eta,\lambda+\epsilon) \leq \lim_{n\to\infty} inf\ \mu(\zeta_n,\eta_n,\lambda)$$

for all $\lambda > 0$ and $0 < \epsilon < \lambda$.

Proof for (a):

By the definition of Revised fuzzy metric space, conditions (iv)

$$\mu(\zeta_n,\eta_n,\lambda) \leq \mu\left(\zeta_n,\zeta,\frac{\epsilon}{2}\right) \oplus (\zeta,\eta,\lambda-\epsilon) \oplus \mu\left(\eta_n,\eta,\frac{\epsilon}{2}\right)$$

$$\lim_{n\to\infty} sup\ \mu(\zeta_n,\eta_n,\lambda) \leq 0 \oplus \mu(\zeta,\eta,\lambda-\epsilon) \oplus 0$$

Hence, $\lim_{n\to\infty} sup\ \mu(\zeta_n,\eta_n,\lambda) \leq \mu(\zeta,\eta,\lambda-\epsilon)$

Proof for (b):

By the definition of Revised fuzzy metric space, conditions (iv),

$$\mu(\zeta,\eta,\lambda+\epsilon) \leq \mu\left(\zeta_n,\zeta,\tfrac{\epsilon}{2}\right) \oplus \mu(\zeta_n,\eta_n,\epsilon) \oplus \mu\left(\eta_n,\eta,\tfrac{\epsilon}{2}\right)$$

$$\mu(\zeta,\eta,\lambda+\epsilon) \leq \lim_{n\to\infty} inf\ \mu(\zeta_n,\eta_n,\epsilon)$$

Corollary 3.3:

If $\lim_{n\to\infty} \zeta_n = a$ and $\lim_{n\to\infty} \eta_n = \eta$

a) $\mu(\zeta,\eta,\lambda) \geq \lim_{n\to\infty} sup\ \mu(\zeta_n,\eta_n,\lambda)$…… (3.3)

$\mu(\zeta,\eta,\lambda) \leq \lim_{n\to\infty} inf\ \mu(\zeta_n,\eta_n,\lambda)$……. (3.4)

for all $\lambda > 0$ and $0 < \epsilon < \lambda$

Theorem 3.4: (Edelstein Contraction Theorem in Revised Fuzzy metric)

Let $(\Sigma,\mu,\oplus)$ be compact Revised Fuzzy metric space. Let $F : \Sigma \to \Sigma$ be a function satisfying

$$\mu(F\zeta,F\eta,.) < \mu(\zeta,\eta,.) \quad (3.5)$$

Then F has fixed point.

Proof:

Let $a \in \Sigma$ and $a_n = F^n\zeta$ $(n \in N)$.

Assume $\zeta_n \neq \zeta_{n+1}$ for each n $(If\ not\ F\zeta_n = \zeta_n)$ consequently $a_n \neq a_{n+1}$ $(n \neq m)$, For otherwise we get

$$\mu(\zeta_n, \zeta_{n+1}, .) = \mu(\zeta_m, \zeta_{m+1}, .) < \mu(\zeta_{m-1}, \zeta_m, .) < \cdots < \mu(\zeta_n, \zeta_{n+1}, .)$$

where $m > n$, which is a contradiction.

Since Σ is compact set, $\{\zeta_n\}$ has convergent sub sequence $\{\zeta_{n_i}\}$.

Let $\eta = \lim_{i\to\infty} \zeta_{n_i}$, Also we assume that η such that $F\eta \in \{\zeta_{n_i}; i \in N\}$.

According to the above assumption, we may now write

$$\mu(F\zeta_{n_i}, F\eta, .) < \mu(\zeta_{n_i}, \eta, .)$$

for all $i \in N$. Then by equation (3.3) we obtain

$$lim\ sup\ \mu(F\zeta_{n_i}, F\eta, \lambda) \leq lim\ \mu(\zeta_{n_i}, \eta, \lambda) = \mu(\eta, \eta, \lambda) = 0$$

for each $\lambda > 0$.

Hence,

$$lim\ F\zeta_{n_i} = F\eta.... \tag{3.6}$$

Similarly $lim\ F^2\zeta_{n_i} = F^2\eta....$ (3.7)

(we recall that $lim\ F\zeta_{n_i} = F\eta$ for all $(i \in N)$, Now observe that,

$$\mu(\zeta_{n_i}, F\zeta_{n_i}, \lambda) \geq \Theta(F\zeta_{n_i}, F^2\zeta_{n_i}, \lambda) \geq \cdots \geq \Theta(\zeta_{n_i}, F\zeta_{n_i}, \lambda)$$

$$\geq \Theta(F\zeta_{n_i}, F^2\zeta_{n_{i+1}}, \lambda) \geq \cdots \geq \Theta(F\zeta_{n_{i+1}}, F^2\zeta_{n_{i+1}}, \lambda)$$

$$\geq \Theta(F\zeta_{n_{i+1}}, F^2\zeta_{n_{i+1}}, \lambda) \geq \cdots \geq 0.$$

for all $\lambda > 0$. $\{\mu(\zeta_{n_i}, F\zeta_{n_i}, \lambda)\}$ and $\{\Theta(F\zeta_{n_i}, F^2\zeta_{n_i}, \lambda)\}$ $(\lambda > 0)$ are convergent to a common limit point . So by equations (3.2) , (3.4) and (3.5) and we get,

$$\mu(\eta, z\eta, \lambda) \leq lim\ inf\ \mu(\zeta_{n_i}, F\zeta_{n_i}, \lambda) = lim\ inf\ \mu(F\zeta_{n_i}, F^2\zeta_{n_i}, \lambda)$$

$$\leq lim\ sup\ \mu(F\zeta_{n_i}, F^2\zeta_{n_i}, \lambda)$$

$$\leq \mu(F\eta, F^2\eta, \lambda)$$

for all $\lambda > 0$. Suppose $b \neq F\eta$, By equation (3.5)

$$\mu(\eta, F\eta, .) > \mu(F\eta, F^2\eta, .)$$

which is a contradiction , because the above function are right continuous ,non - increasing respectively.

Hence $\eta = F\eta$ is a fixed point.

To prove the uniqueness of the fixed point, let us consider $F(\zeta) = \omega$ for some $\zeta \in \Sigma$. Then

$$0 \leq \mu(\zeta, \omega, \lambda) = \mu(F\eta, F\omega, \lambda) \leq \mu(\zeta, \omega, \frac{\lambda}{k}) = \mu(F\eta, F\omega, \frac{\lambda}{k}) \leq \cdots \leq \mu(\zeta, \omega, \frac{\lambda}{k^n})$$

Now, we easily verify that $\{\frac{\lambda}{k^n}\}$ is an s-increasing sequence, then by assumption for a given $\epsilon \in (0,1)$, there exists $n_0 \in N$ such that

$$\mu(\zeta, \omega, \frac{\lambda}{k^n}) \leq \epsilon$$

Clearly,

$$\mu(\zeta, \omega, \lambda) = 0$$

Thus $\eta = \omega$. Hence proved.

CONCLUSION

The main purpose of this paper is to introduce a new class of Banach contraction and Edelstein Contraction **i**n revised fuzzy metric space and to present fixed point theorems.

REFERENCES

1. Alexander Sostak *"George-Veeramani Fuzzy Metrics Revised"* Axioms 2018, 7, 60; doi:10.3390/axioms7030060.
2. Alexander Sostak and Tarkan Öner *On Metric-Type Spaces Based on Extended T-Conorms* Mathematics **2020**, 8, 1097; doi:10.3390/math8071097.
3. George.A, P. Veeramani, *On some results in fuzzy metric spaces, Fuzzy Sets Systems*, 64, (1994), 395-399.
4. Goebel.K and W. A. Kirk, *Topiqs in Metric Fixed Point Theory*, Combridge University Press, New York, (1990).
5. Gregori.V, Samuel Morillas, and AlmanzorSapena, "Examples of fuzzy metrics and applications", Fuzzy Sets and Systems, 170 (2011), 95-111.
6. Grabiec.M, *Fixed points in fuzzy metric space, Fuzzy Sets Systems*, 27(1988), 385-389.
7. Kramosil.I and J. Michalek, *Fuzzy metric and statistical metric spaces, Kybernetika,* 11, (1975), 336-344.
8. Murali Raj.A and Thangathamizh.R, *"Fixed point theorems in revised fuzzy metric space"*, http://dx.doi.org/10.17654/FS026020103.

9. Olga Grigorenko, Juan joseMinana, Alexander Sostak, Oscar Valero *"On t-conorm based Fuzzy (Pseudo) metrics"*, Axioms **2020**, 9, 78;doi:10.3390/axioms9030078

10. Rhoades. E.B, *A Comparison of Various Definitions of Contractive Mappings*, *Trans. Amer. Math. Soc.* 226 (1977), 257-290.

11. Zadeh.L.A, *"Fuzzy sets"*, Inform. Control, 8 (1965),338-353.

THERMAL RADIATION EFFECTS ON MHD UNSTEADY COUETTE FLOW HEAT AND MASS TRANSFER FREE CONVECTIVE IN VERTICAL CHANNELS DUE TO RAMPED AND ISOTHERMAL TEMPERATURE

F. Abdullahi, M.A Sani, D.A. Sani, M.M. Sani, M. Ibrahim, F. Abubakar and I.M. Garba

Department of Mathematics
Waziri Umaru Federal Polytechnic
Birnin Kebbi, Kebbi State
Email: farukabdullahi@wufpbk.edu.ng

Abstract

Numerical investigations were carried out to study thermal radiation effects on magneto-hydrodynamics (MHD) unsteady Couette flow heat mass transfer free-convective in vertical channels due to ramped and isothermal temperature. The governing coupled non-linear partial differential equations of the flow were transformed into non-dimensional form using suitable dimensional quantities. Finite element method (FEM) was employed to find numerical solution of the dimensionless governing coupled boundary layer partial differential equations. The expressions of velocity, temperature, concentration, skin friction, Nusselt number as well as Sherwood number have been obtained and discussed using line graph. From the outcome of the result it was revealed that, increase of porosity parameter K, ratio of mass transfer parameter N, Time parameter t, Eckert number Ec enhances the velocity and temperature while reverse is the case with the with increase of Magnetic parameter M, Radiation parameter tern R and Prandtl number $\Pr$. At y = 0, the fluid skin friction gets enlarged with increase in porosity parameter K, Nusselt number gets increased with increase of Prandtl number $\Pr$ and Sherwood number gets boosted with increase of Eckert number Ec. Similarly, at y = 1 skin friction gets enhanced with increase of porosity parameter K, Nusselt number diminishes with increase of Prandtl number $\Pr$ and Sherwood number gets enlarged with increase of Eckert number Ec.

Keywords: *MHD, thermal radiation effects, isothermal temperature, ramped temperature*

1. Introduction

Studying thermal radiation effects on magneto-hydrodynamics (MHD) has attracted the interest of many researchers in applied mathematics and engineering sciences due to the applications of such flows in the context of aerodynamics. The process by which energy is emitted from one body to another as electromagnetic waves or as moving subatomic particles is known as radiation. Emission of electromagnetic energy results in a decrease in the energy level which is vital in temperature stabilization. Heat transfer problems are classified according to the variable that the temperature depends upon. For example if the temperature is independent of time, the problem is

referred to steady-state problem, while on the other hand if the temperature is a function of time, the problem is classified as unsteady or transient.

The study of MHD flow has attracted a lot of attentions from many researchers as a result of its wide applications in astrophysics and geophysics. It is applied to the study of stellar and solar structures, interstellar matter, and radio propagation through the ionosphere. In engineering, it is applied in MHD pumps, MHD bearings, nuclear reactors, geothermal energy extraction and in boundary layer control in the field of aerodynamics. Animasaun, Raju and Sandeep (2016) analyzed effects of nonlinear thermal radiation and induced magnetic field on viscoelastic fluid flow toward a stagnation point. Similarly Bala, Kumar and Lin (2016) studied the nonlinear coupled evolution equations, which modeled the transient MHD natural convection and mass transfer flow of viscous, incompressible and electrically conducting fluid between two infinite vertical plates. This study was carried out in the presence of the transversal magnetic field, thermal radiation, thermal diffusion and diffusion-thermo effects. They discovered that as the radiation, temperature difference, sustention parameter, thermal-diffusion, diffusion-thermo, and non-dimensional time parameters increase, both the velocity and temperature increase. Furthermore, Ganesh, Gireesha, Manjunatha and Rudraswamy (2017) analyzed the effect of nonlinear thermal radiation on double diffusive free convective boundary layer flow of a viscoelastic nanofluid over a stretching sheet. They discovered increasing values of temperature ratio parameter θ_w extinguishes the rate of heat transfer $|\theta'(0)|$ for fixed Pr and R, also the temperature ratio parameter $\theta_w$and the thermal radiation parameter R have the same effect.

Bhatti, Zeeshan, and Ellahi (2017) studied the effects of heat transfer on particle fluid suspension induced by metachronal. Their study revealed that an increment in thermal radiation R and Casson fluid parameter Δ causes a reduction in the temperature profile when the influence of MHD and thermal radiation are taken into consideration through the help of Ohm's law and Roseland's approximation. Additionally, Ganesh et al. (2017) analyzed two-phase boundary layer flow and heat transfer of a Williamson fluid with fluid particle suspension over a stretching sheet. The region of temperature jump and nonlinear thermal radiation was considered in the energy transfer process. They reported that, the thermal boundary layer thickness gets thinner due to increase in temperature jump parameter. They also revealed that intensifying of β_v and β_t reduces fluid phase velocity and temperature profile. Alao, Fagbade and Falodun (2016) studied the influence of some thermo-physical properties of fluid on heat and mass transfer flow past semi-infinite moving vertical plate. The fluid considered was optically thin in such a way that the thermal heat loss on the fluid is modeled using Rosseland approximation. They revealed that an increase in the thermal radiation parameter leads to the boosting of both the velocity and temperature profiles. They further revealed that the velocity profile as well as the concentration profile gets enhanced with an increase in the Soret number.

In the study of Shagaiya and Simon (2015) the influence of buoyancy and thermal radiation on MHD flow over a stretching porous sheet was analyzed. Their model which highly constituted

nonlinear governing equations was transformed using similarity solution and then solved using homotopy analysis method (HAM). From their research it was found that when the buoyancy parameter increases, the fluid velocity gets enlarged and the thermal boundary layer gets reduced. In case of the thermal radiation, they observed that increasing the thermal radiation parameter produces significant enhancement in the thermal conditions of the fluid temperature. This causes more fluid in the boundary layer due to buoyancy effect, causing the velocity in the fluid to increase. The hydrodynamic boundary layer and thermal boundary layer thicknesses were observed to increase as a result of increasing radiation. Nayak (2017) studied three dimensional (MHD) flow and heat transfer analysis associated with thermal radiation as well as viscous dissipation of nanofluid over a shrinking surface. He found that temperature the thermal boundary gets enhanced due to increase in viscous dissipation which leads to thicker thermal boundary layer. He also revealed that enlarging the temperature is simply increasing the radiation parameter, R. He further revealed that there is an increase in fluid velocity when suction is present at the shrinking surface. Moreover, Rizwan, Nadeem, Hayat and Sher (2015) studied the stagnation point flow of nanofluid with MHD and thermal radiation effects passed over a stretching sheet. Moreover, they considered the combined effects of velocity and thermal slip and found that rising in Hartmann number gives the resistive type flow within the boundary layer; consequently velocity profile shows the decreasing behavior with an increase of M. The thermal slip parameter provides the decreasing behavior in the temperature profile. While on the other hand radiations parameters give rise in temperature profile.

Siva and Anjan (2016), studied finite element analysis of heat and mass transfer past an impulsively moving vertical plate with ramped temperature. From their study the velocity gets intensified with increase of the values of thermal buoyancy force, solutal buoyancy force, permeability parameter and time. Shagaiya and Daniel (2015) investigated the theoretical influence of buoyancy and thermal radiation on MHD flow over a stretching porous sheet. He reported that, increasing the thermal radiation parameter produces significant enhancement in the thermal conditions of the fluid temperature which led to more fluid in the boundary layer due to buoyancy effect, causing the velocity in the fluid to increase. From the analysis of Adamu and Bandari (2018) the thermal and solutal buoyancy parameters on the nanofluid flow, heat, and mass transfer characteristics due to a stretching sheet in the presence of a magnetic field were studied. They discovered that, the axial velocity of the fluid get increased with an increase of both thermal and solutal buoyancy parameter, while the thermal conductivity of the fluid get reduced. In the research of Danjuma, Haliru, Ibrahim and Hamza (2019), the influence of unsteady Heat Transfer to MHD Oscillatory flow of Jeffrey fluid through a porous medium under slip condition analyzed. They reported that, the temperature profile gets enhanced with increasing Peclet number and the velocity profile gets reduced with increasing Hartmann number and Dacy number. Reddy, Raju and Rao and Gola (2017) analyzed the influence of an unsteady magneto-hydrodynamics natural convection on the Couette flow of electrically conducting water at 4^0 C (Pr = 11.40) in a rotating system. The primary velocity, secondary velocity and temperature of water at 4^o C as well as shear stresses and rate of heat transfer were obtained for both ramped temperature and isothermal plates.

The present numerical investigation analyzed finite element analysis of thermal radiation effects on unsteady MHD heat mass transfer Couette flow in free convective vertical channels due to ramped and isothermal temperature. The governing coupled, non-linear, partial differential equations of the flow were solved using finite element method. The velocity, temperature, concentration as well as shear stress have been obtained for both and continuous ramped temperature isothermal plates.

2. Formulation of the Problem

Consider an unsteady free convection flow of an incompressible electrically conducting viscous dissipative fluid past an infinite vertical porous plate. Let the x* -axis be chosen along the plate in the vertically upward direction and the y* axis is chosen normal to the plate. A uniform magnetic field of intensity H_0 is applied transversely to the plate. The induced magnetic field is neglected as the magnetic Reynolds number of the flow is taken to be very small. Initially, the temperature of the plate T^* and the fluid T_w^* are assumed to be the same. The concentration of species at the plate C_w^* and C_0^* are assumed to be the same. At time t*>0, the plate temperature is changed to T_w^*, which is then maintained constant, causing convection currents to flow near the plate and mass is supplied at a constant rate to the plate. Under these conditions the flow variables are functions of time y* and t* alone. The problem is governed by the following equations:

$$\frac{\partial u^*}{\partial t^*} = \frac{\partial^2 u^*}{\partial y^{*2}} + g\beta^{\bullet}(C^* - C_0) - \frac{\sigma \mu_e{}^2 H_0{}^2 u^*}{\rho} - \frac{\nu u^*}{K^*} \tag{1}$$

$$\rho C_p \frac{\partial T^*}{\partial t^*} = k \frac{\partial^2 T^*}{\partial y^{*2}} + \mu \left[\frac{\partial u^*}{\partial y^*}\right]^2 - R^* \theta^* \tag{2}$$

$$\frac{\partial C^*}{\partial t^*} = D_M \frac{\partial^2 C^*}{\partial y^{*2}} \tag{3}$$

The corresponding initial and boundary conditions are:

Case I: Isothermal Temperature

$$\left.\begin{array}{l} t^* \le 0,\ u^* = 0,\ T^* = T_0 \ \ for\ \ all\ \ 0 \le y^* \le L \\ t^* > 0 \left\{ \begin{array}{l} u^* = u,\ T^* = T_w,\ C^* = C_w^* \ \ at\ \ y^* = 0 \\ u^* = 0, T^* = 0^* T,\ C^* = C_w^* \ \ at\ \ y^* = L \end{array} \right. \end{array}\right\}$$

Case II: Continuous Ramped Temperature

$$\left.\begin{array}{l} t^* \le 0,\ u^* = 0,\ T^* = T_0 \ \ for\ \ all\ \ 0 \le y^* \le L \\ t^* > 0 \left\{ \begin{array}{l} u^* = u,\ T^* = T_0 + \dfrac{(T_w^* - T_0)t^*}{T_R},\ C^* = C_w^* \ \ at\ \ y^* = 0 \\ u^* = 0, T^* = 0T,\ C^* = C_w^* \ \ at\ \ y^* = L \end{array} \right. \end{array}\right\} \tag{4}$$

We now introduce the following non- dimensional quantities into the basic equations and initial and boundary conditions in order to make them dimensionless

$$\left.\begin{array}{lll} U_0 = (vg\beta\Delta T)^{1/3}, & \mathrm{L}=\left(\frac{\mathrm{g}\beta\Delta\mathrm{T}}{\mathrm{v}^2}\right)^{-1/3} & \mathrm{T}_R = \frac{(g\beta\Delta T)^{-2/3}}{v^{-1/3}} \\ \Delta T = T_w^* - T_\infty^*, & \mathrm{t}=\frac{\mathrm{t}^*}{\mathrm{T}_\mathrm{R}}, \quad \mathrm{y}=\frac{\mathrm{y}^*}{L}, & \mathrm{r_t} = \frac{r_t^* - T_0}{T_w^* - T_0} \\ u = \frac{u^*}{U_0}, & \mathrm{K}=\frac{\mathrm{K}^*}{\mathrm{v}\mathrm{T}_\mathrm{R}}, \quad \theta=\frac{\mathrm{T}^* - T_0}{T_w^* - T_0}, & \phi=\frac{\mathrm{C}^* - C_0}{C_w^* - C_0} \\ \mathrm{Pr} = \frac{\mu C_P}{k}, & \mathrm{Sc}=\frac{\mathrm{v}}{\mathrm{D_m}}, \quad Ec = \frac{U_0^2}{C_P\Delta T}, & \mathrm{Sr}=\frac{\mathrm{T_w} - T_0}{C_w - C_0} \\ N = \frac{\beta^\bullet(C_w^* - C_\infty^*)}{\beta(T_W^* - T_\infty^*)}, & M = \frac{\sigma\mu_0^2 H_0^2 T_R}{\rho} & \end{array}\right\} \quad (5)$$

On the substitution of equations (5) into (1) - (4) the following governing equations in non-dimensional form are obtained.

$$\frac{\P u}{\P t} = \frac{\P^2 u}{\P y^2} + Gr\theta + Nf - (M + \frac{1}{K})u \quad (6)$$

$$Pr\frac{\partial\theta}{\partial t} = \frac{\partial^2\theta}{\partial y^2} + Ec\left(\frac{\partial u}{\partial y}\right)^2 - \theta R \quad (7)$$

$$Sc\frac{\partial\phi}{\partial t} = \frac{\partial^2\phi}{\partial y^2} \quad (8)$$

The corresponding initial and boundary conditions are

Case I: Isothermal Temperature

$$\left.\begin{array}{l} t \le 0,\ u = 0, \theta = 0, \phi = 0 \ \ for \ \ all \ \ y \\ For\ t \ge 0: \\ u = 1, \theta = 1, \phi = 1 \quad at \ \ y = 0 \\ u = 0, \theta = 0, \phi = 0 \quad at \ \ y = 1 \end{array}\right\}$$

Case II: Continuous Ramped Temperature

$$\left.\begin{array}{l} t \le 0,\ u = 0, \theta = 0, \phi = 0 \ \ for \ \ all \ \ y \\ For\ t \ge 0: \\ u = 1, \theta = t, \phi = 1 \quad at \ \ y = 0 \\ u = 0, \theta = 0, \phi = 0 \quad at \ \ y = 1 \end{array}\right\} \quad (9)$$

3. Method of the Solution

Equations (6) – (8) are a coupled non-linear system of partial differential equations and were to be solved under the boundary conditions (9) using highly validated and robust method known as finite element method (Galerkin approach).

By applying Galerkin finite element method for equation (6) over the element $\ell,\ y_i \le y \le y_j$ is

$$\int_{y_i}^{y_i}\left\{N^T\left[\frac{\partial^2 u}{\partial y^2} - \frac{\partial u}{\partial t} - u(M+\frac{1}{K}) + Nf + q\right]\right\}dy = 0 \tag{10}$$

Equation (10) is reduce to:

$$\int_{y_i}^{y_i}\left\{N^T\left[\frac{\partial^2 u}{\partial y^2} - \frac{\partial u}{\partial t} - M_1 u + P\right]\right\}dy = 0 \tag{11}$$

Where $M_1 = M + \frac{1}{K}$ and $P = \theta + N\phi$

Applying integration by part to equation (10) yield:

$$[N^T \frac{\P u}{\P t}]_{y_i}^{yj} - \int_{y_i}^{y_i} \frac{\P N^T}{\P y}\frac{\P u}{\P y}dy - \int_{y_i}^{y_i} N^T \frac{\P u}{\P t}dy - M_1\int_{y_i}^{y_i} N^T u dy + P\int_{y_i}^{y_i} N^T dy = 0 \tag{12}$$

Dropping the first term of equation (3.18):

$$\int_{y_i}^{y_i} \frac{\P N^T}{\P y}\frac{\P u}{\P y}dy + \int_{y_i}^{y_i} N^T \frac{\P u}{\P t}dy + M_1\int_{y_i}^{y_i} N^T u dy - P\int_{y_i}^{y_i} N^T dy = 0 \tag{13}$$

Let $u^{(e)} = u_i N_i + u_j N_j \Rightarrow u^{(e)} = [N][u]^T$ be a linear piecewise approximation solution over the two nodal element e, $(y_i \le y \le y_j)$ where $u^{(e)} = [u_i \ u_j]$, $N = [N_i N_j]$ also u_i *and* u_j are the velocity component at the i^{th} and j^{th} nodes of the typical element (e) $(y_i \le y \le y_j)$ furthermore, N_i and N_j are basis (or shape) functions defined as follows:

$$N_i = \frac{y_j - y}{y_j - y_i},\ N_j = \frac{y - y_i}{y_j - y_i}$$

Hence equation (13) after simplifying becomes:

$$\int_{y_i}^{y_i}\begin{bmatrix} N_i'N_i' & N_i'N_j' \\ N_i'N_j' & N_j'N_j' \end{bmatrix}\begin{bmatrix} u_i \\ u_j \end{bmatrix}dy + \int_{y_i}^{y_i}\begin{bmatrix} N_iN_i & N_iN_j \\ N_iN_j & N_jN_j \end{bmatrix}\begin{bmatrix} \dot{u}_i \\ \dot{u}_j \end{bmatrix}dy + M_1\int_{y_i}^{y_i}\begin{bmatrix} N_iN_i & N_iN_j \\ N_iN_j & N_jN_j \end{bmatrix}\begin{bmatrix} u_i \\ u_j \end{bmatrix}dy - P\int_{y_i}^{y_i}\begin{bmatrix} N_i \\ N_j \end{bmatrix}dy = 0 \tag{14}$$

Also simplifying equation (14) above we have:

$$\frac{1}{l}\begin{bmatrix}1 & -1\\ -1 & 1\end{bmatrix}\begin{bmatrix}u_i\\ u_j\end{bmatrix}+\frac{l}{6}\begin{bmatrix}2 & 1\\ 1 & 2\end{bmatrix}\begin{bmatrix}\dot{u}_i\\ \dot{u}_j\end{bmatrix}+\frac{M_1 l}{6}\begin{bmatrix}2 & 1\\ 1 & 2\end{bmatrix}\begin{bmatrix}u_i\\ u_j\end{bmatrix}-\frac{lP}{2}\begin{bmatrix}1\\ 1\end{bmatrix}=0 \tag{15}$$

Where $l = y_j - y_i = h$ and prime and dot denotes differentiation with respect to y and t respectively. Assembling the equations for the two consecutive elements $y_{i-1} \le y \le y_i$ and $\mathrm{y_i} \le y \le y_{i+1}$ the following is obtained:

$$\frac{1}{l^2}\begin{bmatrix}1 & -1 & 0\\ -1 & 2 & -1\\ 0 & -1 & 1\end{bmatrix}\begin{bmatrix}u_{i-1}\\ u_i\\ u_{i+1}\end{bmatrix}+\frac{1}{6}\begin{bmatrix}2 & 1 & 0\\ 1 & 4 & 1\\ 0 & 1 & 2\end{bmatrix}\begin{bmatrix}\dot{u}_{i-1}\\ \dot{u}_i\\ \dot{u}_{i+1}\end{bmatrix}+\frac{M}{6}\begin{bmatrix}2 & 1 & 0\\ 1 & 4 & 1\\ 0 & 1 & 2\end{bmatrix}\begin{bmatrix}u_{i-1}\\ u_i\\ u_{i+1}\end{bmatrix}-\frac{P}{2}\begin{bmatrix}1\\ 2\\ 1\end{bmatrix} \tag{16}$$

Now if we consider the row corresponding to the node i to zero with $l = h$, from equation (16) the difference schemes reads:

$$\frac{1}{h^2}(-u_{i-1}+2u_i-u_{i+1})+\frac{1}{6}(-\dot{u}_{i-1}+4\dot{u}_i+\dot{u}_{i+1})\frac{M_1}{6}(u_{i-1}+4u_i+u_{i+1})=P \tag{17}$$

Using the trapezoidal rule on (17), the following system of equations in Crank-Nicolson method are obtained as:

$$A_1 u_{i-1}^{n+1}+A_2 u_i^{n+1}+A_3 u_{i+1}^{n+1}=A_4 u_{i-1}^{n}+A_5 u_i^{n}+A_6 u_{i+1}^{n}+P^* \tag{18}$$

Similarly, by solving (7) and (8) using the same method we have:

$$B_1 q_{i-1}^{n+1}+B_2 q_i^{n+1}+B_3 q_{i+1}^{n+1}=B_4 q_{i-1}^{n}+B_5 q_i^{n}+B_6 q_{i+1}^{n}+Q^* \tag{19}$$

$$C_1\phi_{i-1}^{n+1}+C_2\phi_i^{n+1}+C_3\phi_{i+1}^{n+1}=C_4\phi_{i-1}^{n}+C_5\phi_i^{n}+C_6\phi_{i+1}^{n} \tag{20}$$

Where:

$$A_1 = 2-6r+rM_1h^2, \quad A_2 = 8+12r+rM_1h^2, \quad A_3 = 2-6r+rM_1h^2$$

$$\mathrm{A_4} = 2+6r-rM_1h^2, \quad A_5 = 8-12r-4rrM_1h^2, \quad A_6 = 2+6r-rM_1h^2$$

$$B_1 = Pr-3r, \quad B_2 = 4Pr+6r, \quad B_3 = \mathrm{Pr}-3r \quad \mathrm{B_4} = Pr+3r,$$

$$\mathrm{B_5} = 4Pr-6r, \quad \mathrm{B_6} = Pr+3r$$

$$C_1 = Pr - 3r, \qquad C_2 = 4Pr + 6r\,, \qquad C_3 = \Pr - 3r$$

$$C_4 = Pr + 3r, \qquad C_5 = 4Pr - 6r, \qquad C_6 = Pr + 3r$$

$$P^* = 12rh^2(\theta_i^n + N\phi_i^n), \quad \text{and} \quad Q^* = 6r\,\Pr\,Ec\left(\left[\frac{\partial u}{\partial y}\right]^2 - R\theta\right)$$

With $r = \frac{k}{h^2}$ and h and k are the mesh size along y direction and time direction respectively. Index i refers to space and j refers to the time. In equations (18), (19) and (20), taking $i = 1(1)n$ and using the initials and boundary conditions (9), the following system of equations is obtained

$$A_i X_i = B_i \qquad i = 1(1)n$$

Where A_i matrices of are order n and X_i and B_i are column matrices having n components. The solution of the system of equation are obtained using Thomas algorithm for velocity, temperature and concentration. For various parameters the results are computed and p resented graphically.

The skin friction, Nusselt number and Sherwood number are important physical parameters for this type boundary layers flow. With known values of velocity, temperature and concentration fields. The skin-friction at the plate is given by non-dimensional form:

$$\tau = \left[\frac{\partial u}{\partial y}\right]_{y=0,1} \tag{21}$$

The rate of heat transfer coefficient can be obtained in the terms of Nusselt number in non-dimensional form as

$$N_u = -\left[\frac{\partial \theta}{\partial y}\right]_{y=0,1} \tag{22}$$

The rate of mass transfer coefficient cab be obtained in terms of Sherwood number in non-dimensional form given by

$$S_h = -\left[\frac{\partial \phi}{\partial y}\right]_{y=0,1} \tag{23}$$

4. Results and Discussion

In order to analyze the effects various parameters on flow field in the boundary layer region, Finite element method was employed to solve equations (6) to (8) under the boundary conditions (9). We studied the effects Prandtl number $\Pr$, Radiation parameter R, Eckert number Ec Schmidt

number Sc, magnetic parameter M, porosity parameter K, Buoyancy effect parameter r_t, ratio of mass transformation (N) on fluid velocity, temperature and concentration and they were presented graphically. $\Pr = 0.71, R = 0.5, Ec = 0.1, Sc = 0.5, M = 0.5, K = 0.5\ r_t = 0.5, N = 0.5$. The values above were adopted to be default parameters values under the present study. There velocity profiles are presented in the following figures:

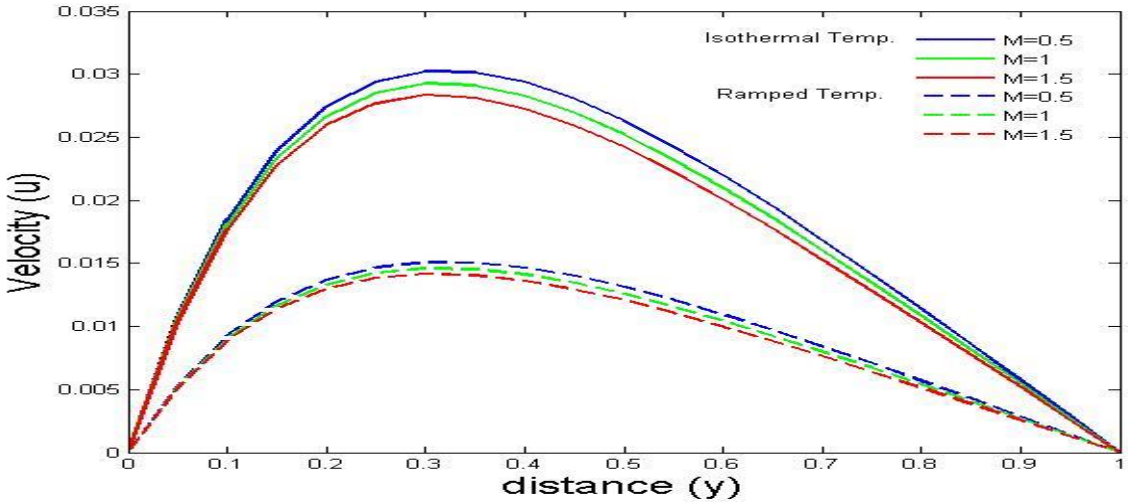

Figure 1: Effect of M on velocity profile

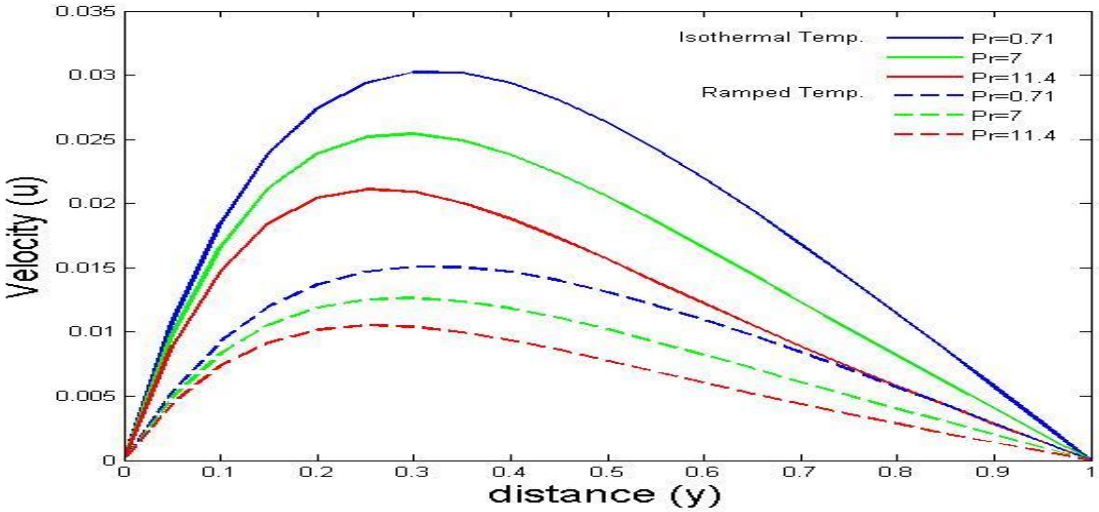

Figure 2: Effect Pr on velocity profile

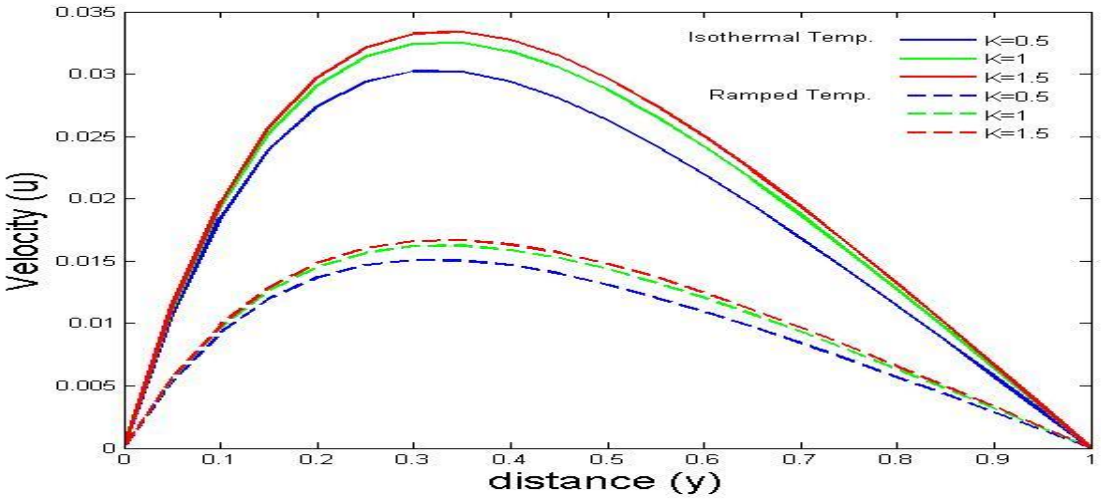

Figure 3: Effect of K on velocity profile

Figure 1 gives the details about the control of magnetic parameter M on velocity for both isothermal and ramped plate. From that figure it is noticed that the velocity begins to reduce at all point of the flow field by increasing the values of magnetic parameter M. This is true since magnetic parameter produce resistive force, which acts opposite direction to the fluid motion. Similarly, Figure 2 gives the details about the control Prandtl number $\Pr$ on fluid velocity for both isothermal and ramped plate. From that figure it is noticed that fluid velocity begins to diminish at all point of the flow field by increasing the values of Prandtl number $\Pr$. While Figure 3 gives the details control about porosity parameter K on fluid velocity for both isothermal and ramped plate and it is also observed that fluid velocity begins to increase at all point of the flow field on increasing the values porosity parameter K.

Figure 4 demonstrates the influence of the ratio of mass transfer parameter N on the fluid velocity for both isothermal and ramped plate. It is observed that the fluid velocity gets enlarged by increasing the values of the ratio of mass transfer parameter N for both isothermal and ramped plate. While Figure 5 demonstrate the influence of Radiation parameter term (R) on the fluid velocity for both isothermal and ramped plate. It is also clearly observed that the fluid velocity gets reduced for both isothermal and ramped plate by increasing the values of Radiation parameter term (R).

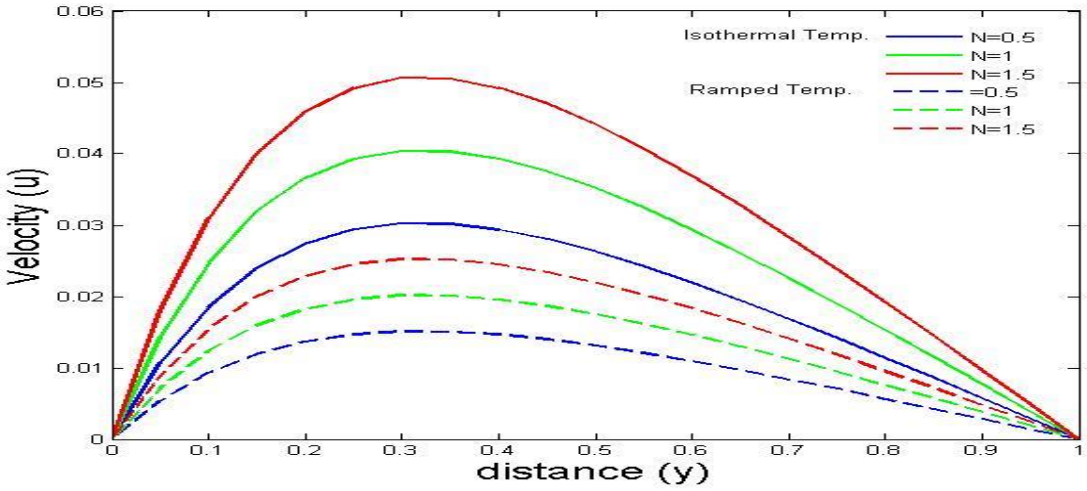

Figure 4: Effect of N on velocity profile

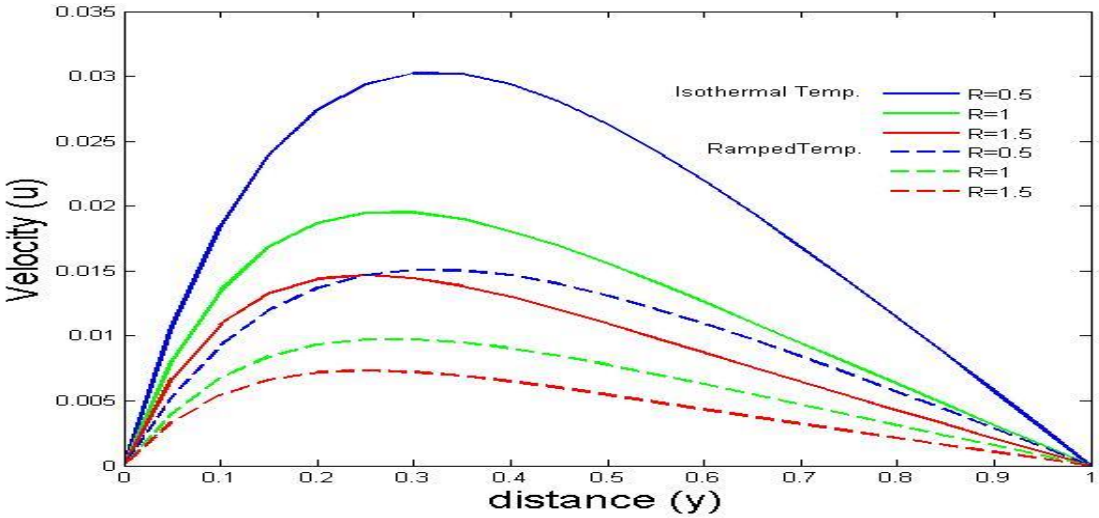

Figure 5: Effect of R on velocity profile

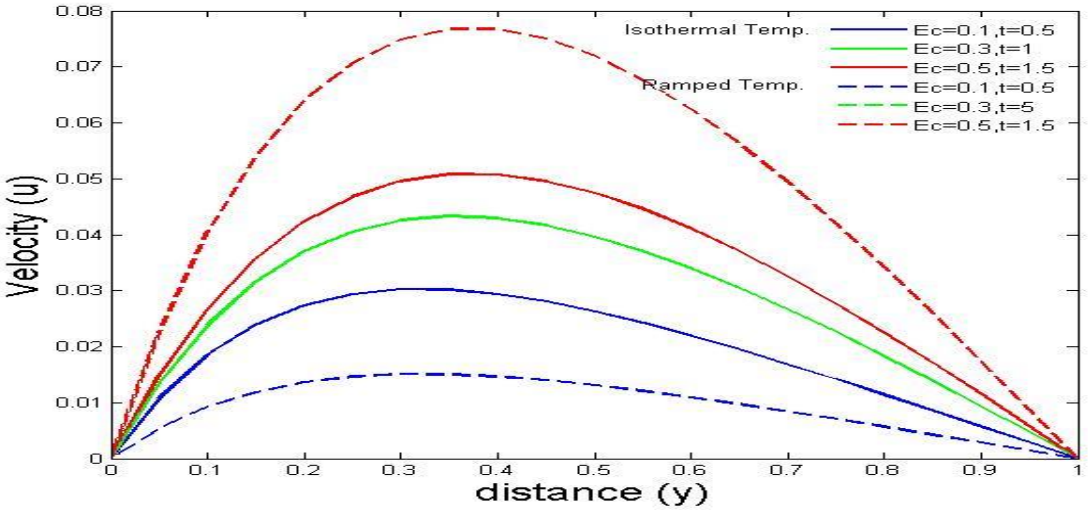

Figure 6: Effect the different values Ec and t on velocity profile

Figure 6 displays the effect of Eckert number Ec and time t parameter on the fluid velocity for both isothermal and ramped plate. It is observed that the velocity get significant enhancement by increasing the values of Ec and time parameter t for both isothermal and ramped plates. There temperature profiles are presented on the following figures:

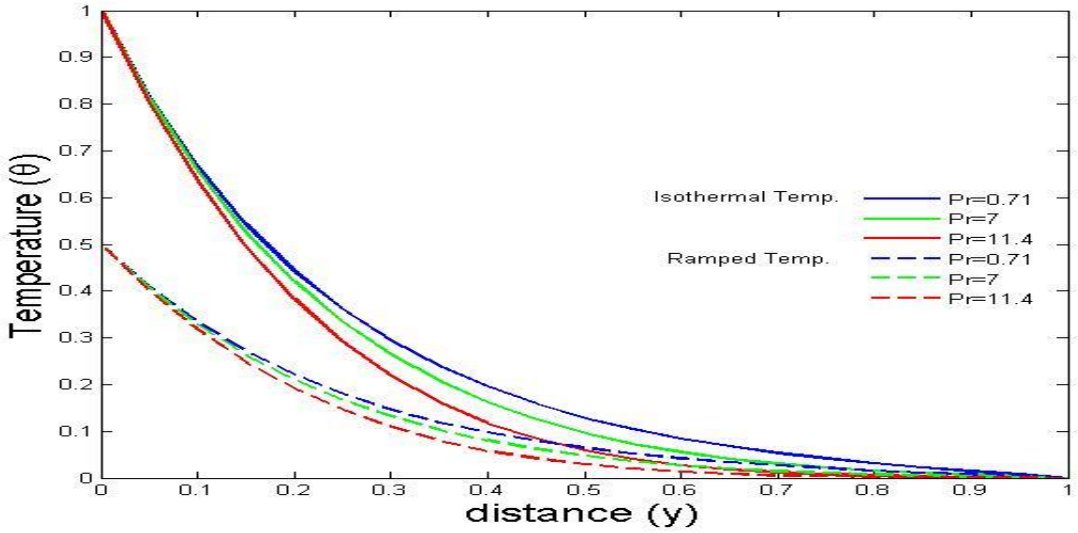

Figure 7: Effect Pr and on temperature profile

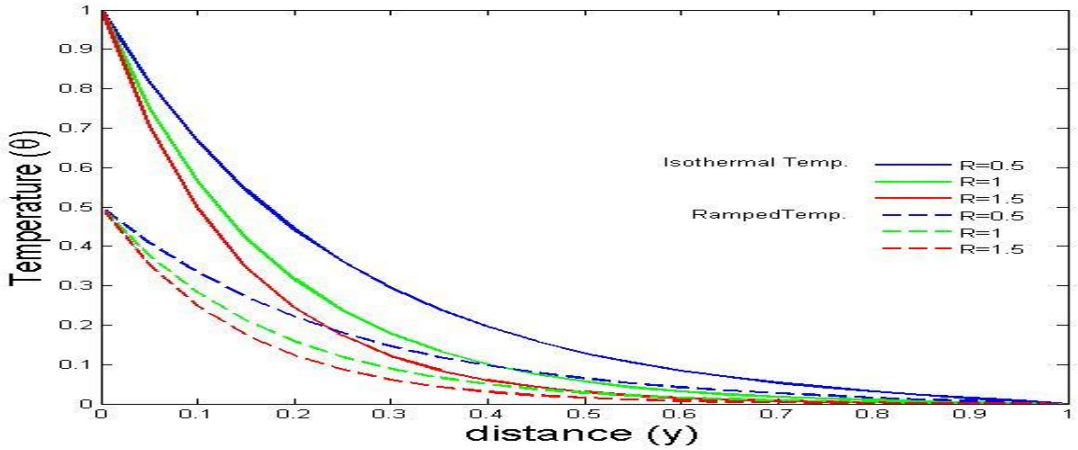

Figure 7: Effect R and on temperature profile

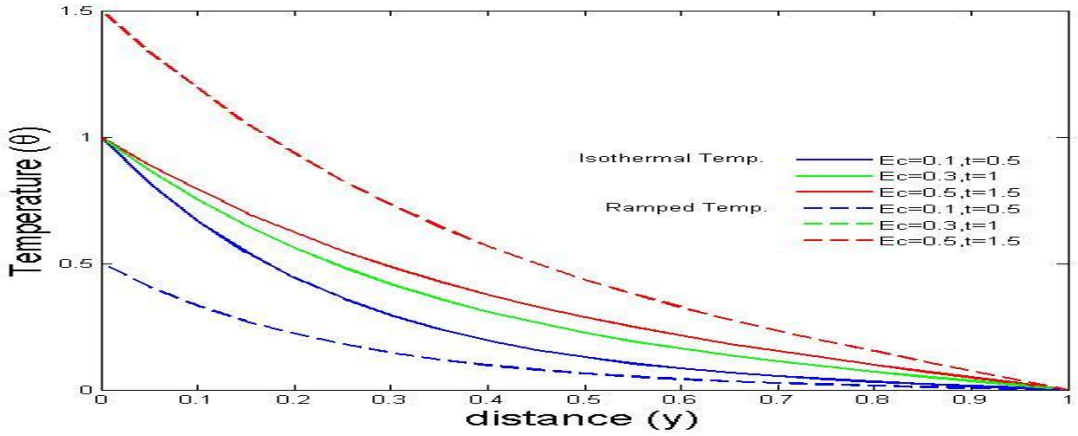

Figure 9: Effect the different values Ec and t on temperature profile

Figure 7 depicts the influence of Prandtl number Pr on fluid temperature for both isothermal and ramped plate. It is revealed from that figure the fluid temperature diminishes by increasing the values of Prandtl number Pr. Similarly figure 8 depicts the influence of radiation parameter term R on fluid temperature for both isothermal and ramped plate. It is also revealed from the figure that figure the fluid temperature gets reduced by increasing the values of Radiation parameter term R.

Figure 9 displays the effect of Eckert number Ec and time t parameter on the fluid temperature for both isothermal and ramped plate. It is observed that the temperature profile gets enlarged by increasing the values of Eckert number Ec and time parameter t for both isothermal and ramped plate.

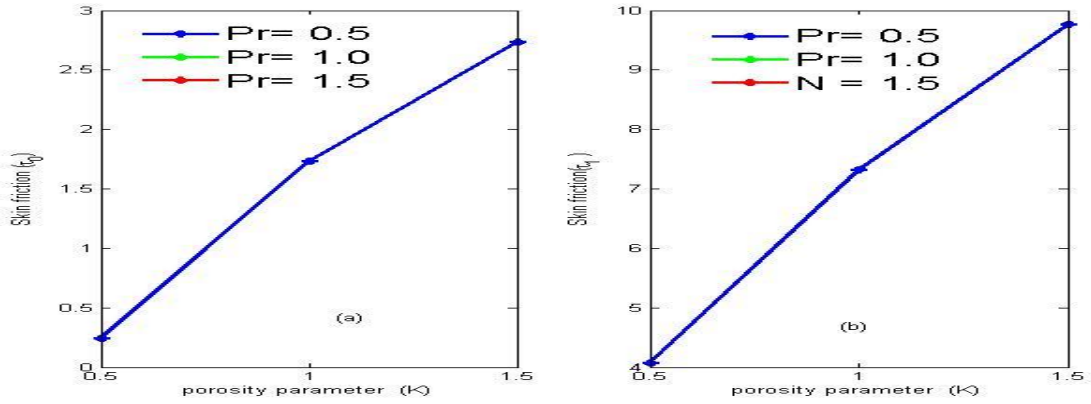

Figure 10(a) &10(b): Effect Pr and K on Skin friction

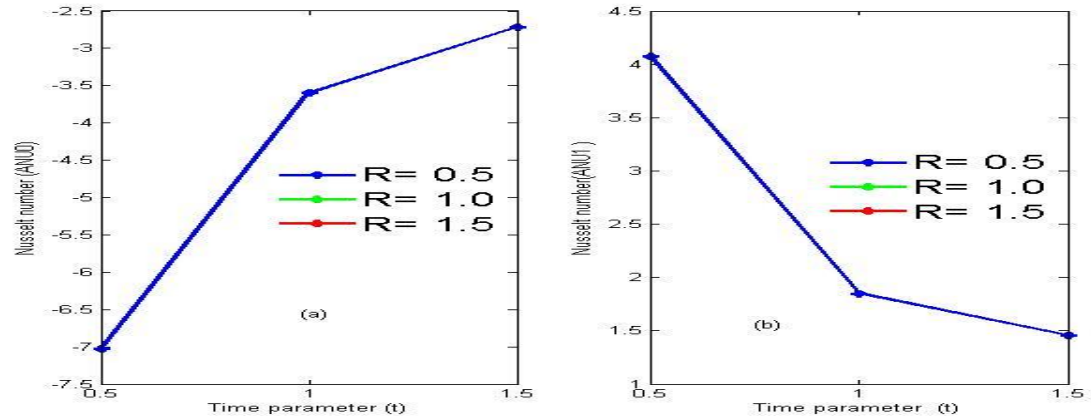

Figure 11(a) &11(b): effect t and R on Nusselt number

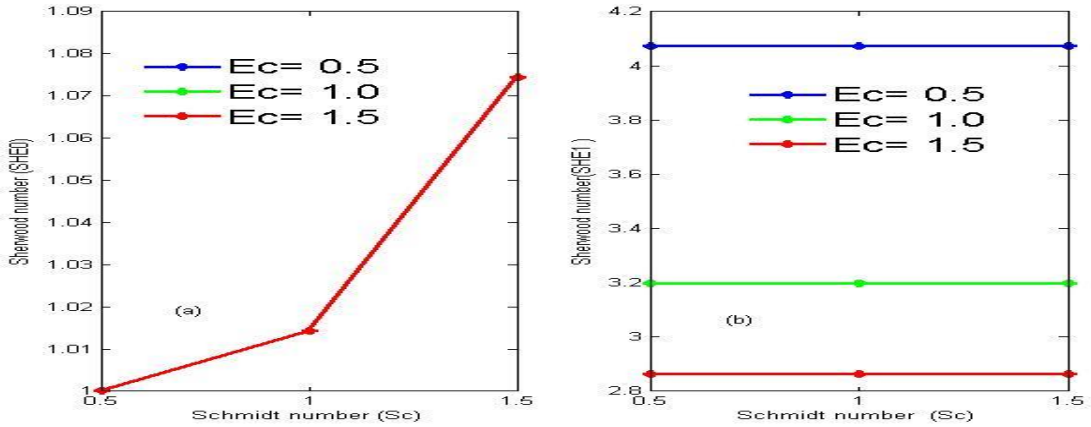

Figure 12(a) &12(b): effect Ec and Sc on Sherwood number

Figure 10(a) and 10(b) displays the effect of Prandtl number Pr and porosity parameter K on the fluid skin friction. It is clearly seen that, increase in Prandtl number has no significant effect on skin friction in both Figure 10(a) and 10(b). While increase in porosity parameter K has boosting

effect on skin friction in Figure 10(a) and 10(b). Similarly, Figure 11(a) and 11(b) displays the effect of time parameter and radiation parameter on the Nusselt number. It is clearly observed that in Figure 11(a) increase time parameter t has significant enhancing effect on Nusselt number and increase in radiation parameter has no significant effect on Nusselt number. In Figure 11(b) Nusselt decreases with increasing time parameter t and radiation parameter has no significant effect on Nusselt number. Figure 12(a) and12 (b) displays the effect of Eckert number Ec and Schmidt number Sc on Sherwood number and it is seen that Schmidt number has increasing effect on Sherwood number in Figure 12 (a) and has no significant effect on Sherwood number in Figure 12 (b). Increase Eckert number has no significant effect on Sherwood number in Figure 12(a) and has significant increasing effects on Sherwood number in Figure 12 (b).

5. Conclusion

In this paper, we studied the thermal radiation effects on unsteady heat and mass transfer Couette flow of free convective vertical channels due to ramped and isothermal temperature. From the study, the following conclusions were drawn:

i. Increase of porosity parameter K, ratio of mass transfer parameter N, Eckert number Ec time parameter t enhances the velocity while reverse is the case with the increase of Magnetic parameter M, Radiation parameter tern R and Prandtl number Pr .

ii. Similarly increase of Eckert number Ec and time parameter t enhances the temperature profile and reverse is the case with the increase of Magnetic parameter M, Prandtl number Pr and Radiation parameter R.

iii. Prandtl number has no effects on skin friction at y = 0 and y = 1, skin friction at y=0 and y=1 gets enlarged with the increase of porosity parameter K.

iv. Increase in radiation parameter R has no effects on Nusselt number at y = 0 and y = 1, but increase in Prandtl enhances the Nusselt number at y = 0 and it diminishes it at y = 1.

v. Schmidt number has boosting effects on Sherwood number at y = 0 and has no effects in Sherwood number at y = 1. While Eckert number has no effects on Sherwood number at y=0 and has significant enlarging effects on Sherwood number at y = 1.

References

1. Adamu, G. C., and Bandari, S. (2018). Buoyancy Effects on MHD Flow of a Nanofluid over a Stretching Sheet with Chemical Reaction. *International Journal of Innovative Research in Science, Engineering and Technology*; 7(11), 2319-8753

2. Alao F. I., Fagbade A. I. & Falodun, B. O. (2016). Effects of Thermal Radiation, Soret and Dufour on an Unsteady Heat and Mass Transfer flow of a Chemically Reacting Fluid past a Semi-Infinite Vertical Plate with Viscous Dissipation. *Journal of the Nigerian Mathematical Society*; 35(2016) 142-158.

2. Animasaun, I. L., Raju, C. S. K. & Sandeep, N. (2016). Unequal Diffusivities Case of Homogeneous Heterogeneous Reactions within Viscoelastic Fluid flow in the presence of Induced Magnetic-field and Nonlinear Thermal Radiation. *Alexandria Engineering Journal* 55, 1595-1606.

3. Bala, I. Y., Kumar, B. J. & Lin, J. (2016). Combined Effects of Thermal Diffusion and Diffusion-Thermo Effects on Transient MHD Natural Convection and Mass Transfer Flow in a Vertical Channel with Thermal Radiation. *International Journal of Scientific Research*; 7, 2354-2373.

4. Bhatti, M. M., Zeeshan, A. & Ellahi, R. (2017). Heat Transfer with Thermal Radiation on MHD Particle fluid Suspension Induced by Metachronal Wave. *Pramana Journal of Physics;* (2017), 39-48. DOI 10.1007/s12043-017-1444-6.

5. Danjuma, Y.I., Haliru, A.A., Ibrahim, M & Hamza, M.M. (2019). Unsteady Heat Transfer to MHD Oscillatory Flow of Jeffrey fluid in a Channel Filled with Porous Material. *International Journal of Scientific and Research Publications*, 9 (7), 2250-3153.

6. Ganesh, K. K., Gireesha B. J., Manjunatha S. & Rudraswamy N. G. (2017). Effect of Nonlinear Thermal Radiation on Double-Diffusive mixed Convection Boundary Layer Flow of Viscoelastic Nanofluid over a Stretching Shee. *International Journal of Mechanical and Materials Engineering;* 10(11), 71-83.

7. Ganesh, K. K., Gireesha B. J., Manjunatha S. & Rudraswamy N. G. (2017). Non Linear Thermal Radiation Effect on Williamson Fluid with Particle-Liquid suspension past a Stretching Surface. *Elservier Journal*; 7(2017), 3196-3202.

8. Nayak, M. K. (2017). MHD 3D Flow and Heat Transfer Analysis of Nano Fluid by Shrinking Surface Inspired by Thermal Radiation and Viscous Dissipation. *International Journal of Mechanical Sciences;* 124-125(2017), 185-193.

9. Prabhakar, R. B. (2016). Mass Transfer Effects on an Unsteady MHD Free Convective Flow of an Incompressible Viscous Dissipative Fluid Past an Infinite Vertical Porous Plate. *International Journal of Applied Mechanics and Engineering*; 21(1), 143-155.

10. Reddy, G. J., Raju, R. S., Rao, J. A. & Gorla, R. S. R. (2017). Unsteady MHD Heat Transfer in Couette Flow of Water at 4^{o}C in a Rotating System with Ramped Temperature via Finite Element Method. *International Journal of Applied Mechanics and Engineering;* 22(1), 145-161.

11. Rizwan, U. L. H., Nadeem, S., Hayat, K. Z. & Sher A. N. (2017). Thermal Radiation and Slip Effects on MHD Stagnation point Flow of Nano Fluid over a Stretching Sheet. *Physics E;* 65(2015), 17-23.

12. Shagaiya, D. S. & Daniel, S. K. (2015). Effects of Buoyancy and Thermal Radiation on MHD Flow over a Stretching Porous Sheet using Homotopy Analysis Method. *Alexandria Engineering Journal;* 54, 705-712.

13. Shagaiya, Y. D. & Simon, K. D. (2015). Effects of Buoyancy and Thermal Radiation on MHD Flow over a Stretching Porous Sheet using Homotopy Analysis Method. *Alexandria Engineering Journal;* 54(2015), 705-712.

14. Siva, R. S. & Anjan, K. S. (2016). Finite Element Analysis of Heat and Mass Transfer past an Impulsively Moving Vertical Plate with Ramped Temperature. *Journal of Applied Science and Engineering*; 19(4), 385-392.

THE ASSESSMENT OF CARBON DIOXIDE (CO2) ADSORPTION AND SPATIAL BIOMASS DISTRIBUTION MAPPING IN THE RESERVOIR OF HINBOUN HYDROPOWER PROJECT

S.Phoummixay[1,*], Biswadip Basu Mallik[2], T.Khampasith[1], V.Somchay[1], K.Phouphavanh[1],P.Sengkeo[1], S.Sivakone[1]

[1] Environmental Engineering Department, Faculty of Engineering, National University of Laos.

[2]Department of Basic Science & Humanities, Institute of Engineering & Management, Salt Lake Electronics Complex, Kolkata- 700091. West Bengal. India.

[*] Corresponding author, E-mail: phoummixay2011@gmail.com.

Abstract

Geographical Information System (GIS) is an excellent tool to be employed with computer control system and play very significant role for database management, storing, capture, mapping and data analysis which includes vector and raster data. This study is mainly to focus on: (i) to study on the tree volumes, carbon storages and analyze the adsorption of carbon dioxide (CO_2), (ii) to estimate the existing biomass within the reservoir and (iii) to create the spatial biomass distribution maps. Consequently, the distribution maps are described and indicated in low to high biomass density within the study area. Hence, this study has found that: there are 10,365.3 m^3 of the total volume, 421.423 kg of total Carbone storage, 1,542.41kg of total CO_2 absorption and 36,346.48 tons of total Biomass within the study area.

Keywords: *GIS, Biomass, Carbon Dioxide, Adsorption, Dam.*

1. INTRODUCTION

Lao government has set forest strategy and targeted to restore and increase the forest cover to be 70% by 2020 [1].It means that 8.2 million hectares of land need to be planted, Carbon dioxide emission has been increased gradually since 2000 and 2013 there was 3,199 Kilotons at highest concentration in Lao PDR [2,3,4]. It is caused of global warming and climate change as encountering [5]. Carbon absorption of the trees are natural way to reduce global warming issue and save the global from high temperature around the global, it also increases the oxygen for the people and living and nonliving thing [6].

2. LITERATURE REVIEW

Currently, GIS is developed and employed commonly in multi-tasks for instance: science, engineering and relevant works [7]. Spatial biomass distribution is integrated between data collection from field work and ArcGIS software application [8]. In particular, Arc toolbox is a wise tool that applies to interpolate with Kriging method [9], in order to deal with biomass spatial distribution of each sampling point within the reservoir area of Hinboun Hydroelectric Plant [10], the Kriging methods were calculated and generated the raster files of the biomass distribution based on data analysis [11] and were stored in the database as attribute data, entire

data was employed the statistical function to analyze and then be transferred from Microsoft Excel to Arc GIS by Geospatial method [12].

3. METHODOLOGY

The study is conducted and followed the research methodology as indicated in Fig 1.

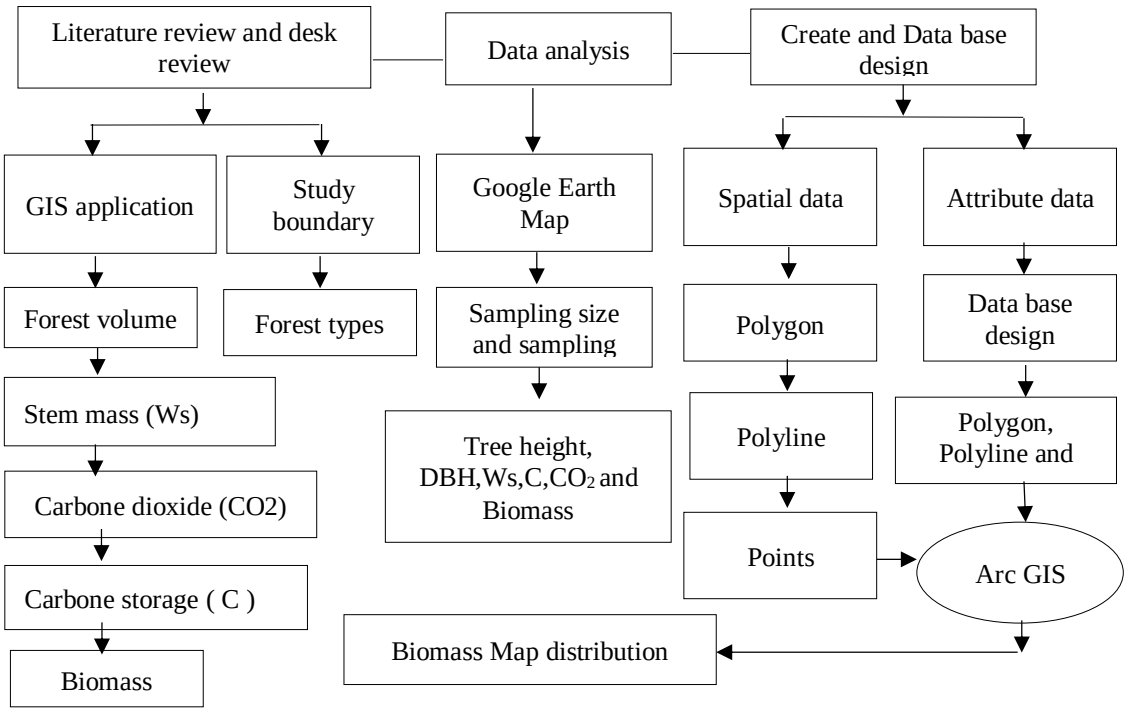

Fig1. Research methodology

A. Site study and sampling data collection

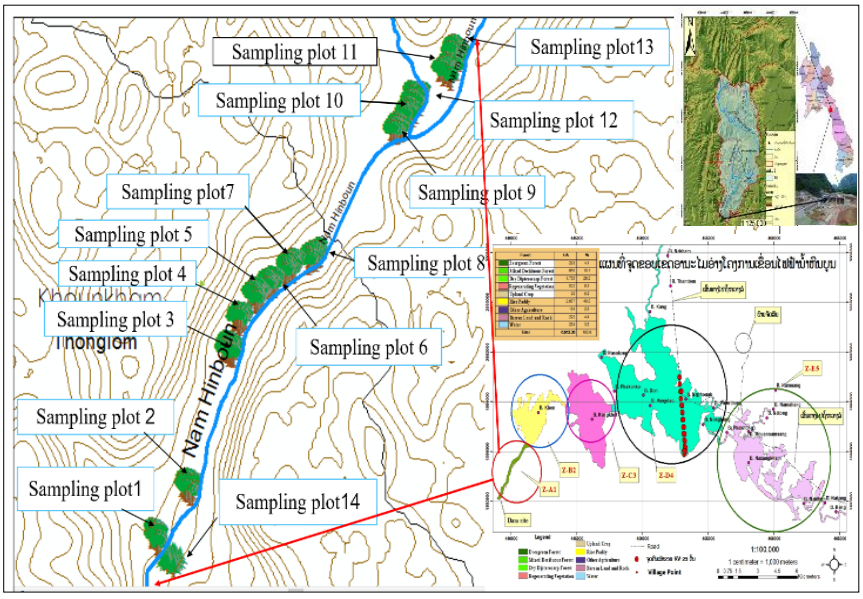

Fig2. Study area and sampling plots

Hinboun Hydro Power is a project that belongs to the Electricite Du Laos (EDL) to generate the electricity and support to Local need, it is located approximately 3 km above Thonglom Village to the East, Hinboun district, Khammouane Province and also approximately 30 kilometers downstream of the existing Theun Hinboun Dam and 60 km away and North of the confluence area of Nam Hinboun River and Mekong River. The type of dam is a run-off river concrete diversion dam which the main purpose is to generate the electricity for local use, low and high point is 167 masl and 468 masl [13], respectively, the study will cover only Z-A1 which is 60.78 ha, there are 14 sampling locations where were collected data as shown in Fig 2.

B. Formulas and Equations

$$W_s = 0.0509 \times D \times H \quad [1]$$

$$C = W_s \times 0.5 \quad [2]$$

$$Abs(CO_2) = C \times (\frac{44}{12}) \quad [3]$$

$$V = D^2 \times (\frac{\pi}{4}) \times h \times f \quad [4]$$

$$Biomass = (\frac{W_s \times V \times 800}{1000}) \quad [5]$$

Where:

W_s: Stem mass [kg]

C: Carbone Storage [kg]

$Abs(CO_2)$: Carbon dioxide absorption [Kg]

V: Volume [m^3]

f :Factor = 0.65

C. Data analysis and Biomass calculation

Based on data collection at sampling sites. Therefore, data was manipulated and analyzed to obtain the biomass volume [14, 15] as indicated in Fig 3.

Sampling points	Ws (kg)	V (m^3)	C(Kg)	Co2(Kg)	Biomass (Tons)	Biomass (Tons) /year
1	75.622	931.679	37.811	138.388	3303.858	9.05
2	64.573	797.5	32.287	118.169	2978.174	8.16
3	64.222	791.263	32.111	117.526	2519.148	6.90
4	60.785	743.388	30.393	111.237	2909.89	7.97
5	66.833	822.758	33.417	122.304	3068.079	8.41
6	39.124	477.814	19.562	71.597	978.442	2.68
7	59.068	729.297	29.534	108.095	2454.142	6.72
8	47.505	583.38	23.752	86.934	1657.757	4.54
9	46.148	566.088	23.074	84.451	1253.235	3.43
10	44.219	542.3	22.109	80.921	1275.022	3.49
11	61.251	750.304	30.626	112.09	2270.052	6.22
12	59.891	737.384	29.945	109.6	2430.282	6.66
13	72.363	892.649	36.182	132.424	4587.172	12.57
14	81.241	999.472	40.62	148.671	4661.232	12.77
Total	**842.845**	**10,365.28**	**421.423**	**1542.407**	**36346.485**	**99.57941**

Fig3. Sampling points and Biomass calculation

4. RESULT AND DISCUSSION

Figure 4 shows relationship between biomass and carbon absorption and also biomass and carbon storage within the study area, according to the finding, root mean square is 0.838 and 0.839, respectively. It means that the more biomass, the more absorption within the trees as well as the carbon storage.The distribution maps. Figure 5, 6, 7, 8 and 9 are described and indicated in low to high biomass density within the study area.**T**he low biomass density is meant that, those areas are not much richness of biodiversity and adsorption carbon dioxide is not rather good, the high biomass density is relevant to the abundance of the forest cover due to most of the standing trees are enriched and sustained; they are adsorptive carbon dioxide very well. Therefore, the forest cover will support and mitigate global warming and also climate change issue Among of 14 sampling points, the biomass distributions

Are mostly covered at plot 14 and 13 and 1 which are 4661.232 kg, 4587.172 kg and 3303.858 kg, respectively. The biomass distribution is covered very less at Plot 6, 9 and 10 which are 978.442 kg, 1253.235 kg and1275.022 kg, respectively.

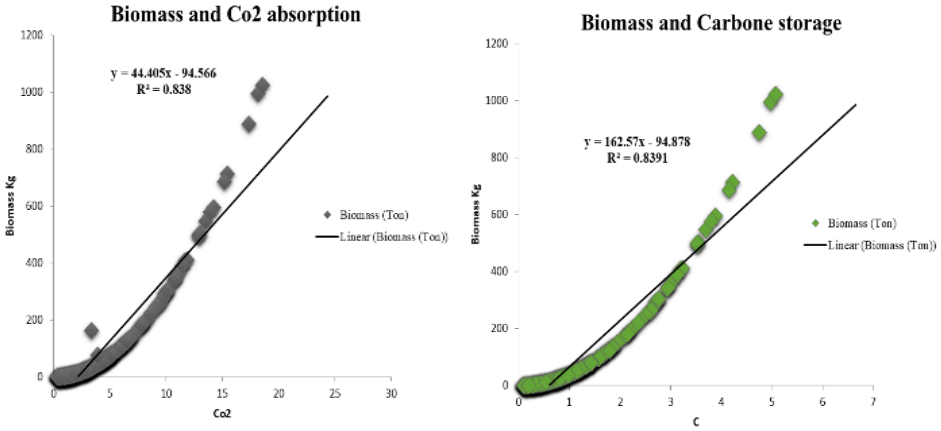

Fig4. Biomass, Carbon Storage and CO2 absorption model

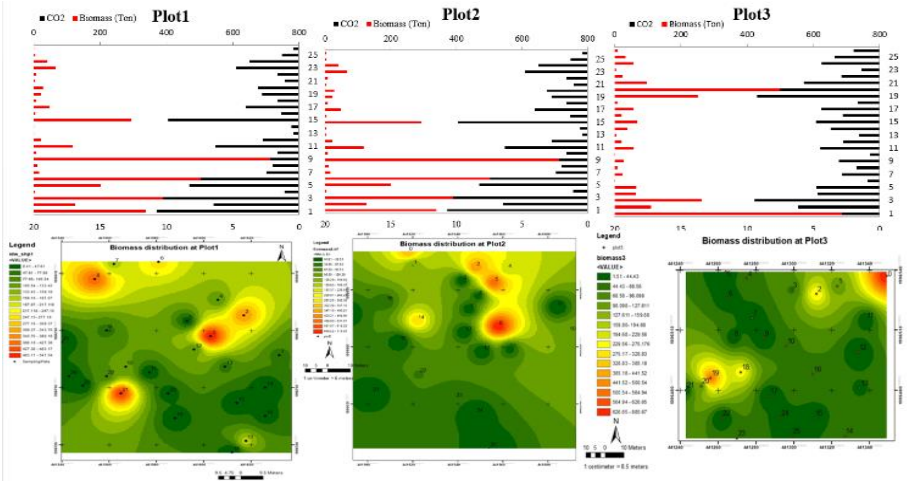

Fig5. Biomass Distribution at Plot 1, 2 and 3

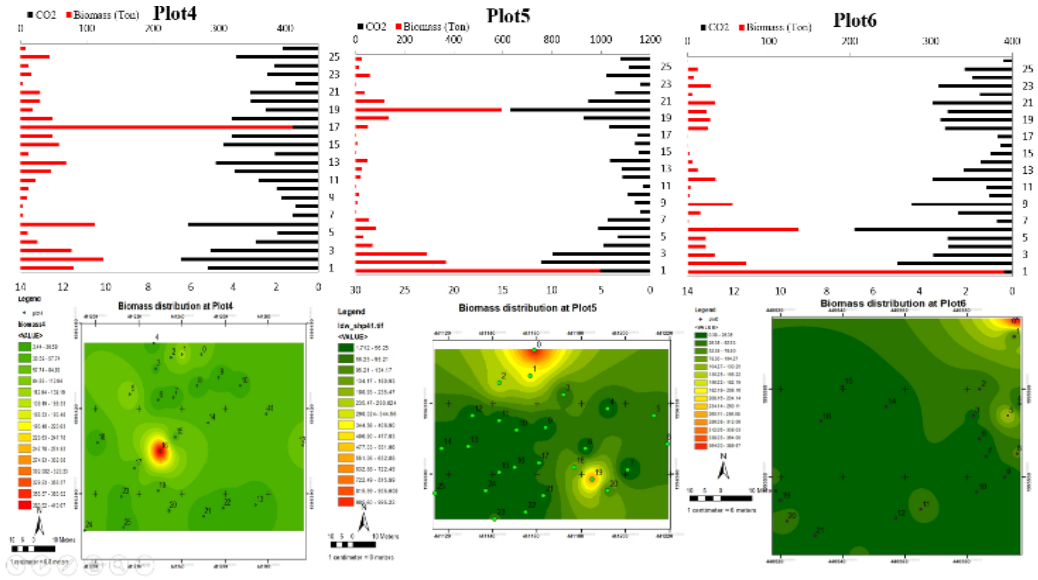

Fig6. Biomass Distribution at Plot 4, 5 and 6.

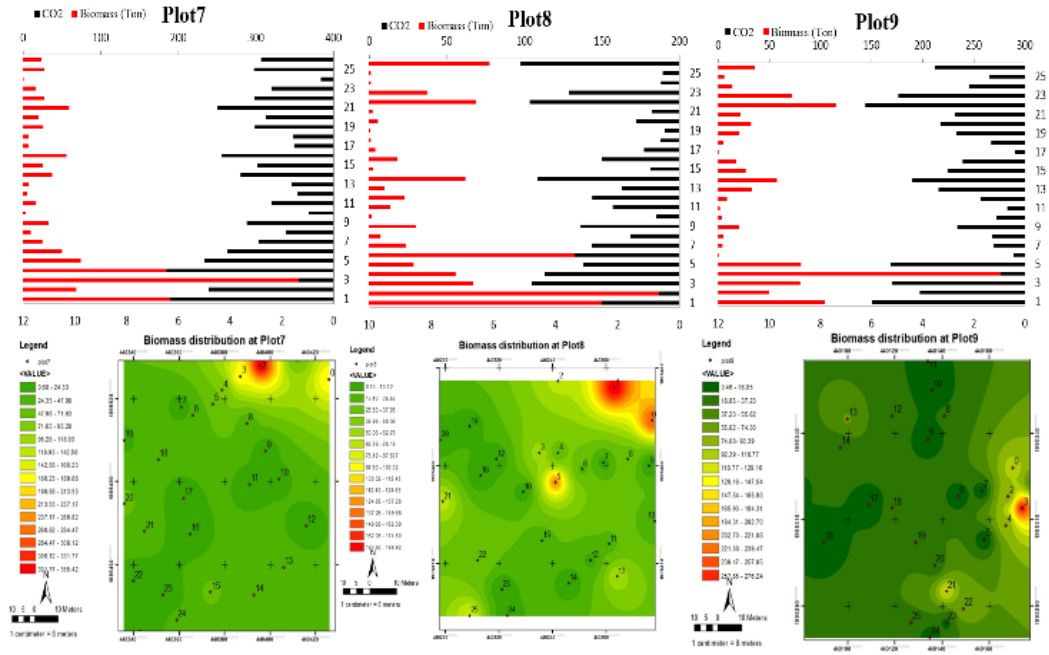

Fig7. Biomass Distribution at Plot 7,8 and 9

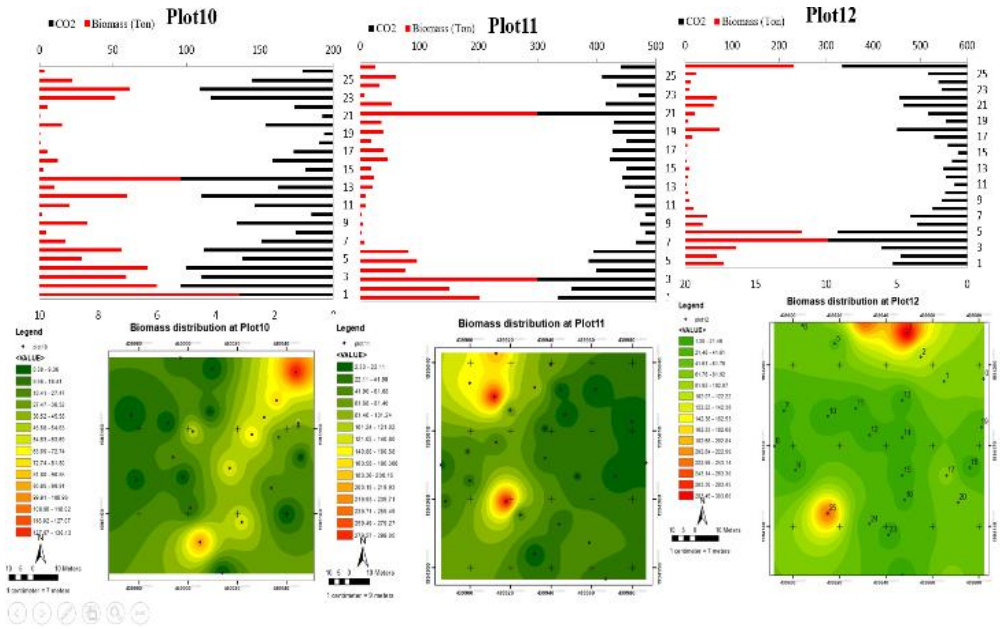

Fig8. Biomass Distribution at Plot 10, 11 and 12

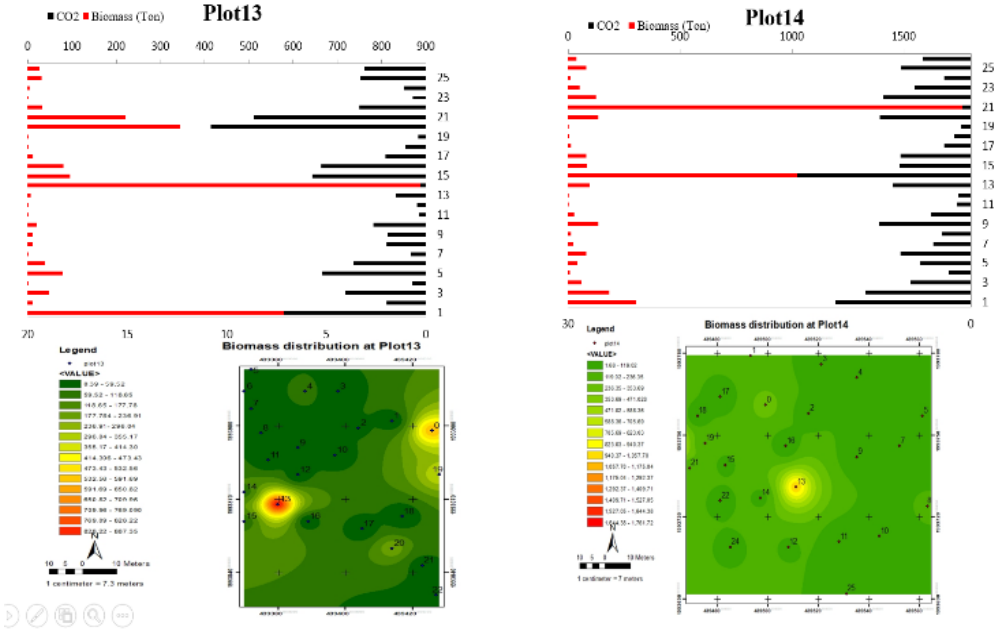

Fig9. Biomass Distribution at Plot 13 and 14

5. CONCLUSION

This paper is presented the integrated ArcGIS and excel sheet working together from the site to deskwork by employing the Biomass formula to manipulate and map. Therefore, the study results within the Z-A1are as followings:

The biomass distribution coverage at plot 1,13 and 14 are significantly to environment and biodiversity conservation, due to they are considered as good carbon dioxide absorption, at Plot 6,9 and 10 are considered as low carbon dioxide absorption and the other plots are classified

as medium. Therefore, increasing of the sustainable Biomass will be vital factor that will support and mitigate global warming and also climate change issue in both down and up scaling.

In addition, Biodiversity Offset should be compensated when forest is cut and burned in order to sustain the forest and wildlife and also climate change issue.

ACKNOWLEDGMENT

Author would like to thank the board committees of Nam Hinboun hydropower project to collect data and their support during site survey and also thanks to all who contributed their hospitality to assist the study since it completed. Additionally, thanks to Visavakhone Engineering & Construction Co.,Ltd for their financial support.

REFERENCES

[1] Ministry of Natural Resources and the Environment (MoNRE),” National Biodiversity Strategy and Action Plan for Lao PDR 2016-2025. Vientiane Lao PDR”,2016.
[2]World Bank, “Lao PDR carbon (Co2) emission 1996-2019”, [Online], Available:https://www.macrotrends.net/countries/LAO/lao-pdr/carbon-co2-emissions, 2019.
[3]Sorphasith Xaisongkham, Syvanh Phonasa, Khaysy Srithilat and Honglin Yuan “Carbon dioxide emissions and the prospects for Lao PDR's economic self-development”, June 2019.
[4] Muntean, M., Guizzardi,D.,Schaaf,E., Crippa,M.,Solazzo,E., Oliver,J,G,J.,Vignati,E. Fossil “CO2 emssions of all world countries-2018
[5]report”,2018, [Online], Available: https://countryeconomy.com/energy-and-environment/co2-emissions
[6] Biswjit Mukhopadhyay ,”Global Warming – A Threat to the Planet”,2013.
[7] Graciela Tejada , Eric Bastos Görgens , Fernando Del Bon Espírito-Santo , Roberta Zecchini Cantinho and Jean Pierre Ometto ”Evaluating spatial coverage of data on the aboveground biomass in undisturbed forests in the Brazilian Amazon”,2019.
[8] Geoffery J. Meaden , José Aguilar-Manjarrez ,”Advances in geographic Paper information systems and remote sensing for fisheries and aquaculture”,2013.
[9] Na Li, Gaodi Xie,Changshun Zhang, Yu Xiao, Biao Zhang, Wenhui Chen ,Yanzhi Sun and Shuo Wang, “Biomass Resources Distribution in the Terrestrial Ecosystem of China”, 2015.
[10]Aba SC , Ndukwe OO , CJ Amuand KP Baiyeri ,”The role of trees and Plantation agriculture in mitigating global climate change”, 2017.
[11] Nam Hinboun Hydro Power, “Environmental Social Management Monitoring Plan report”, 2012.
[12] Tomislav Hengl, “A Practical Guide to Geostatistical Mapping”, 2009.
[13] S.Phoummixay,” Introduction to Geographical Information System”, 2018, ch.1.
[14] Electricite Du Laos ,”Project design document form for CDM project activities, version 8.0”,2017.
[15] P.Khamphet, “Forest survey and inventory manual”, 2015.
[16] Asian Development Bank (ADB),”Project performance audit report on the Theun-Hinboun Hydropower project (Loan 1329-LAO[SF]) in the Lao People’s Democratic Republic”,2002.

APPLICATION OF ZZ-TRANSFORM WITH HOMOTOPY PERTURBATION METHOD FOR SOLVING HIGHER-ORDER BOUNDARY VALUE PROBLEMS

George Albert Toma

Department of Mathematics

Aleppo University, Aleppo, Syria

Email: george.toma.1987@gmail.com

Abstract

In this paper, a new hybrid scheme for solving the higher-order boundary value problems is introduced. the presented approach is based on combination of the ZZ-transform method with the homotopy perturbation method to find the solutions of boundary value problems. To show the power of the proposed technique, several examples are tested and the comparison results are tabulated.

Keywords: *ZZ-transform method, homotopy perturbation method, hybrid scheme, higher-order, boundary value problems*.

INTRODUCTION

Higher-order boundary value problems arise in many engineering and applied sciences applications, therefore the researchers have been interested in this type of problems. there are many numerical and analytical methods used to solve the higher-order boundary value problems such as Adomian decomposition method [1,2], differential transform technique [3], Quintic B-spline collocation method [4], chebychev polynomial technique [5], iterative method [6], developed Euler-collocation method [7] and variational iteration method [8].

The aim of this paper is to suggest a new hybrid method combines the ZZ-transform with the homotopy perturbation method to find the solutions of higher-order boundary value problems that are difficult to solve via classical methods. the new proposed technique exploits the advantage of the ZZ-transform and the homotopy perturbation method (HPM) to introduce a new scheme with high accuracy.

The organization of the paper is as follows. In Section 2, the definition of ZZ-transform is introduced. In Section 3, the proposed hybrid method is presented. In section 4, some numerical examples are tested. Finally, Section 5 provides conclusions of the work.

DEFINITION OF ZZ-TRANSFORM

In 2016, the integral transform "ZZ-transform method" was introduced by Zain Abadin Zafar [9]. ZZ-transform technique is similar to the other transforms such as Sumudu and Laplace transforms.

Definition [9]:

let $f(x)$ be a function defined for all $x \geq 0$. The ZZ-transform of a function $f(x)$ is described as follows

$$H\left(f(x)\right) = Z(v,s) = s\int_0^{\infty} f(v\,x)e^{-sx}dx$$

THE PROPOSED SCHEME

In this section, the methodology of the presented method is explained by detail as follows:

Consider the following n-th order boundary value problem

$$v^{(n)}(x) = f\left(x, v, v', ..., v^{(n-1)}\right) \tag{1}$$

With boundary conditions

$$v(0) = \alpha_0, v'(0) = \alpha_1, ..., v^{(n-1)}(0) = \alpha_{n-1}$$

Where f is a continuous function on $[0,1]\times D$, D is an open subset of R^{n-1} and α_i are real numbers.

Taking the ZZ- transform on (1), we find

$$\frac{s^n}{v^n}H(v) - \sum_{k=0}^{n-1}\frac{s^{n-k}}{v^{n-k}}v^{(k)}(0) = H\left[f\left(x, v, v', ..., v^{(n-1)}\right)\right]$$

Then we have

$$H(v) = \frac{v^n}{s^n}\sum_{k=0}^{n-1}\frac{s^{n-k}}{v^{n-k}}v^{(k)}(0) + \frac{v^n}{s^n}H\left[f\left(x, v, v', ..., v^{(n-1)}\right)\right] \tag{2}$$

Now, we construct the homotopy on (2) yields

$$H(v) = \frac{v^n}{s^n}\sum_{k=0}^{n-1}\frac{s^{n-k}}{v^{n-k}}v^{(k)}(0) + p\frac{v^n}{s^n}H\left[f\left(x, v, v', ..., v^{(n-1)}\right)\right] \tag{3}$$

Where $p \in [0,1]$ is an embedding parameter.

According to the homotopy perturbation method the solution of (3) can be written as a power series in *p*

$$v = \sum_{i=0}^{\infty} p^i v_i \tag{4}$$

Substituting (4) into (3), we get

$$H\left(\sum_{i=0}^{\infty} p^i v_i\right) = \frac{v^n}{s^n}\sum_{k=0}^{n-1}\frac{s^{n-k}}{v^{n-k}}v^{(k)}(0) + p\frac{v^n}{s^n}H\left[f\left(x, \sum_{i=0}^{\infty} p^i v_i, \sum_{i=0}^{\infty} p^i v_i', ..., \sum_{i=0}^{\infty} p^i v_i^{(n-1)}\right)\right]$$

Comparing the coefficients of terms with identical powers of p and taking the inverse ZZ-transform and we get the approximate solution of (1) where $p = 1$

$$v = \sum_{i=0}^{\infty} v_i$$

NUMERICAL EXAMPLES

In this section, to test the accuracy of the proposed method several examples are presented

Example .1

Consider the following ninth-order boundary value problem:

$$v^{(9)}(x) = -9e^x + v(x) \quad , \quad 0 \le x \le 1 \tag{5}$$

With boundary conditions

$$v^{(i)}(0) = 1 - i \quad ; i = 0,1,2,3,4$$
$$v^{(i)}(1) = -i\,e \quad ; i = 0,1,2,3$$

Taking the ZZ- transform on (5), finds

Then
$$\frac{s^9}{v^9}H(v) - \frac{s^9}{v^9}v(0) - \frac{s^8}{v^8}v'(0) - \frac{s^7}{v^7}v''(0) - \frac{s^6}{v^6}v^{(3)}(0) - \frac{s^5}{v^5}v^{(4)}(0) - \frac{s^4}{v^4}v^{(5)}(0) - \frac{s^3}{v^3}v^{(6)}(0)$$
$$-\frac{s^2}{v^2}v^{(7)}(0) - \frac{s}{v}v^{(8)}(0) = -9H\left(1 + x + \frac{x^2}{2!} + \frac{x^3}{3!} + \frac{x^4}{4!} + \frac{x^5}{5!} + \frac{x^6}{6!}\right) + H(v)$$

we have

$$H(v) = 1 - \frac{v^2}{s^2} - 2\frac{v^3}{s^3} - 3\frac{v^4}{s^4} + \alpha_1\frac{v^5}{s^5} + \alpha_2\frac{v^6}{s^6} + \alpha_3\frac{v^7}{s^7} + \alpha_4\frac{v^8}{s^8}$$
$$-9\left(\frac{v^9}{s^9} + \frac{v^{10}}{s^{10}} + \frac{v^{11}}{s^{11}} + \frac{v^{12}}{s^{12}} + \frac{v^{13}}{s^{13}} + \frac{v^{14}}{s^{14}} + \frac{v^{15}}{s^{15}}\right) + \frac{v^9}{s^9}H(v) \tag{6}$$

Now, we construct the homotopy on (6) then we find

$$H(v)=1-\frac{v^2}{s^2}-2\frac{v^3}{s^3}-3\frac{v^4}{s^4}+\alpha_1\frac{v^5}{s^5}+\alpha_2\frac{v^6}{s^6}+\alpha_3\frac{v^7}{s^7}+\alpha_4\frac{v^8}{s^8}$$
$$-9\left(\frac{v^9}{s^9}+\frac{v^{10}}{s^{10}}+\frac{v^{11}}{s^{11}}+\frac{v^{12}}{s^{12}}+\frac{v^{13}}{s^{13}}+\frac{v^{14}}{s^{14}}+\frac{v^{15}}{s^{15}}\right)+p\,\frac{v^9}{s^9}H(v) \quad (7)$$

Substituting (4) into (7), we get

$$H\left(\sum_{i=0}^{\infty}p^i v_i\right)=1-\frac{v^2}{s^2}-2\frac{v^3}{s^3}-3\frac{v^4}{s^4}+\alpha_1\frac{v^5}{s^5}+\alpha_2\frac{v^6}{s^6}+\alpha_3\frac{v^7}{s^7}+\alpha_4\frac{v^8}{s^8}$$
$$-9\left(\frac{v^9}{s^9}+\frac{v^{10}}{s^{10}}+\frac{v^{11}}{s^{11}}+\frac{v^{12}}{s^{12}}+\frac{v^{13}}{s^{13}}+\frac{v^{14}}{s^{14}}+\frac{v^{15}}{s^{15}}\right)+p\,\frac{v^9}{s^9}H\left(\sum_{i=0}^{\infty}p^i v_i\right) \quad (8)$$

Comparing coefficients of terms with identical powers of p in (8), we get

$$p^0: H(v_0)=1-\frac{v^2}{s^2}-2\frac{v^3}{s^3}-3\frac{v^4}{s^4}+\alpha_1\frac{v^5}{s^5}+\alpha_2\frac{v^6}{s^6}+\alpha_3\frac{v^7}{s^7}+\alpha_4\frac{v^8}{s^8}$$
$$-9\left(\frac{v^9}{s^9}+\frac{v^{10}}{s^{10}}+\frac{v^{11}}{s^{11}}+\frac{v^{12}}{s^{12}}+\frac{v^{13}}{s^{13}}+\frac{v^{14}}{s^{14}}+\frac{v^{15}}{s^{15}}\right) \quad (9)$$

$$p^1: H(v_1)=\frac{v^9}{s^9}H(v_0) \quad (10)$$

Taking the inverse ZZ- transform of (9) and (10) yields

$$v_0=1-\frac{x^2}{2!}-2\frac{x^3}{3!}-3\frac{x^4}{4!}+\alpha_1\frac{x^5}{5!}+\alpha_2\frac{x^6}{6!}+\alpha_3\frac{x^7}{7!}+\alpha_4\frac{x^8}{8!}$$
$$-9\left(\frac{x^9}{9!}+\frac{x^{10}}{10!}+\frac{x^{11}}{11!}+\frac{x^{12}}{12!}+\frac{x^{13}}{13!}+\frac{x^{14}}{14!}+\frac{x^{15}}{15!}\right)$$

$$v_1=\frac{x^9}{362880}-\frac{x^{11}}{39916800}-\frac{x^{12}}{239500800}-\frac{x^{13}}{2075673600}+\alpha_1\frac{x^{14}}{87178291200}$$
$$+\alpha_2\frac{x^{15}}{1307674368000}+\alpha_3\frac{x^{16}}{20922789888000}+\alpha_4\frac{x^{17}}{355687428096000}$$
$$-\frac{x^{18}}{711374856192000}-\frac{x^{19}}{13516122267648000}-\frac{x^{20}}{270322445352960000}$$
$$-\frac{x^{21}}{5676771352412160000}+\ldots$$

Table.1 shows the errors obtained by using the proposed method and the HPM

Table. 1 comparison results for Example 1

X	Error of basic HPM [10] N=12	Error of proposed method N=1	Error of proposed method N=2
0	0	0	0
0.1	3.6 e -09	5.24615 e -11	3.21489 e -15
0.2	3.4 e -09	1.82732 e -10	5.21147 e -14
0.3	4.6 e -09	1.66867 e -09	8.32226 e -14
0.4	1.4 e -09	3.30718 e -09	3.21478 e -14
0.5	4.5 e -09	4.66982 e -09	1.11248 e -14
0.6	6.0 e -06	4.40412 e -09	2.32148 e -14
0.7	3.1 e -09	2.91342 e -09	9.32547 e -14
0.8	2.4 e -09	1.11459 e -09	2.00147 e -14
0.9	4.5 e -10	1.12556 e -10	5.36987 e -16
1	0	4.38011 e -12	3.31214 e -17

Example .2

Consider the following tenth-order boundary value problem:

$$v^{(10)}(x) = e^{-x} v^2(x) \quad , \quad 0 \le x \le 1 \tag{11}$$

With …

$$v^{(2i)}(0) = 1 \quad , \quad v^{(2i)}(1) = e \quad ; i = 0,1,2,3,4$$

Taking the ZZ transform on (11), we find

$$\frac{s^{10}}{v^{10}} H(v) - \frac{s^{10}}{v^{10}} v(0) - \frac{s^9}{v^9} v'(0) - \frac{s^8}{v^8} v''(0) - \frac{s^7}{v^7} v^{(3)}(0) - \frac{s^6}{v^6} v^{(4)}(0) - \frac{s^5}{v^5} v^{(5)}(0) - \frac{s^4}{v^4} v^{(6)}(0)$$
$$- \frac{s^3}{v^3} v^{(7)}(0) - \frac{s^2}{v^2} v^{(8)}(0) - \frac{s}{v} v^{(9)}(0) = H\left(e^{-x} v^2(x)\right)$$

Then we have

$$\frac{s^{10}}{v^{10}} H(v) = \frac{s^{10}}{v^{10}} + \alpha_1 \frac{s^9}{v^9} + \frac{s^8}{v^8} + \alpha_2 \frac{s^7}{v^7} + \frac{s^6}{v^6} + \alpha_3 \frac{s^5}{v^5} + \frac{s^4}{v^4} + \alpha_4 \frac{s^3}{v^3} + \frac{s^2}{v^2}$$
$$+ \alpha_5 \frac{s}{v} v^{(9)}(0) + H\left(e^{-x} v^2(x)\right) \tag{12}$$

Now, we construct the homotopy on (12) and then we get

$$\frac{s^{10}}{v^{10}} H(v) = \frac{s^{10}}{v^{10}} + \alpha_1 \frac{s^9}{v^9} + \frac{s^8}{v^8} + \alpha_2 \frac{s^7}{v^7} + \frac{s^6}{v^6} + \alpha_3 \frac{s^5}{v^5} + \frac{s^4}{v^4} + \alpha_4 \frac{s^3}{v^3} + \frac{s^2}{v^2}$$
$$+ \alpha_5 \frac{s}{v} v^{(9)}(0) + p\, H\left(e^{-x} v^2(x)\right)$$

Substituting (4) into (12), we get

$$\frac{s^{10}}{v^{10}}H\left(\sum_{i=0}^{\infty}p^{i}v_{i}\right)=\frac{s^{10}}{v^{10}}+\alpha_1\frac{s^{9}}{v^{9}}+\frac{s^{8}}{v^{8}}+\alpha_2\frac{s^{7}}{v^{7}}+\frac{s^{6}}{v^{6}}+\alpha_3\frac{s^{5}}{v^{5}}+\frac{s^{4}}{v^{4}}+\alpha_4\frac{s^{3}}{v^{3}}+\frac{s^{2}}{v^{2}}$$
$$+\alpha_5\frac{s}{v}v^{(9)}(0)+pH\left(e^{-x}\sum_{i=0}^{\infty}p^{i}v^{2}{}_{i}\right) \quad (13)$$

Comparing coefficients of terms with identical powers of p in (13) and taking the inverse ZZ transform, then we have

$$v_0=1+\alpha_1 x+\frac{x^{2}}{2!}+\alpha_2\frac{x^{3}}{3!}+\frac{x^{4}}{4!}+\alpha_3\frac{x^{5}}{5!}+\frac{x^{6}}{6!}+\alpha_4\frac{x^{7}}{7!}+\frac{x^{8}}{8!}+\alpha_5\frac{x^{9}}{9!}$$

$$v_1=\alpha_4\frac{x^{10}}{3628800}+\frac{x^{11}}{39916800}+\alpha_1\frac{x^{12}}{479001600}+\frac{x^{13}}{6227020800}+\alpha_2\frac{x^{14}}{87178291200}$$
$$+\frac{x^{15}}{435891456000}+\frac{23x^{16}}{20922789888000}+\frac{x^{17}}{2487324672000}$$
$$+\frac{x^{18}}{9094280832000}+\alpha_3\frac{37x^{19}}{1520563755110400}+\ldots$$

Table.2 shows the errors obtained using HPM [10] and the proposed technique

Table 2. Comparison results for Example 2

X	Error of basic HPM [10] N=12	Error of proposed method N=1	Error of proposed method N=2
0	0	0	0
0.1	1.41 e -06	7.08926 e -06	7.56813 e -11
0.2	2.69 e -06	1.34854 e -05	1.59841 e -10
0.3	3.70 e -06	1.85623 e -05	4.23997 e -10
0.4	4.35 e -06	2.18242 e -05	3.55066 e -10
0.5	4.58 e -06	2.29508 e -05	3.02838 e -10
0.6	4.36 e -06	2.18314 e -05	3.90509 e -10
0.7	3.71 e -06	1.85736 e -05	7.76822 e -10
0.8	2.69 e -06	1.34961 e -05	5.02812 e -10
0.9	1.42 e -06	7.09561 e -06	1.56949 e -10
1	2.00 e -09	2.10487 e -07	2.01456 e -13

Example .3

Consider the following twelfth-order boundary value problem:

$$v^{(12)}(x)=2e^{x}v^{2}(x)+v^{(3)}(x) \quad , \quad 0\le x\le 1 \quad (14)$$

With the boundary conditions

$$v^{(2i)}(0)=1 \quad , \quad v^{(2i)}(1)=e^{-1} \quad ; i=0,1,2,3,4,5$$

Taking the ZZ- transform on (14), we find

$$\frac{s^{12}}{v^{12}}H(v)-\frac{s^{12}}{v^{12}}v(0)-\frac{s^{11}}{v^{11}}v'(0)-\frac{s^{10}}{v^{10}}v''(0)-\frac{s^{9}}{v^{9}}v^{(3)}(0)-\frac{s^{8}}{v^{8}}v^{(4)}(0)$$
$$-\frac{s^{7}}{v^{7}}v^{(5)}(0)-\frac{s^{6}}{v^{6}}v^{(6)}(0)-\frac{s^{5}}{v^{5}}v^{(7)}(0)-\frac{s^{4}}{v^{4}}v^{(8)}(0)-\frac{s^{3}}{v^{3}}v^{(9)}(0)$$
$$-\frac{s^{2}}{v^{2}}v^{(10)}(0)-\frac{s}{v}v^{(11)}(0)=H\left(2e^{x}v^{2}(x)+v^{(3)}(x)\right)$$

And the same technique as Example 1 and Example 2, we get

$$v_0=1+\alpha_1 x+\frac{x^2}{2!}+\alpha_2\frac{x^3}{3!}+\frac{x^4}{4!}+\alpha_3\frac{x^5}{5!}+\frac{x^6}{6!}+\alpha_4\frac{x^7}{7!}+\frac{x^8}{8!}+\alpha_5\frac{x^9}{9!}+\frac{x^{10}}{10!}+\alpha_6\frac{x^{11}}{11!}$$

Table. 3 presents the comparison of errors obtained using HPM [10] and the proposed method

Table 3. Comparison results for Example 3

X	Error of basic HPM [10] N=12	Error of proposed method N=1	Error of proposed method N=2
0	0	0	0
0.1	1.61 e -07	2.64363 e -07	1.02489 e -12
0.2	3.07 e -07	5.02929 e -07	6.32871 e -12
0.3	4.22 e -07	6.92193 e -07	2.22147 e -12
0.4	4.97 e -07	8.13636 e -07	6.21478 e -12
0.5	5.22 e -07	8.55511 e -07	9.63257 e -12
0.6	4.97 e -07	8.13637 e -07	2.11478 e -12
0.7	4.22 e -07	6.92105 e -07	6.32547 e -12
0.8	3.07 e -07	5.02821 e -07	3.22578 e -12
0.9	1.61 e -07	2.64332 e -07	3.29874 e -12
1	2.00 e -10	1.02146 e -09	5.62221 e -16

Conclusion

In this study, the proposed hybrid scheme is successfully combined the homotopy perturbation method with the ZZ-transform method to solve higher-order boundary value problems. The main advantage of the proposed scheme is that there is no need to calculate a large number of integrals as in the classical methods. in addition, the proposed scheme gave results which are more accurate compared to the homotopy perturbation method. Therefore the proposed scheme is effective and successful for solving higher-order boundary value problems.

References

1. Alhayani, W. "Adomian decomposition method with Greens function for solving twelfth-order boundary value problems". Appl. Math. Sice. 9, 353-368 (2015)

2. Wazwaz, A. "The modified Adomian decomposition method for solving linear and nonlinear boundary value problems of tenth-order and twelfth-order". Int. J. Nonlinear Sci. Numer. Simul. 1, 17-24 (2000)

3. Opanuge, A., Okagbue, H., Edeki, S., Agboola, O. "Differential transform technique for higher order boundary value problems". Mod. Appl. Sci. 9, 224-230 (2015)

4. Viswanadhm, k., Raju, Y, "Quintic B-spline collocation method for tenth order boundary value problems". Int. J. Comput. Appl. 51, 975-989 (2012)

5. El-Gamel, M. "Chebychev polynomial solutions of twelfth-order boundary-value problems". Br. J. Math. Comput. Sci. 6, 13-23 (2015)

6. Ullah, I., Khan, H., Rahim, M. "Numerical solutions of higher order nonlinear boundary value problems by new iterative method". Appl. Math. Sci. 7, 2429-2439 (2013)

7. El-Gamel, M., Adel, W. "Numerical Investigation of the Solution of higher-order boundary value problems via Euler matrix method". Sociedad Espanola de Mathematica Aplicada SOMA, Springer (2017)

8. Noor, M., Mohyud-Din, S. "Solution of tenth-order boundary value problems by variational iteration technique". J. Appl. Math. Comput. 28, 123-131 (2008)

9. Zafar, Z. "ZZ transfrm method, International journal of Advanced Engineering and Global Technology", vol. 4, Issue-1, 1605-1611 (2016)

10. Nadjafi, J., Zahmatkesh, S."Homotopy perturbation method (HPM) for solving higher order boundary value problems (BVPs)". Applied Mathematical and computational sciences-Mili publication, V. 1, 199-224 (2010)

JOURNAL OF MATHEMATICAL SCIENCES & COMPUTATIONAL MATHEMATICS

OCTOBER 2021 | VOLUME 3 | No. 1

Contents Page No.